JOINT HIGHWAY RESEARCH PROGRAM
PROJECT 72-03-3

EVALUATION OF
BITUMINOUS MIXES IN PAVEMENT STRUCTURES

INTERIM REPORT II

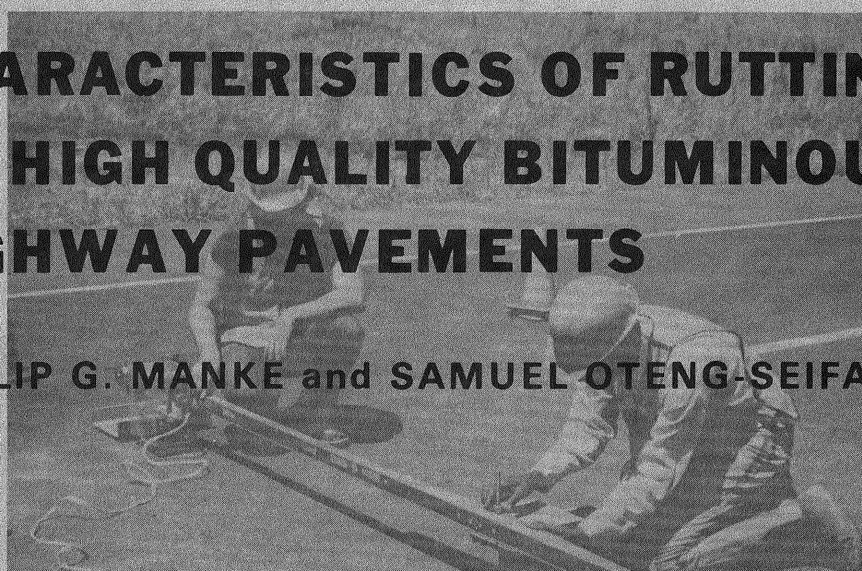

CHARACTERISTICS OF RUTTING ON HIGH QUALITY BITUMINOUS HIGHWAY PAVEMENTS

PHILLIP G. MANKE and SAMUEL OTENG-SEIFAH

In turn:
~~KAA~~
~~Witteveen~~
Oehler

SCHOOL OF CIVIL ENGINEERING
OKLAHOMA STATE UNIVERSITY
STILLWATER, OKLAHOMA

EVALUATION OF BITUMINOUS MIXES IN PAVEMENT STRUCTURES

INTERIM REPORT II

CHARACTERISTICS OF RUTTING ON HIGH QUALITY BITUMINOUS HIGHWAY PAVEMENTS

by

Phillip G. Manke
Project Director

and

Samuel Oteng-Seifah
Research Assistant

Research Project 72-03-3
Joint Highway Research Program

conducted for the

State of Oklahoma, Department of Highways

by the

School of Civil Engineering
Office of Engineering Research
Oklahoma State University
Stillwater, Oklahoma

December, 1975

PREFACE

Rutting on high quality flexible pavement is due to traffic action and is a functional as well as a structural type of failure. That is, it interferes with the quality of ride expected from such a surface and can be detrimental to safe vehicle operation. Excessive rutting is an indication that the integrity of one or more of the material layers in the pavement system was not sufficient to withstand the imposed traffic loads. Surface attrition and subgrade deformations also contribute to this type of failure.

This report discusses the results of a research study of rutting conducted by the school of Civil Engineering at Oklahoma State University. This research endeavored to: 1) accurately determine the depth of ruts and the shape of the transverse pavement profile, and 2) detect evidence of the contribution of the bituminous bound materials to this type of failure in heavy-duty asphalt pavement structures. The research did not deal directly with the influence or contribution to rutting of the subgrade soils and non-bituminous base materials.

Support for this study was provided by the State of Oklahoma Department of Highways and this support is gratefully acknowledge.

Phillip G. Manke

Samuel Oteng Seifah

TABLE OF CONTENTS

(continued)

LIST OF FIGURES

Figure | Page

LIST OF TABLES

CHAPTER I

INTRODUCTION

Statement of Problem

Rutting, as evidenced by vertical deformations in the wheelpaths on flexible pavement surfaces, is a serious highway performance problem in Oklahoma. Rutting is due to traffic action and it affects the quality of ride on a pavement in two distinct ways. First, rutting tends to define the position of vehicle wheels on the pavement, i.e., wheels slightly displaced tend to be directed back to points of maximum rutting, making steering more difficult at high vehicle speeds. Second, rutting tends to channelize and retain free surface water along the wheelpaths during and after rainfall. This surface water acts at the tire-pavement interface to form an effective lubricant so that the intended frictional resistance at this interface is not mobilized and surface slickness results. In extreme cases, the interfacial phenomenon referred to as "hydroplaning" occurs and this is a definite traffic safety hazard. This channelization also allows drainage of more surface water into intersecting or transverse cracks and thus into the underlying pavement layers to deteriorate the asphalt-bound materials (11), and to soften the subgrade materials.

Method and Scope of Study

Field and laboratory observations indicate three major modes of rutting. Regarding the bituminous bound layers, these modes are:

1) post-construction differential densification of one or more of the pavement layers, 2) shear failure or lateral displacement of material in one or more layers from beneath the wheelpaths, and 3) surface wear or errosion of surface material under traffic. In addition, densification (consolidation) and/or shear failures in the non-bituminous bound base and subgrade materials can influence the total amount of rutting. In a specific case, each of these factors may act singularly or in various combinations.

The primary objective of this research was to investigate rutting on high quality flexible pavements and to detect, where possible, evidence of contribution of the bituminous bound pavement materials to this type of failure. This research did not deal directly with the influence or contributions to rutting of the subgrade soils and the non-asphalt bound base materials.

A transverse profile apparatus was developed to plot the profile of the pavement surface perpendicular to the centerline. Rut depths could be scaled directly and humps outside the wheelpath locations detected from the transverse profile tracings. Heaving or humping adjacent to ruts was considered an indication of outward or lateral creep of material from beneath the wheelpaths.

Four inch diameter (10.16 cm.) cores of the asphalt bound pavement materials were recovered at selected points across the pavement. The percent density values of the respective subdivisions of the core samples were determined and compared. Significant differences in the percent density values between materials in the wheelpath locations and those outside the wheelpaths were considered as evidence of differential

densification. Correlation between laboratory densities and the corresponding field measured surface nuclear-densities at the selected sites was also attempted.

Stereo photography was employed to obtain quantitative estimates of differential wear in the wheelpath locations. Also, visual rating of the pavement surface conditions was made at each test site so as to provide comparative data for the study of trends at these locations.

Sixteen test sites were selected on two interstate highway systems (I-35 and I-40) in Oklahoma. Performance of four test sites on flexible pavement sections constructed on each of the following types of base course materials was studied: 1) hot mix sand asphalt (HMSA), 2) soil-cement base (SCB), 3) black base (BB), and 4) stabilized aggregate base course (SABC).

Classical statistical methods, using the Statistical Analysis System (SAS) computer program, was employed in the analysis of test data. Traffic volumes were not counted at the time of testing and the recorded in-service age of the pavement sections at the test sites were estimated from construction completion records obtained from the research section of the Oklahoma Department of Highways (ODH).

The field study of the test sites was made <u>after</u> rutting had occurred. The approximate ages of the pavement sections at the time of the study ranged from 36 to 169 months. For this reason, exact amounts of surface deformations and densification in the pavement layers could not be determined. Measurement of rut depths and other surface deformations was based on a hypothetical datum or transverse profile at age zero, i.e., an assumed transverse profile at the time the pavement was opened to traffic.

CHAPTER II

RESEARCH BACKGROUND

Pavement Deformations

Elastic Deformations

Under applied wheel loads, bituminous pavements undergo both elastic and plastic deformations (3, 4). These deformations occur in both the longitudinal and the transverse directions to form a deflection basin. The elastic deformations are recoverable upon removal of the load. However, complete recovery is gradual and depends on the magnitude and duration of load, temperature, and stiffness properties of the pavement materials. Sometimes, complete recovery of this portion of deformation is not achieved before subsequent load coverages.

Theories for predicting elastic deformations (14, 24, 39) consider the pavement material as an ideal material of some kind and assume that the primary response of the pavement structure can be defined by its mechanical state as a result of the applied loads. Laws of classical physics are then employed to determine the stress-strain relationships and to formulate constitutive equations (mathematical models) of response. Because of the viscoelastic behavior of the bituminous material, the complexities in the behavior of subgrade materials, and the fact that the bituminous pavement constitutes a layered system, deformation values

obtained using these methods are approximate. The degree of accuracy resulting from use of any of these theories will depend on how close the assumptions (upon which the theory was developed) relate to the field conditions. Some of the commonly used theories of elastic response include: 1(Boussinesq's theory (39), 2) Burmister's theory (6), 3) Westtergaard's theory (39), and 4) discrete models (24).

Plastic Deformations

This portion of the total deformation is unrecovered after removal of the applied load, i.e., the deformation remains permanent. Unlike elastic deformations, plastic deformations are cummulative and depend on the magnitude and duration of loading, temperature, and the stress history of the material (1, 15, 24). Basic concepts of material behavior and constitutive laws of plasticity are currently used to predict the onset of plastic behavior. However, because the stress-strain relationships in the plastic range are generally non-linear, the magnitude of deformations are not uniquely determined by stresses. Though seldom used, numerous criteria have been proposed for predicting plastic behavior, and these are based on a concept of either stress, strain or strain energy (24, 37).

Viscoelastic Response

Viscoelasticity attempts to represent the behavior of real materials by combining time-dependent response and time-independent response models (1, 24). There are two types of viscoelastic models: linear viscoelastic, and non-linear viscoelastic models.

Two basic elements are used to develop a linear viscoelastic (one dimensional) model. These models use a spring to represent elastic behavior and viscous behavior is represented by a dashpot with stress proportional to the rate of strain. Linear viscoelastic models employ a basic stress-strain rule to combine the two portions of the model. The basic rule states that when the two elements are placed in series (Maxwell model), the stress is the same in each element, but the total strain is the sum of the strain in each element. When the two elements are placed in parallel (Kelvin model) the strain is the same in each element, but the total stress is the sum of the stresses in each element. These models are discussed in detail by Nair and Chang (24).

Linear viscoelastic models are the most widely used in bituminous pavement analysis because of their relative simplicity and the closeness with which they predict field behavior. Barksdale and others (1) have compared measured and computed responses using a linear viscoelastic model. They computed both elastic and permanent deflections for a 3-layer pavement system on the AASHO test road. The computed response was in close agreement with the measured response. Even so, viscoelastic theory only provides a realistic approximation of the actual behavior of a bituminous pavement system.

Non-linear viscoelastic models only exist as theoretical tools. They have not been applied to the analysis of pavement structures because of the complexity of the theory, the difficulty in experimentally determining the material functions, and the problems associated with developing solutions to the non-linear boundary value problems (24).

Phenomenon of Rutting

Field and laboratory observations indicate different modes of rutting. Foster (12) has observed a situation in which high asphalt content mixes shoved out from under the path of traffic wheels and bulged up on the sides (lateral creep). Similarly, studies by Regal (29) indicated a tendency for bituminous surfaces to rub and shove when constructed from aggregates having "humps" in their gradation. At a symposium on Pavement Evaluation, Hartronft (25) cited examples of decreased density of stone base course materials between wheelpaths and referred to this phenomenon as an apparent permanent loss of density. This situation may be due to dilation resulting from lateral displacement of the base material from beneath the adjacent wheelpaths.

Wissa (13) and McLeod (23) are of the opinion that pavement mixtures undergo densification under traffic. In a general discussion on the effects of load repetition on bituminous mixtures, Wissa remarked that, with repetitions of loads, strains to reach a maximum strength tend to decrease as densification occurs, i.e., previous densification tends to increase the resistance of the mixture to further densification. In a detailed study of the performance of full-depth asphalt bases, Shook and others (32) found surface rutting to be related to the vertical compressive strain and the vertical compressive stress at the subgrade surface. Studies by Nabil (18) have confirmed this relationship.

Marks and Ford (22) have also studied the effect of density on surface performance of bituminous mixtures. In their field investigation, study cores obtained adjacent to initial reference cores indicated

increased densities in the surface course materials ranging from 0.5 percent to 7.5 percent of Marshall Laboratory density. It was also found that the average rut depth increased with increases in the percent density change of the natural gravel mixtures used in the study.

Shoving or lateral displacement (lateral creep) and post-construction densification do not appear to be the only factors that contribute to rutting. Wear of surface materials can also contribute significantly to rutting as was reported by Britton (4). Evidence of pavement wear has also been observed in performance studies using studded and non-studded tires (9).

Rut depths on high class pavements are usually very small (maximum values around 0.5 in. (1.27 cm.), however, data from large scale road tests indicate rutting on highway pavements can be substantial. Ramsey (28) has reported rut depths up to 1.8 in. (4.57 cm.) on pavement sections constructed on granular base course materials in Nebraska. A British full-scale pavement design experiment (20) also recorded rut depths exceeding 3.0 ins. (7.62 cm.). Similarly, data from the AASHO road test (35) indicated excessive rut depths on the order of 4.0 ins. (10.16 cm.).

Mechanisms of Rutting

Densification

The mechanism of densification is best understood by considering the stress conditions occurring under the action of a moving load. When a wheel load moves past an element of material located beneath the surface of the pavement system, the element is subject to stress states

similar to that shown in Fig. 1 (3). Consider a particular situation in which the moving load is at position A. If the tire-pavement interfacial friction is neglected, the orientation of the two principal stresses acting on an element located under position B will be as shown by the broken lines. As the load moves past position A towards position B, the orientation of the principal stresses gradually changes and finally assumes the orientation indicated by the bold lines when the load reaches position B. That is, each element of material under the pavement surface is subject to a simultaneous build up of stresses (σ_1 and σ_3). As these stresses build up, a rotation of the stress axis occurs. The tendency of this rotation and stress build up is to encourage reorientation of aggregate particles in the paving mixture, followed by degradation (if the stresses are large enough) and, finally, a decrease in void content and an increase in density. On the other hand, dilation (increase in volume) of the material may occur if the mixture has already attained maximum density.

The mechanism of densification may also be explained by any of the viscoelastic response models or systems consisting of a combination of elastic springs and dash pots. Representing the materials beneath the thin wearing surface by a viscoelastic medium and assuming no lateral escape of material occurs, it can be shown that the load directly decreases the volume of the material and the unrecovered portion of the deformation after removal of the load is a measure of densification due to the applied load.

Densification can also occur as a result of temperature cycling. Ellis and others (8) have noticed significant increases in density of Marshall briquettes subject to temperature cycling. They attributed

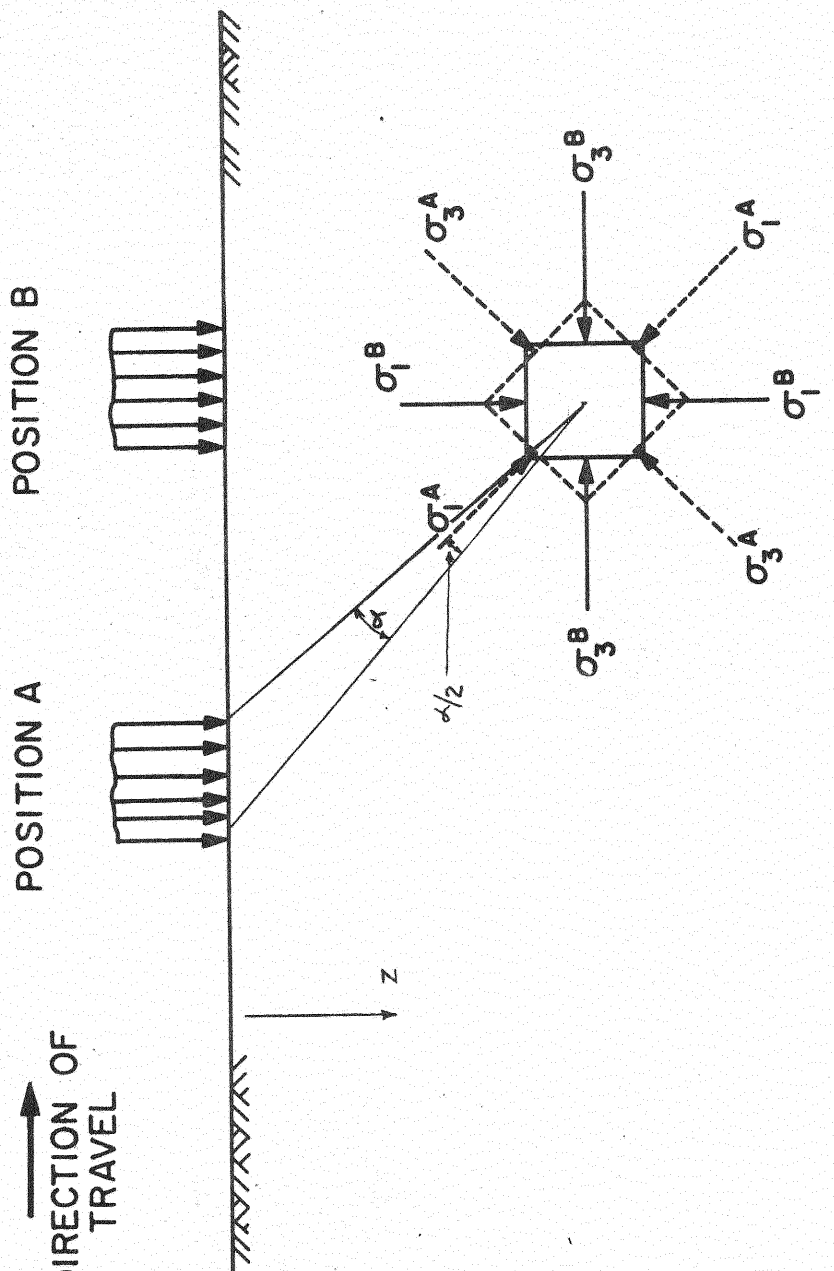

Figure 1. Rotation of Stress Axes of an Element Under a Moving Load

this type of densification to the behavior of the asphalt binder during heating and cooling. Asphalt cement increases in volume by approximately 3.0 percent over a 100°F (37.7°C) rise in temperature. Over the temperature range of the experiment, the asphalt binder was considered to have expanded in volume about twenty times more than the aggregate in the mixture. This expansion caused the binder material to flow into the air voids in the briquette. Upon cooling the asphalt cement contracted and pulled the aggregate particles closer together by the action of surface tension. This caused the air voids to decrease and the briquette to shrink. Their experimental data associated increasing densification with: 1) highly absorptive aggregates, 2) low viscosity asphalt cement, and 3) high asphalt content. It is believed that this type of densification is not a contributing factor to pavement rutting, however, thermal densification will develop large contraction stresses in the paving mixture.

Review of the compressive stress distribution in materials under a surface load shows large stresses approaching the contact pressure, in the surface layer (6). This means there is a greater prospect of densification in the surface or wearing course of a pavement than in the underlying layers where the stresses are smaller (Fig. 2a). However, the magnitude of stress due to a wheel load in a material layer is dependent on the strength or modulus of elasticity of the given layer and that of the overlying layer. Thus, the stress at a given depth may be sufficiently great to cause densification in the material layer. This would apply in particular to layers having a low stability and high void content.

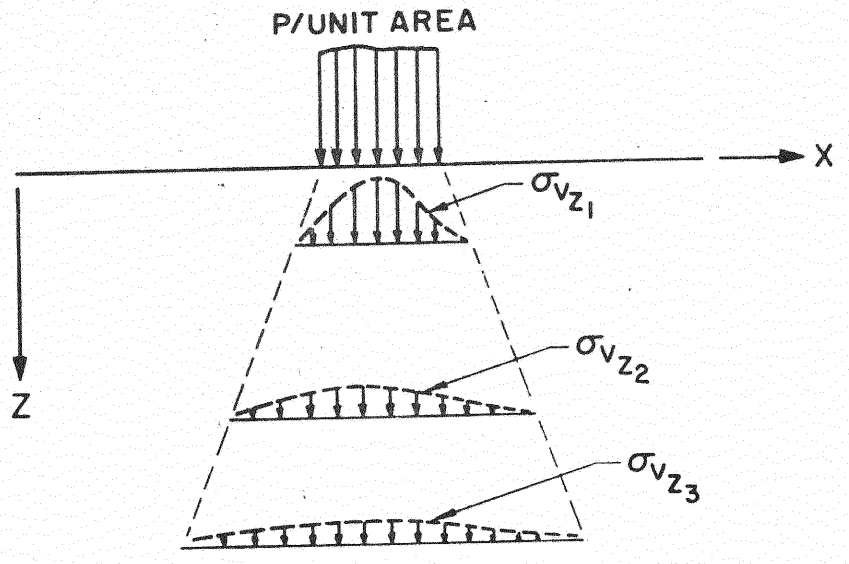

(a) DISTRIBUTION OF VERTICAL STRESSES

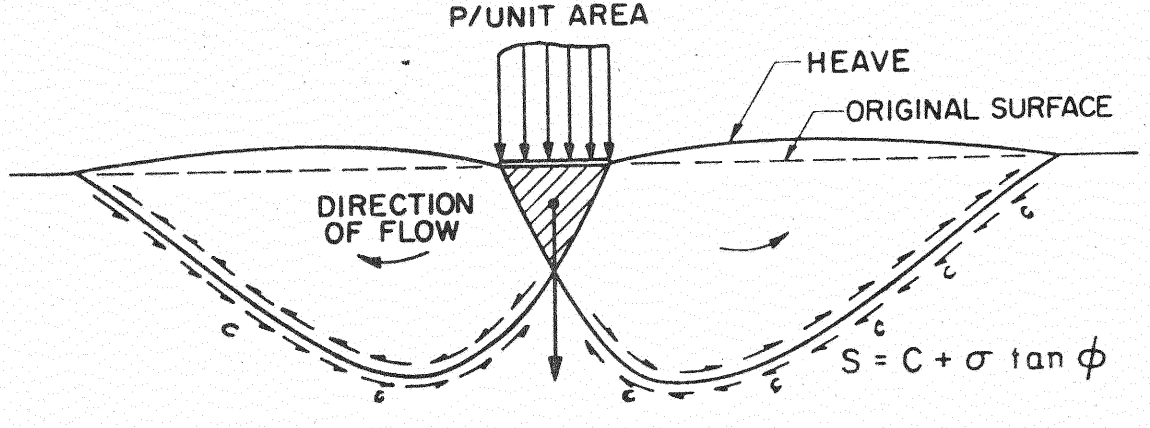

(b) SHEAR FAILURE

Figure 2. Behavior of Paving Material Under Loaded Areas

The contribution of densification to rutting can be illustrated by considering a column of bituminous mixture confined by rigid boundaries at the sides and at the base (Fig. 3). Assume this column of material changes in volume from V_0 to V_1 as a result of the applied load P. The height H_0 of the column is reduced to H_1 and the density of the column of material is increased, thereby, reducing the void content in the material. The percent decrease in air void content can be shown to be directly proportional to the percent decrease in height of the column of material.

Lateral Displacement

In addition to tensile and compressive stresses, the vertical compressive stress pulses acting on the pavement tend to induce shearing stresses in the pavement layers. The induced shearing stresses are resisted by the cohesive strength and the inter-particle frictional resistance developed in the compacted mixture. When the induced shearing stresses exceed the shearing strength of the mixture, plastic flow of the materials beneath the loaded area occurs (39). Lateral flow of materials from beneath the loaded area is evidenced by upheaval of surfaces adjacent to the loaded area (Fig. 2b).

In bituminous pavement structures, lateral creep may occur in the surface layer, base course, or in the subgrade soil. These modes of failure are illustrated in Fig. 4,5, and 6. If an initial transverse profile graph of a new pavement surface was made prior to traffic use, then any subsequent upheaval of the surface adjacent to the wheelpaths could be measured. The transverse location of the heaved surface with respect to the wheelpath would provide an indication of the layer in which lateral creep had occurred. The amount of vertical heave of the

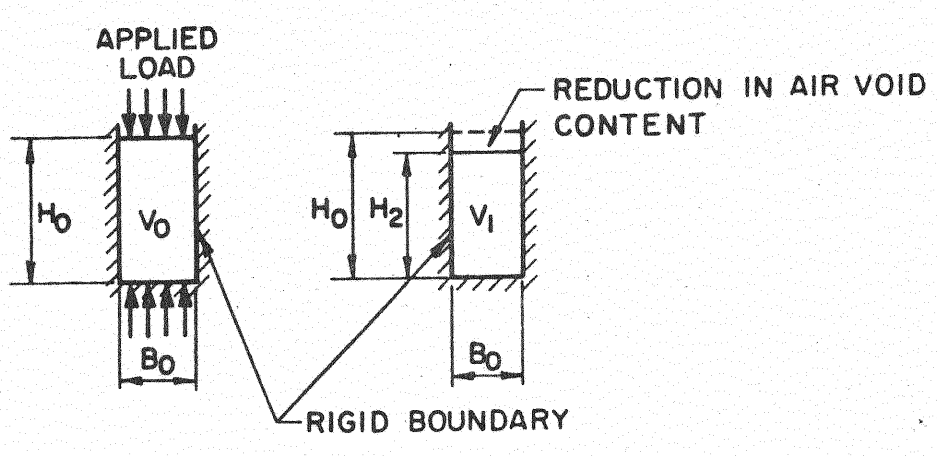

INCREASE IN PERCENT DENSITY $\propto$ DECREASE IN VOID CONTENT,

AND

$\propto$ PERCENT DECREASE IN SPECIMEN HEIGHT

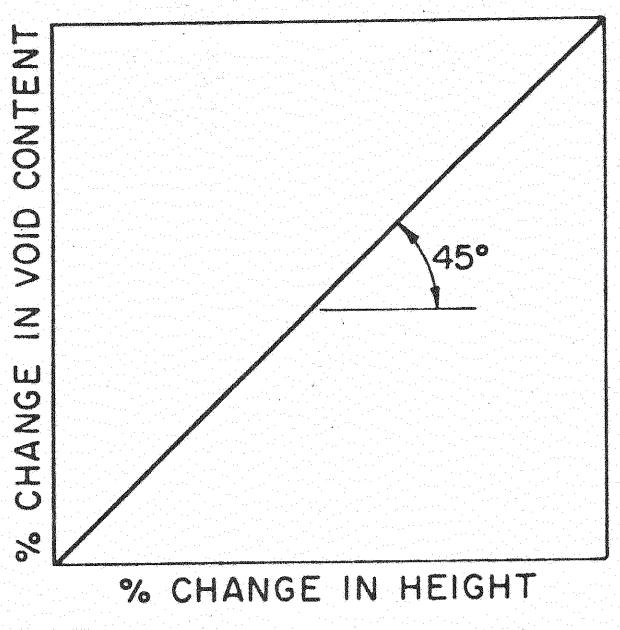

Figure 3. Effects of Densification on Layer Thickness

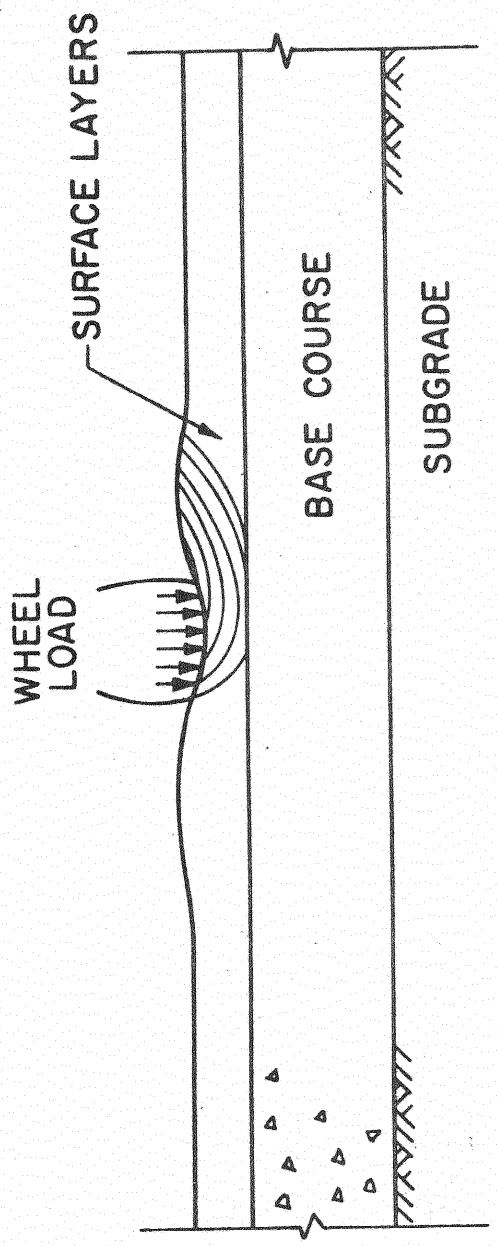

Figure 4. Lateral Creep (Shear Failure) in Surface Layers

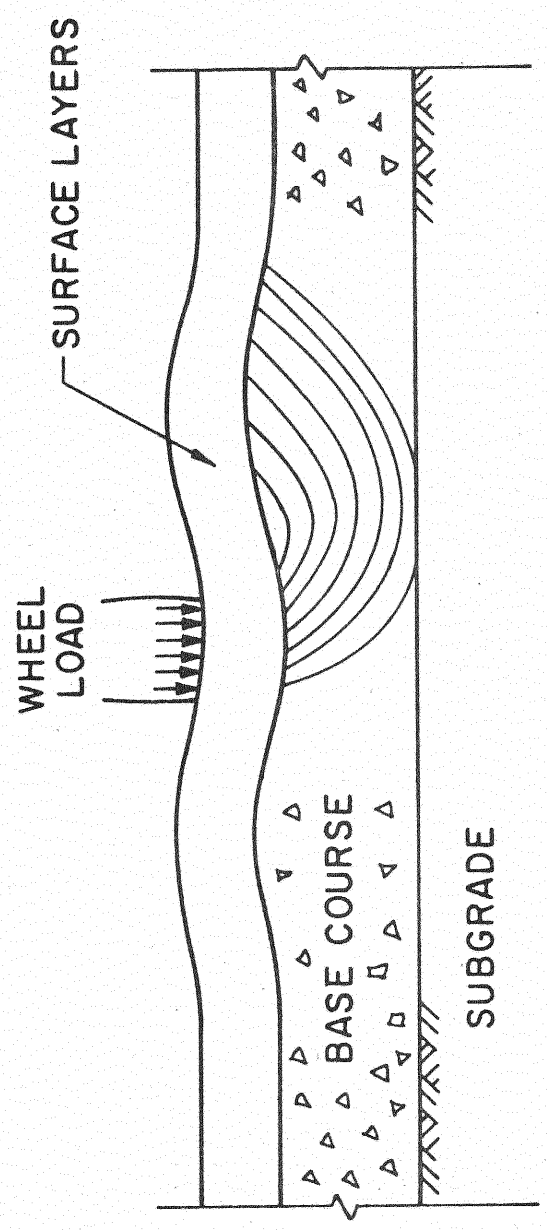

Figure 5. Lateral Creep (Shear Failure) in Base Course

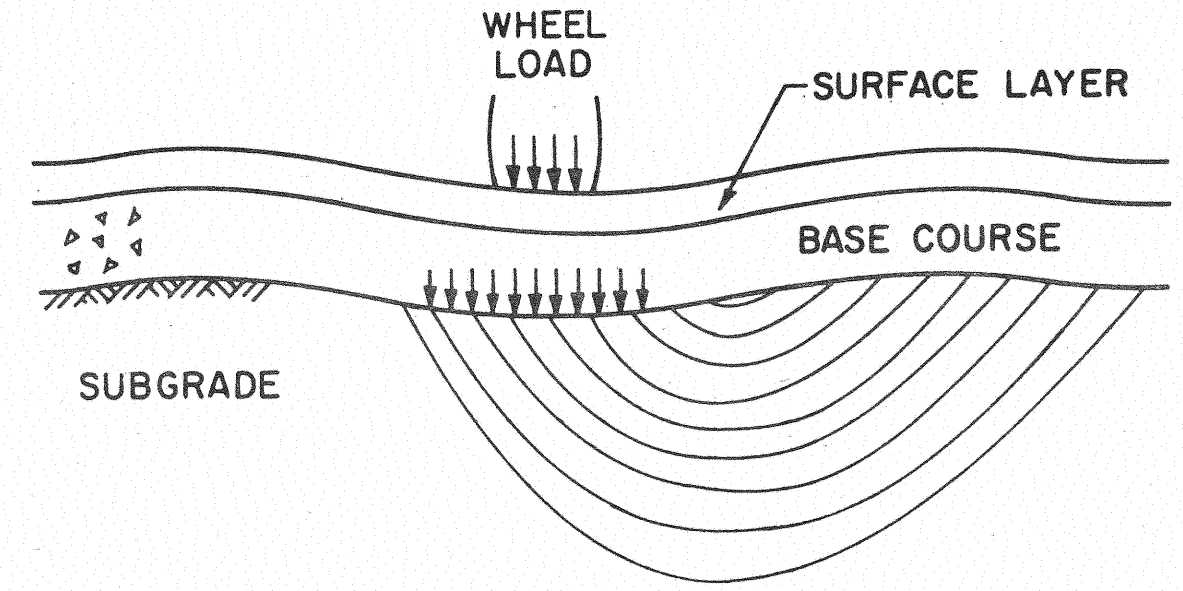

Figure 6. Lateral Creep (Shear Failure) in Subgrade Soil

adjacent surfaces would provide an estimate of the rut depth resulting from lateral flow of material from beneath the wheelpath. Estimates obtained this way are highly approximate because of volumetric changes the pavement materials undergo in service, and the complex behavior of the subgrade soil.

Surface Wear

Wear of pavement surfaces is due to frictional stresses developed at the tire-pavement interface as a result of resistance to rotation of the tire offered by the surface materials. It is a complicated phenomenon and depends on several factors including: the nature of vehicle tire; type of tread or stud; strength characteristics of the surface mixture; the nature of traffic and environmental conditions. On bituminous pavements, the slippage stresses which the tire applies to the pavement surface tend to polish, fracture, loosen and pulverize the matrix.

According to Keyser (19) bituminous surfaces are worn by a combination of three processes: 1) pulverization, cutting and attrition of the surface matrix; 2) fragmentation and loosening of the mineral aggregate; and 3) loosening and dislodging of aggregate particles.

Keyser found the matrix at the pavement surface to wear very rapidly in the beginning. As the asperity or projection of the coarse aggregate increased, the rate of wear of the matrix became constant and corresponded to the rate of wear of the coarse aggregate. Thus, the nature of wear depended to a greater extent on the relative wear resistance of the constituent coarse aggregate and the mortar or matrix of the surface mixture. Keyser also found wear was lowest at about $32^{o}F$ ($0^{o}C$) and increased with increasing or decreasing temperature. He attributed this

behavior to changes in rigidity of the rubber tires and the stiffness of the bituminous mixture with temperature.

For pavements receiving all year round traffic with standard automobile tires, surface wear takes place at very slow rates, and magnitudes of wear are usually very small. Preus (27) has observed depths of wear on both bituminous and portland cement concrete pavements for traffic using both studded and non-studded tires. His study of wear using non-studded tires showed 0.008 in. (0.02 cm.) wear depth on a bituminous surface compared with 0.006 in. (0.015 cm.) on a portland cement pavement, after 4.0 million tire passes. Under field conditions, however, greater depths of wear can be expected on bituminous surfaces. This increased wear is attributed to loss in adhesion of the matrix and loss in hardness and strength of the surface aggregates resulting from the presence of water and changes in temperature.

CHAPTER III

EXPERIMENTAL DESIGN

By definition, the terminology "design of experiment" refers to the specification of treatments whose effects are to be investigated, the selection and the arrangement of the experimental units to which specific treatments are to be applied, and the specification of measurements to be made on each experimental unit (10).

Initially, it was planned to use a purely statistical approach in this investigation. However, as in the case of many other field research programs, existing limitations required some departure from the classical statistical approach. Some of these limitations pertained to: 1) safety of the research personnel on high-speed highways, 2) time restrictions related to completing certain phases of the study within an established time frame, 3) existence of a particular base course material at an appropriate experimental design location on the Oklahoma interstate highway system, and 4) precise transverse location of the wheelpaths in the respective traffic lanes.

For this investigation, types of base course materials were referred to as "treatments". Test sites were selected on flexible pavement sections of interstate highways constructed on four types of base course materials. These base course materials are the four major types commonly specified by the Oklahoma Department of Highways: Hot Mix Sand Asphalt

(HMSA), Soil-Cement Base (SCB), Black Base (BB), and Stabilized Aggregate Base Course (SABC) (34).

The individual test sites were considered as "experimental units" and were picked from locations on two interstate highways in Oklahoma. These highways, Interstate 35 (north-south) and Interstate 40 (east-west), roughly divide the state into four quadrants. To be able to detect possible regional differences resulting from climatic variations and the subsequent differences in subgrade moisture contents, variations in subgrade soil types and differences in traffic characteristics, it was thought that the "completely randomized block design" (10) would be most effective. However, the field limitations mentioned above did not permit use of the randomized block design. Tentative selection of the test sites (experimental units) was based on performance data obtained from the research section of the Oklahoma Department of Highways. This information indicated the design average daily traffic volumes (design ADT) of the two interstate highways, the construction completion dates, and existing paving materials of respective pavement sections on these highways. The data also included Benkelman beam deflections and "A-frame" rut depth measurements at approximately 176 yds. (160 m.) intervals. From this performance data, possible test sites were selected.

Preliminary visits were made to possible test sites to: 1) evaluate the extent of sight distance available to on-coming motor vehicles, 2) check the vertical and the horizontal alinement, 3) check for the existence of the indicated type of base course materials, 4) visually examine and rate the surface characteristics including estimates of the extent of rutting, 5) study the general geometric design characteristics in the vicinity, and 6) mark suitable test locations as possible

candidates for final selection. Whenever a site was found to lie on curved section (horizontal or vertical) or near interchanges, a substitute test site in the same vicinity was picked. Each test site was permanently identified by attaching a 4.0 in. x 6.0 in. (10.2 cm. x 15.2 cm.) orange painted sheet metal marker to the right-of-way fence. For the test sites on Interstate 35, the markers were located at measured odometer distances north of the appropriate south boundary line of the county in which the test site was located. If the location of the site happened to be in the southbound traffic lanes, the distance was measured in the northbound traffic lanes. The location was temporarily identified in the northbound lane and then projected transversely to the west right-of-way fence adjacent to the southbound lanes, where it was permanently marked as described above. The sites on Interstate 40 were similarly located and identified. The only exception was that all distances were measured east of the west county line in the eastbound traffic lane.

In order to assure the safety of the study personnel on these high speed highways, the governing criteria for site selection was that the test sites had to lie on straight tangent sections. This was needed so that drivers of on-coming vehicles could be given sufficient distance to effectively perceive and react safely to the changed road conditions caused by the study operations. A minimum of one-half mile (804 m.) of unobstructed sight distance was considered necessary to meet this safety requirement.

To keep the volume of experimental data within limits practical to the planned time schedule, a total of sixteen test sites meeting the aforementioned requirements were finally selected for investigation. These included four test sites, comprising two minimum and two maximum

rut depth sections of pavements constructed on each of the four types of base course materials (HMSA, SCB, SABC, and BB). The resulting allocation of base course materials (treatments) to the test sites (experimental units), though not completely randomized, was considered as a completely randomized experiment (10, 33) instead of the intended randomized block design. In other words, eventhough the effects of regional differences on performance were somehow allowed for, the final site selection procedure did not permit direct statistical investigation of the influence of regional differences on the performance of the individual types of base course materials.

The data collected from both the field and the laboratory portions of this investigation are referred to as "measurements" in the above statistical definition of "design of experiment". Specification of types of measurements to be made on the test sites were dictated by the prevailing field conditions and lack of desirable information on individual test sites. Absence of initial in-place densities of the asphalt-bound paving materials at the selected test sites required the determination of percent densities instead of the existing bulk densities alone. To obtain the percent density values, two other laboratory values were required: the in-place bulk specific gravities and the theoretical maximum specific gravities of the existing pavement materials. Standard procedures for measurement of the theoretical specific gravity were reviewed in terms of their relative advantages and Rice's Method (36) was found to be the most appropriate. This procedure, in turn, required that "undisturbed" samples be taken from the layered system at appropriate points across the pavement surface. Four-inch diameter core specimens were considered convenient.

It was also decided that a nuclear technique (7) be employed to measure the in-place bulk densities in addition to the laboratory methods of measurement of the core samples. The major reason for this additional field measurement was to determine, if possible, a correlation between the nuclear densities and the conventional laboratory densities. If good correlation were found, the destructive laboratory procedure could be replaced by the faster non-destructive nuclear method for all future research or field testing involving measurement of in-place bulk densities.

In order that the pavement surface configuration could be clearly observed, and to accurately measure the rut depths in the wheelpaths and possible heaves immediately outside the wheelpaths, it was decided that continuous plots of the transverse profiles at the individual test sites were required. Most of the existing profilometers or road meters (26) were found to be incapable of producing the required continuous tracings. Furthermore, the sizes of those which could possibly be modified to do the job made them unfeasible, so a portable transverse profile gage was developed for this research investigation. In addition to plotting the transverse profiles, the cross-slopes of the pavement surface could also be determined with this equipment.

Some means of measuring or estimating the amount of attrition in the wheelpaths was desirable. It was found that a quantitative estimate of attrition could be made by means of stereo-photography (30, 31). Stereo-pairs of 35 mm. photographs taken at appropriate transverse points on the pavement surface were required. Comparison of projections of the surface aggregates in the wheelpaths with those outside the wheelpaths would provide estimates of relative attrition or frictional wear of surfaces in the wheelpaths.

For comparative purposes, two other sets of data were needed. These were: 1) estimates of the in-service pavement age, and 2) pavement surface condition rating (qualitative) (38). The final field layout of test points at a given test site is illustrated in Fig. 7. The geographical locations of the test sites selected for this study are described in Appendix A.

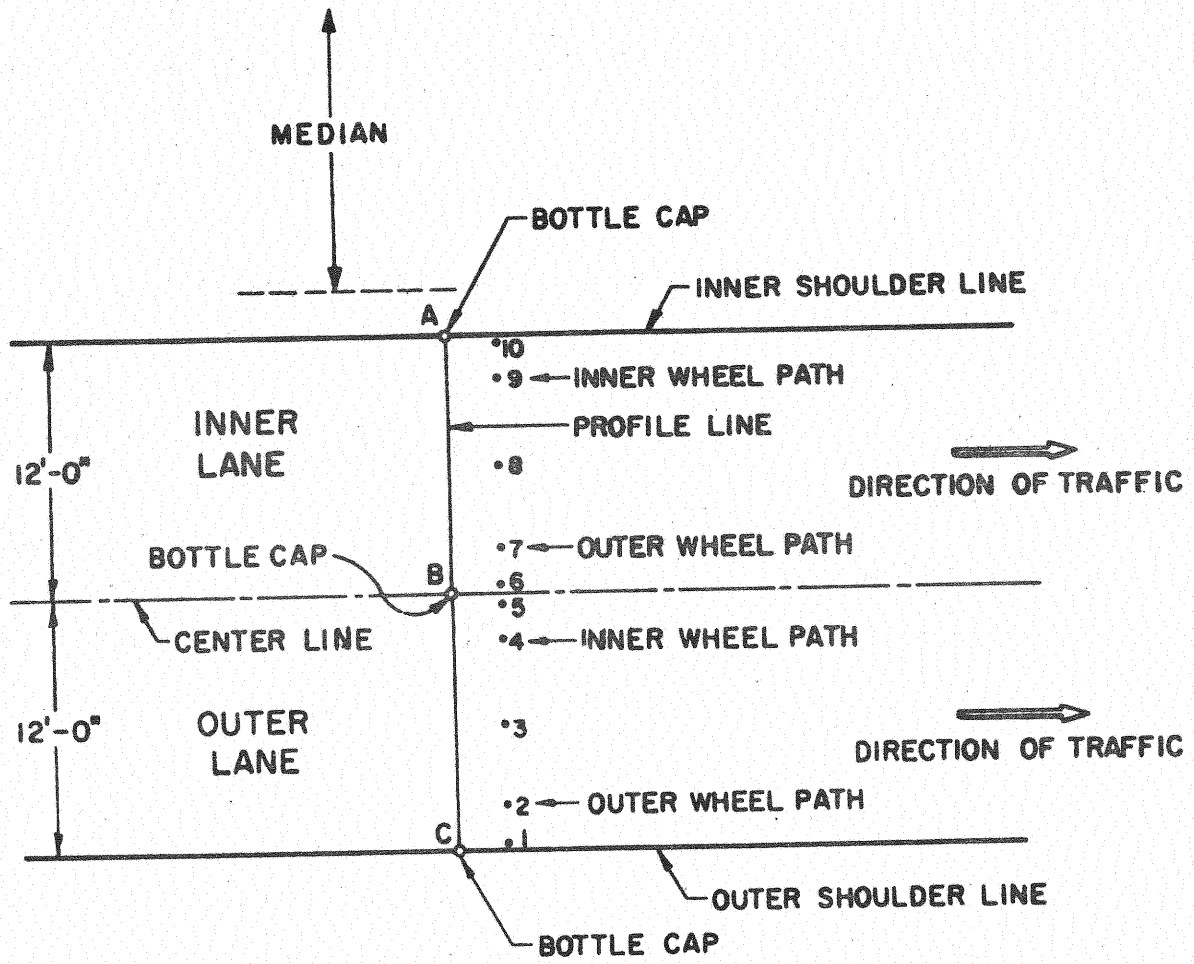

Figure 7. Layout of Transverse Test Point Locations at a Test Site

CHAPTER IV

DEVELOPMENT OF TRANSVERSE PROFILE GAGE AND EQUIPMENT

A continuous profile tracing apparatus, the "transverse profile gage", was developed for this and future research because the existing profilometers were designed primarily for longitudinal profile studies. The few that were designed for transverse profiles were too large to handle easily and cost more than the research project could afford. The portable types of equipment, including the "A-frame" and the electronic rut depth gage (35), are only capable of producing point estimates of rut depths. Also, their operational procedures require knowledge of the transverse location of the wheelpath whose rut depth is to be estimated, and their accuracy depends, to a large extent, on the curvature or configuration of the rut. Because these variables are usually unknown, measurements made with these instruments are only approximate and can be highly erroneous, making them unsuitable for research studies which require reasonably accurate measurements of rut depths or upheaval of pavement surfaces.

The transverse profile gage was developed to provide a portable and accurate means of obtaining continuous transverse profile graphs. In addition to the measurement of rut depths and heaves outside of the wheelpaths, the plotted transverse profile graphs provide permanent records of these conditions at a specific time in the service life of a pavement and

can be used in future studies. The equipment could also be employed to check the transverse profile tolerances usually specified in the construction of highway pavements.

Transverse Profile Gage

Essentially, the transverse profile gage consists of: 1) a straight edge, 2) a cross-slope device, 3) a trolley system, 4) an "X-Y" recorder, and 5) electrical installation equipment.

Straight Edge

The straight edge was designed to serve as a guide rail and a datum plane for the trolley system. The major design requirements were: 1) that the unit be subject to a minimum amount of temperature distortion, 2) that its weight be kept to a minimum to facilitate transportation to and handling at the site, 3) that its length be sufficient to span, at least, one traffic lane of an interstate highway, and 4) that its supports be adjustable in height to provide means of increasing or decreasing the relative elevations of the datum plane at the support points.

Temperature distortion was a major problem in the selection of a suitable member. In addition to the unavoidable expansion and contraction, a metallic section undergoes twisting and warping when subjected to sudden temperature change. These distortions could add to the factory or mill imperfections which alone might be greater than was desirable.

The weight of the member was also a problem. The unit had to be transported to and from the site and it also has to be handled several times at the site. Under the expected conditions, it was considered that

any member that was heavier than one person could conveniently handle would create both handling and safety problems. Also, the weight of the member would encourage flexural deflections. For this study, flexural deflections exceeding 0.05 in. (0.13 cm.) were considered excessive.

To provide a member that was less subject to temperature distortion and yet light in weight, the straight edge was made from magnesium-alloy carpenter's framing levels. Two standard 6.50 ft. (1.98 m.) long carpenters levels (1.0 in. [2.54 cm.] wide x 2.25 in. [5.72 cm.] deep I-section) were spliced together on the web with two 1.5 in. (3.81cm.) wide x 8.0 in (20.32 cm.) long aluminum-alloy plates, 0.31 in. (0.79 cm.) thick to provide continuity. The spliced connection was bolted along the mid-depth of the web with four 0.25 in. (0.64) diameter bolts so the built-up member could be taken apart by removing two bolts for transportation to and from the site. The built-up member had a finished length of 13.0 ft. (3.96 m.). The member was also bracketed at its mid-length with a dismountable aluminum-alloy bracket, 38.0 in. (96.52 cm.) long and 2.0 in. (5.08 cm.) thick, to provide the desired regidity and to provide a means of support at the mid-span (Fig. 8).

The straight edge was supported at the ends and at the center. The end supports utilized 12.0 in. (30.48 cm.) lengths of standard 10.0 in. (25.40 cm.) x 2.5 in. (6.35 cm.) structural steel channel sections as a base plate which was supported on three leveling screws. These screws were 0.75 in. (1.915 cm.) diameter bolts, 3.0 in. (7.62 cm.) long, with spherically shaped ends so the height of the base plate from the pavement surface could be varied and the entire base leveled by adjusting the screws. The stem of the end support system utilized a standard 2.0 in. (5.08 cm.) x 2.0 in. (5.08 cm.) structural steel angle 12.0 in. (30.48

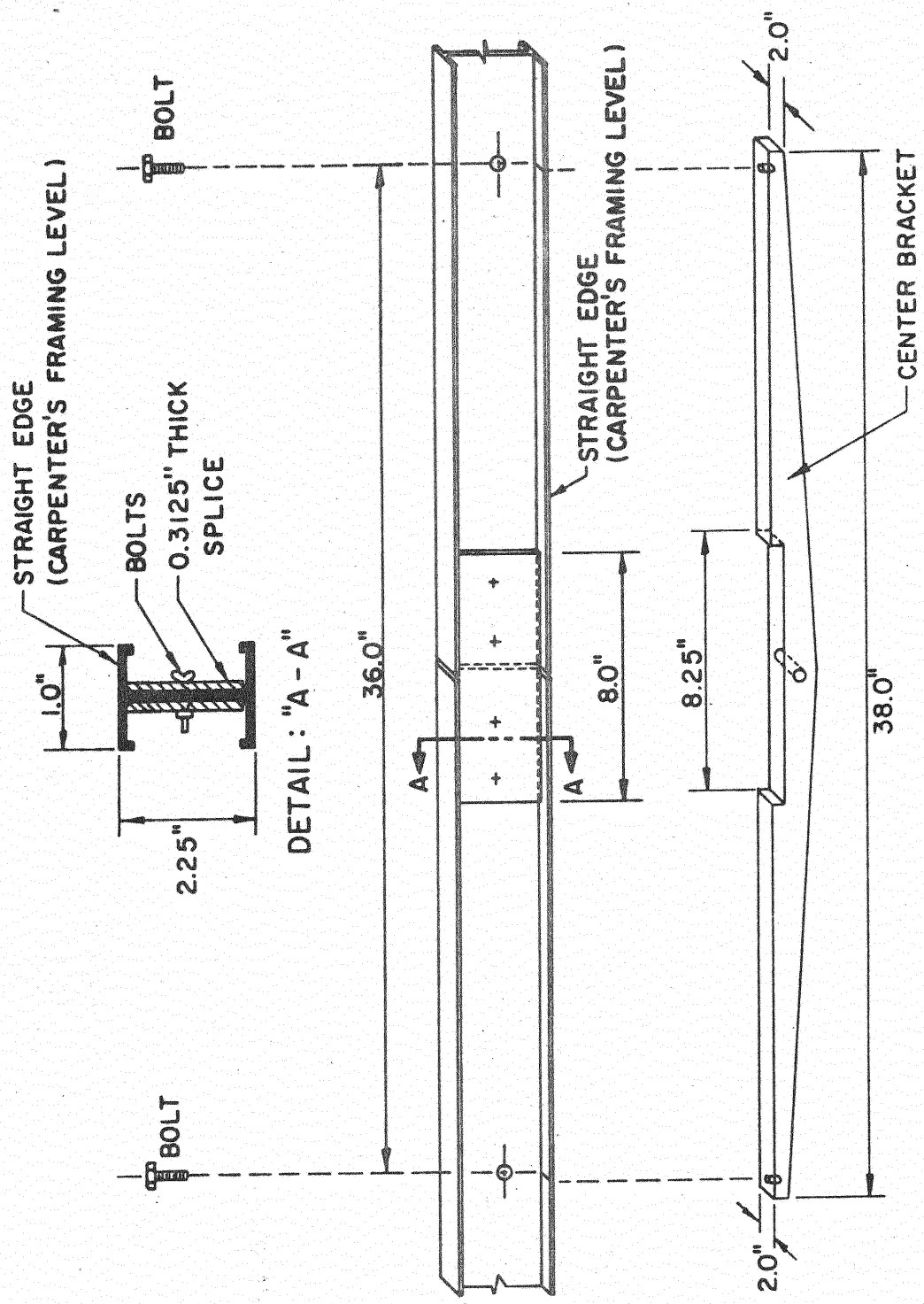

Figure 8. Fabrication of Straight Edge

30.48 cm.) long which was centered and welded at its lower end to the side of the base plate such that the stem stood vertically when the base plate was level. A 0.5 in. (1.27 cm.) diameter by 3.0 in. (7.62 cm.) long steel bolt was screwed to the stem to provide a horizontal abutment for the straight edge (Fig. 9). The straight edge was fastened to the face of the stem by a 0.5 in. (1.27 cm.) diameter bolt.

The center support of the system was made from three pieces of 0.5 in. (1.27 cm.) thick steel plates and one piece of a standard 8.0 in. (20.32 cm.) x 6.0 in. (15.24 cm.) structural steel T-section as shown in Fig. 9. The threaded steel rod was bolted at its lower end to the horizontal leg of the T-section to form a vertical shaft which supported the center bracket of the straight edge. A brass nut, bevel-pointed at the contact end, provided a bearing surface for the bracket. The brass nut also provided a means of adjusting the elevation of the straight edge at this point. A second brass nut firmly held the bracket at a desired elevation when tightened.

Cross-Slope Device

This was a simple accessory that was attached to the straight edge to estimate the average cross-slope of the pavement surface for each traffic lane of the highway.

A selected 15.0 in. (38.10 cm.) length was cut from a standard 1.0 in. (2.54 cm.) x 1.0 in. (2.54 cm.) extruded aluminum-alloy angle. One leg (vertical) of the member was notched at a distance of 1.0 in. (2.54 cm.) from one end. The other leg (horizontal) was also notched at a distance of 12.0 in. (30.48 cm.) from the same end. The vertical leg was pivoted to the face of the stem of one of the straight edge end supports by

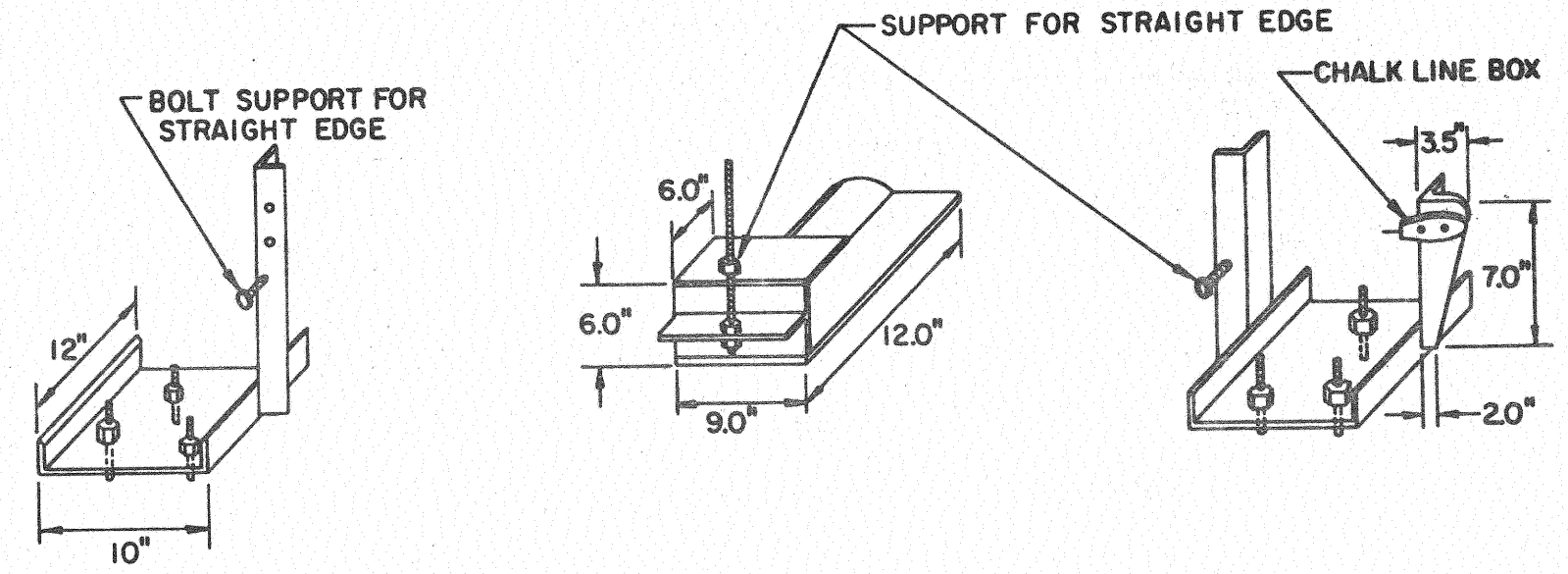

Figure 9. Straight Edge Support System

bolting through the notch such that the angle would lie flat on the top surface of the straight edge when free to do so. A dial gage with thousandths of an inch graduations was attached to the web of the straight edge (by a bolt) at a distance of 12.0 in. (30.48 cm.) from the end of the straight edge so that the neck of the dial gage shaft would freely slide into the notch cut through the horizontal leg of the angle section. A torpedo type spirit level was placed on the top surface of the horizontal leg to complete the fabrication of the device.

To measure the average cross-slope of a highway pavement, the straight edge was first set up transversely across the pavement so that the height of the top flange above the pavement surface was equal at the two end support points. Any mid-span deflection of the straight edge was removed by adjusting the height of the center support (a detailed procedure for setting up the profile gage is discussed later). The aluminum angle was adjusted to lie flat on the top of the straight edge. This position established the datum line parallel to a line joining the pavement surfaces at the end support points. The dial gage was set to zero and the free end of the aluminum angle was raised vertically until the bubble in the spirit level moved to a level position. The observed dial gage reading was the average cross-slope of the pavement surface in inches per foot.

The Trolley System

The trolley of the transverse profile gage consists of: 1) a 15-turn, 2-ohm Helipot helical potentiometer, 2) a 0.5 in. (1.27 cm.) diameter by 4.75 in. (12.06 cm.) long 2-ohm linear potentiometer with 1.5 in. (3.81 cm.) travel, 3) 5.0 in. (12.70 cm.) diameter teflon actuating wheel, 4) four 1.5 in. (3.81 cm.) diameter by 2.5 in. (6.35 cm.) long

nylon rail track wheels, and 5) a 9.0 in. (22.86 cm.) x 12 in. (30.48 cm.) aluminum suspension plate 0.5 in. (1.27 cm.) thick. Functionally, the heilical potentiometer scales the transverse displacements while the vertical potentiometer gages the vertical displacements of the actuating wheel (Fig. 10).

The rail track wheels were cut from a 1.75 in. (4.45 cm.) diameter nylon rod and machined so that the cylindrical web would freely track along the flanges of the straight edge (Fig. 8). The four track wheels were bolted along their cylindrical axes to the upper portion of the steel suspension plate. The two rows (upper and lower) of track wheels were centered to fit the straight edge flanges, as explained above, and to provide a smooth ride along the entire span of the straight edge.

The actuating wheel was cut from 0.75 in. (1.91 cm.) thick teflon sheet. The outer circumference was slightly crowned and grooved. A 0.19 in. (0.48 cm.) diameter circular rubber ring was placed in the groove on the outer circumference of the wheel to provide a smooth ride on the pavement surface and to minimize permanent circumferential deformations in the teflon wheel. Also, the rubber ring could easily be replaced should excessive wear occur or the material deteriorate.

The mounting ring on the shaft of the helical potentiometer was fitted to an opening cut at the centroid of the actuating wheel. The protruding end of the potentiometer shaft was bolted to one end of a pivot arm, the other end of which was hinged to the aluminum suspension plate. There was sufficient tolerance at the hinged connection for free rotation of the wheel system about this point. The wheel system was sufficiently mass-weighted, approximately 5 lbs. (2.27 kg.), to keep the actuating wheel in continuous contact with the pavement surface.

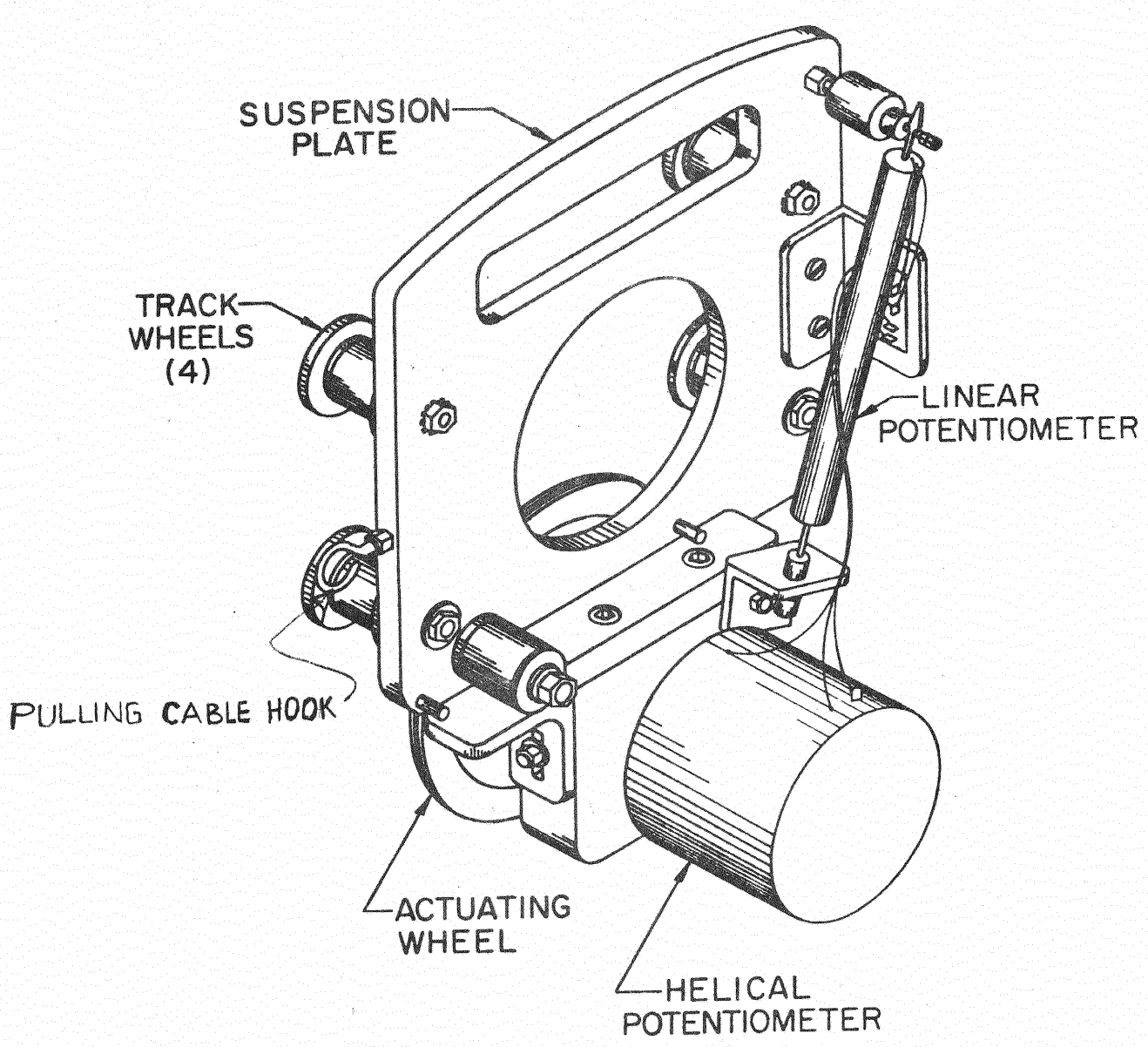

Figure 10. Transverse Profile Gage Trolley Unit

The linear potentiometer was similarly mounted by attaching one end to the suspension plate and the other to the axle of the actuating wheel such that the body of the potentiometer was approximately vertical when the shaft of the potentiometer was at its midpoint of the travel. This position of the shaft was designated as the datum for the linear potentiometer so that both positive (subsidence) and negative (upheaval) deformations could be measured. The sensitive portions (the potentiometers) of the trolley system were shielded with a plexiglass cover attached to the suspension plate.

A small reel of fine copper cable was bolted to one end support of the straight edge and the end of the cable was hooked to the aluminum suspension plate of the trolley as shown in Fig. 10. With this arrangement, the trolley could be manually reeled in one direction at a fairly uniform speed from one end of the straight edge to the other. In this way, induced structural vibrations in the straight edge could be minimized and undue deflections that might result from "push loads" on the trolley system eliminated. The field set up of the transverse profile gage is shown in Fig. 11.

Electrical Installation System

Fig. 12 shows a diagramatic sketch of the electrical installation system employed with the trolley system and the "X-Y" recording equipment. Using a standard automobile battery cable, electrical current from a 12 volt pickup battery was passed through a safety switch and through a low resistance relay switch system to the 200 watt/115 volt D.C. to A.C. inverter. The inverter supplied the appropriate alternating current (AC) to the Hewlett Packard "X-Y" recorder. The potentiometers used direct

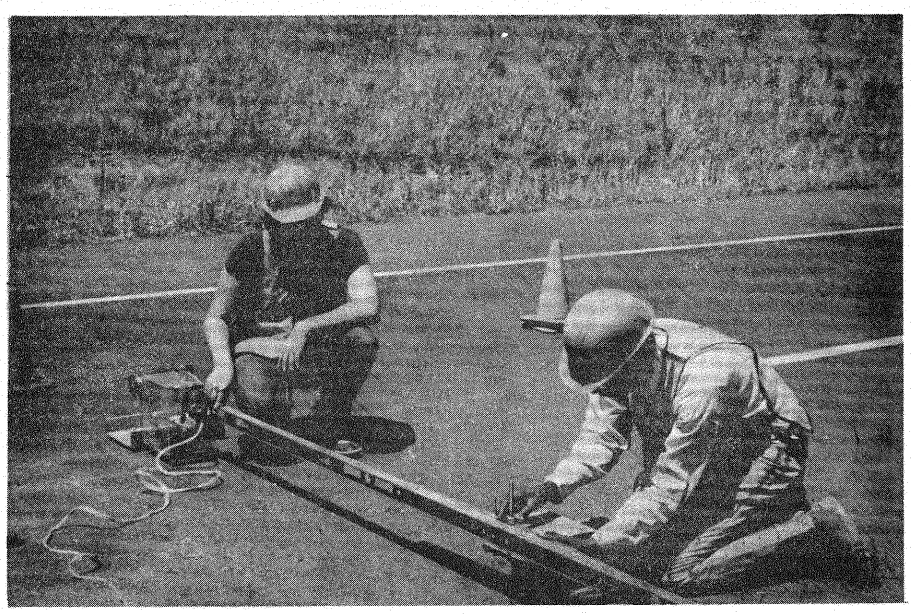

Figure 11. Straight Edge and Trolley Unit

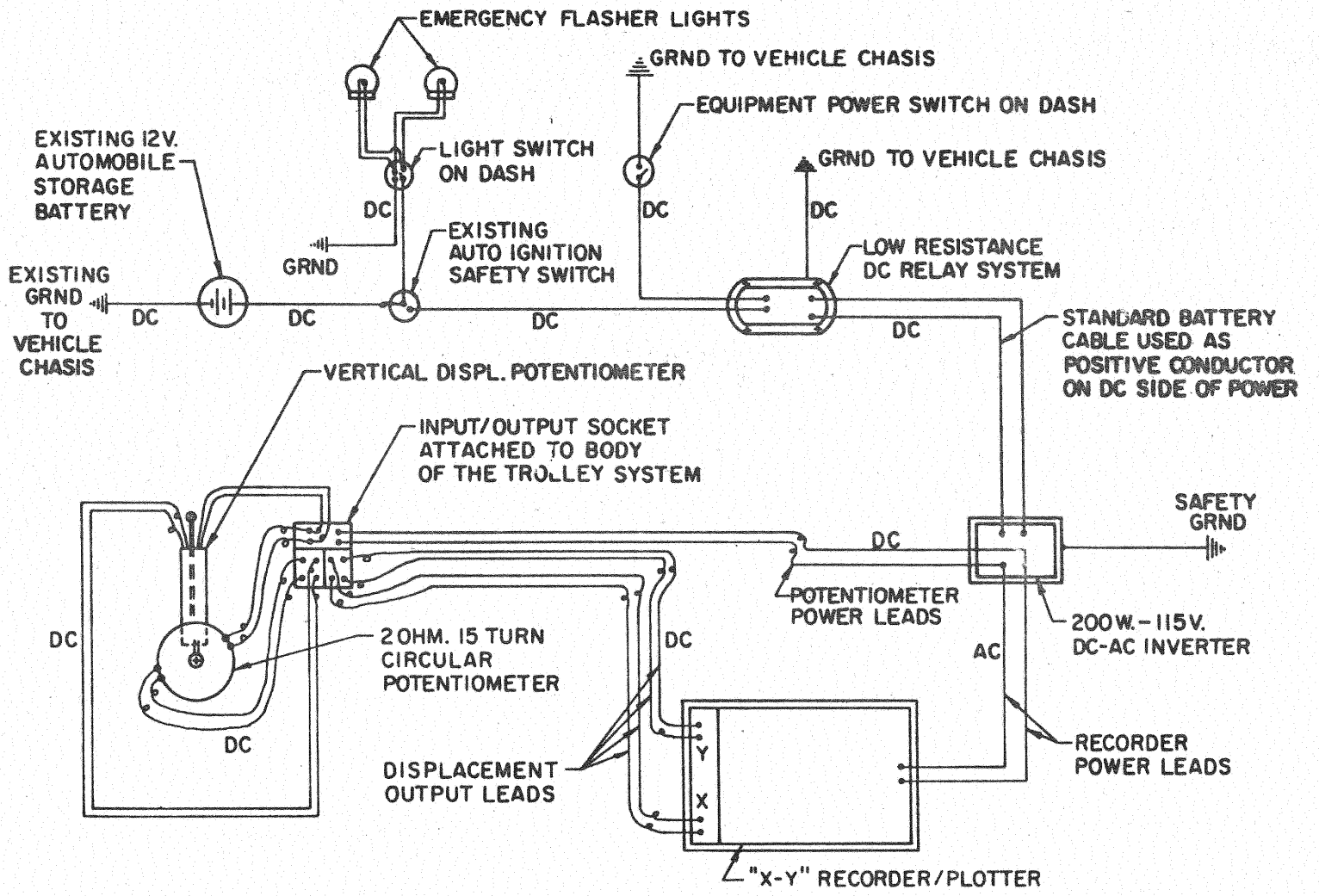

Figure 12. Electrical Installation Diagram

current from the storage battery. Both the input to and the output from the potentiometers were passed through a socket unit which was attached to the trolley system. In this fashion, the number and lengths of the electrical leads could be minimized. These power leads and the displacement output leads from the potentiometers to the "X-Y" recorder were taped together into a single 6-wire conductor cable.

The negative to ground (vehicle chasis) system of electrical installation was adopted. The equipment power switch, attached to the dash of the pickup, was installed on the electrically negative conductor. The low resistance electrical power relay switch system was installed on the positive conductor to serve as a circuit breaker, i.e., electrical current from the storage battery would flow through the installation system only when the equipment power switch was turned to the "ON" position. If the positive conductor had been directly connected to the storage battery, the electrical circuit would be complete whenever the bare end of the positive conductor contacted any metallic part (body) of the vehicle, a condition that would create a serious fire hazard. A second safety provision was built into the system by passing the positive conductor cable through the vehicle's ignition safety switch system. A third safety provision consisted of grounding the inverter to take care of probable stagnant electrical power in this unit.

Fig. 12 also shows the electrical circuit diagram employed to power the emergency flasher lights. These dome type flasher units with magnetic bases were placed on the cab of the pickup to provide additional warning to on-coming vehicular traffic of the restrictions created by the study operations on the highway.

Calibration of the Transverse Profile Gage

Trolley Unit

The first tests made on the performance of the profile gage were those involving linearity and reproducibility of results. A parking lot on the campus of Oklahoma State University which had some rutted areas was selected for the preliminary testing. A section of this parking lot was blocked to traffic and the profile gage was set up in this location.

Initially, a plot of the pavement surface was made so that the surface characteristics could be studied and the suitability of the location for calibration purposes evaluated. A fine chalk line was then drawn along the path of the gage's actuating wheel. Using a steel tape, distances of 1, 3, 6, 9, and 11 feet (0.30, 0.91, 1.83, 2.74, and 3.35 m.) were measured from the starting point and marked off along the chalk line on the pavement. A trial scale was selected on the "X-Y" recording equipment. The trolley unit was then reeled along the measured path. The recorded distances were compared with the measured distances traversed. This process was repeated numerous times using different recorder scales. A high degree of accuracy and reproducibility of the profile tracings was observed in these trials. Subsequently, a horizontal scale of 0.5 volts/in. was selected as the most convenient and practical for field work and a calibration factor was determined for this scale setting.

From the initial plot of the surface profile of the parking lot area, a relatively level section along the path of the profile gage was selected on the plot and the corresponding location on the pavement surface was identified by moving the actuating wheel back and forth until the position of the plotter pen coincided with the midpoint of the selected section.

A 0.13 in. (0.33 cm.) thick plexiglass plate 2.5 in. (6.35 cm.) wide and 6.0 in. (15.24 cm.) long was taped to the pavement surface at this point with masking tape. A vertical scale of 0.5 volt/in. on the recording equipment was selected, the actuating wheel was reeled slowly over the plexiglass plate and the profile of this surface obstruction plotted. This procedure was repeated using other plotter scales of 1.0, 2.0, 5.0, and 10.0 volt/in. and for plate thicknesses of 0.25, 0.375, 0.5, 0.75, and 1.0 in. (0.64, 0.95, 1.27, 1.91, and 2.54 cm.). Comparison of the plotted heights of these calibration plates on the various profile traces showed that the gage was capable of accurately reproducing vertical deviations within this range. Convenient recorder scales of 0.5 and 1.0 volt/in. were selected for field usage and calibration factors for these settings were determined.

Cross-Slope Device

The specified procedure for measurement of cross-slope was followed by three operators at various locations in the parking lot area. Each operator recorded the observed average gradient of a location without moving the supports of the straight edge. Typical results were as follows:

Operator No.	Observed Gradient in/ft.	Average of Obsns. in/ft.
1	0.0028	
2	0.0026	0.0027
3	0.0029	

While the observed cross-slope values varied slightly from one operator to the other, the data shows that the observed gradients were within

reasonable tolerances. Subsequent calibration checks showed similar reproducibilities and excellent agreement with the measured cross-slopes.

Laboratory Calibration

To check for any adverse effects of wind and temperature variations on the profile gage the calibration processes described above were repeated in the Asphalt Laboratory of the School of Civil Engineering. In the laboratory, the air was relatively still and the room temperature was held approximately constant at $77^{o}F$ ($25^{o}C$).

New calibration data was obtained and compared with the previous field calibration data. Good agreement between the two sets of data was observed, i.e., there was very little, if any, variance in the performance of the profile gage for the conditions under which the two sets of the calibration data were obtained. The profile gage was subsequently considered acceptable for the purposes for which it was designed.

CHAPTER V

TEST PROCEDURES

This research investigation can be divided into two parts or phases relative to the procedures employed in collecting data and core samples at the field test sites and those used in the laboratory to analyze the pavement materials and stereo-photographs.

Field Testing

Safety

Safety of research personnel on the highway was a deciding factor in the design of the field operations. All field work was terminated or cancelled whenever there was any form of precipitation at the test site. Similarly no work was carried out whenever visibility was poor or whenever traffic volumes became larger than a single traffic lane could handle. While these actions were expensive in terms of both time and money, they were considered necessary to minimize the danger of traffic accidents.

Workmen, research equipment and highspeed traffic do not operate too well together on an interstate highway without some means of separation. To avoid any unfortunate accident, one lane of the highway was kept open to traffic while the other was blocked for field tests. Each field test site was preceded by appropriate advance signing to warn the motorist at

least 880 yards (800 meters) from the work area. This was followed by directional signals, a flagman and finally a physical barrier to block the lane undergoing field tests to vehicular traffic. The directional markers and barriers were then switched to allow work in the other lane. All signing, signalling, blocking, and flagging were done by personnel from Research and Development, and other respective Divisions of the Oklahoma Department of Highways.

Setting Up the Profile Equipment

Having blocked the test lane to all vehicular traffic, a chalk line was used to mark the pavement surface perpendicular to the center line. Two bottle caps were nailed to the pavement surface to mark the ends of this transverse line at the shoulder and the centerline of the pavement.

The straight edge (gage rail) was then set up, as described previously, directly over the chalk line by shifting the end supports laterally. The trolley unit was moved to one end of the straight edge (a bottle cap point) and the height of the support at this end was adjusted so that the vertical potentiometer shaft was positioned at the midpoint of its effective travel distance. The trolley unit was then moved to the other end and the height adjusting process was repeated. This assured that the two ends of the gage rail were the same height above the pavement surface.

A string line was stretched along the top surface of the gage rail between the end support points. The height of the rail at the middle support point was then adjusted until the top surface of the rail just touched the string line. Adjustment of the middle support was also made for the lateral alinement or straightness of the rail. In this way, the top surface of the straight edge was set parallel to an imaginary line

joining the bottle cap points at the edges of the pavement lane. This imaginary line was considered as the datum for subsequent profile measurements.

Profile Tracings

After making the appropriate output and input power connections, the helical potentiometer was set to zero by moving the trolley unit to its starting position at one end of the straight edge. The trolley unit was reeled from this point to the other end of the straight edge and the resulting linear and vertical displacements were recorded on a standard 8.5 in. (21.59 cm.) x 11.0 in. (27.94 cm.) graph paper by the "X-Y" recorder. This was in the form of a continuous plot on the graph paper and this tracing indicated the transverse profile of the pavement surface (at a selected recorder scale) along the path of the actuating wheel.

Location of Wheelpaths

If rutting has occurred on a bituminous highway pavement, then the most frequently traveled pavement surfaces, i.e., those areas receiving the greatest number of wheel-load coverages, will show a concave profile. The relatively less traveled surfaces, on the other hand, will remain practically unchanged from the original profile or will possibly show some convexity. On medium to heavily rutted pavements, therefore, the points where the surface profile changes direction (a maximum or minimum point on the plot) will very closely define the location of the center of the wheelpaths and the approximate midpoint of the distance between the wheelpaths, respectively.

The following procedure was used to locate the vehicle wheelpaths and the approximate midpoint of the wheelpaths on the pavement surface. After obtaining an accurate plot of the transverse profile of the pavement surface, points of maximum depression and points of maximum upheaval as indicated where the surface profile significantly changed direction were marked on the plotted profile. The actuating wheel of the trolley unit was wheeled back and forth on the pavement surface until the position of the plotter pen coincided with one of the identified points on the profile tracing. The corresponding point on the pavement surface was then marked. This process was repeated until all the required points (center of wheelpaths and midpoint of the distance between wheelpaths) were identified on the pavement surface. Five points per traffic lane were selected along the profile line for further tests. These points are shown in Fig. 7.

Profile Measurements

Lack of an original profile of the pavement surface at a test site made it rather difficult to determine the total deformation the surface had undergone since the roadway was opened to vehicular traffic. For this reason, the observed profile measurements were considered as approximate values of the variables whose magnitude were being measured, and were based on measurements from defined datums. Rut depth was measured as the maximum vertical displacement of the surface in the wheelpath from a straight line whose ends formed tangents to the transverse profile curve at the adjacent points of maximum elevation. All rut depth measurements were scaled directly from the profile tracings and recorded in inches.

Upheaval of the pavement surfaces immediately outside the wheelpaths is an indication of lateral creep of material from beneath the wheelpaths. It was known from design records that the surface of the pavements at the study sites had been designed to have a uniform cross-slope for the lanes in a given traffic direction. Since an original transverse profile of the pavement surfaces was not available, a straight line joining the end support points of the straight edge was assumed to be the original surface. Based on this assumption, upward displacements of the pavement surface above this base line were scaled directly from the profile tracings. The maximum upward displacement measured in the manner was considered as the probable heave resulting from lateral creep. Very small displacements could be measured and these measurements were recorded in inches.

Measurement of Cross-Slope

The cross-slope device was attached to the straight edge and connected to the indicator dial gage. With the device lying flat on the top surface of the straight edge, the dial gage was set to zero. The free end of the cross-slope device was then raised vertically until the bubble in the torpedo level moved into a level position. The observed gage reading was recorded as the average cross-slope (in inches per foot) of the pavement surface.

Stereo-Photos

An offset line, parallel to and 12.0 in. (30.48 cm.) from the profile line in the direction of traffic, was marked on the pavement. The selected test points on the profile line were laterally transferred to this

offset line. Stereo-photographs of the pavement surface were then taken at these points. The stereo-photo box described by Schonfeld (31), a 35 mm. Kodak Retina IV single reflex camera, and an automatic 80 shot electronic flash accessory were used to make these photographs. Interpretation of these photographs is described later under Laboratory Testing

Nuclear Density Measurements

A Troxler Series 2400 Compac Surface Density/Moisture Gage was used to obtain the nuclear density measurements. Following both the manufacturer's Instruction Manual (17) and the ASTM Method of Test D-2950 (16), a standard count for the nuclear gage was taken in the morning and at noon of each day of operation. Prior to each standard count, a series of tests were made to check for drift and malfunction. Tests for reproducibility of results were also conducted at each test point to make sure the recorded density counts were representative for the pavement materials beneath the respective test points. Using the backscatter method of test, density counts were obtained for each of the previously selected test points. These counts were later converted to density units (pounds per cubic foot) using the manufacturer's calibration data.

Surface Condition Rating

A surface condition evaluation was included in this investigation to establish, in terms of a suitable qualitative index, the overall condition of the pavement surface at the test locations. The surface condition rating format suggested by Winnitoy (38) was modified to include the following conditions:

1. General structural condition,

2. Degree of weathering,
3. Uniformity,
4. Crack condition, and
5. Surface wear/excess asphalt.

Each of these conditions was rated in terms of serviceability indices ranging from 1.0 to 5.0. A typical rating form is shown in Fig. 13.

Core Drill Operations

The core drill equipment and personnel were provided by the Research and Development Division of the Oklahoma Department of Highways. Using a 4.0 in. (10.16 cm.) diameter core drill, the angular speed and the rate of penetration were regulated to obtain core specimens with minimum possible disturbance of the material layers. Full thickness cores, ranging from 6.0 in. (15.24 cm.) to 14.0 in. (35.56 cm.) of the asphalt bound pavement materials, were cut at the ten selected test points along the previously described offset line. These cores were cut at the same points where the nuclear density measurements were obtained. Each core specimen was immediately identified, wrapped in plastic bags, and stored in a heat insulated container. Individual core specimens in the container were separated from each other with layers of sponge rubber before transporting them from the site to the laboratory for further tests.

Laboratory Testing

Cutting Core Specimen

Each pavement core was cut into five subdivisions with a diamond edged concrete saw. The subdivisions included the surface course, leveling course, and top third, middle third, and bottom third of the base

SURFACE CONDITION RATING

Rated by _____ Date _____ Base Course type _____

Site Description _____ Age of pavement (months) _____

Rated for (Job) _____ Pavement on: cut / fill / Nat. grade

Rating Code	Gen. Str. Condition	Surf. wear Excess Asphalt	Weathering	Uniformity	Crack Condition			Remarks
					Opening	Abrasion	Multiple	
5	--Good	--None	--None	--Good	--Hairline	--None	--None	
	-	-	-	-	-	-	-	
	-	-	-	-	-	-	-	
	-	-	-	-	1/16	-	-	
	-	-	-	-	-	-	-	
4	--Long. crk	--Slight	--slight	--Streaked	--	--Slight	--Slight	
	-	-	-	-	-	-	-	
	-	-	-	-	1/8	-	-	
	-	-	-	-	-	-	-	
	-	-	-	-	-	-	-	
3	--Map crk	--Moderate	--Moderate	--Crk.-filling	--	--Moderate	--Moderate	
	-	-	-	-	-	-	-	
	-	-	-	-	1/4	-	-	
	-	-	-	-	-	-	-	
	-	-	-	-	-	-	-	
2	--Allig.crk	--Severe	--Severe	--Blotchy	--	--Severe	--Severe	
	-	-	-	-	-	-	-	
	-	-	-	-	1/2	-	-	
	-	-	-	-	-	-	-	
	-	-	-	-	-	-	-	
1	--Erosion	--Abrasion /bleeding	--Erosion	--None uniform	-- greater than 1/2	--Abrasion	--Erosion	

Figure 13. Surface Condition Rating Form

course materials. Only the asphalt bound pavement materials were included in these subdivisions. The average thicknesses of the individual subdivisions were measured, recorded, and then marked on the cores before sawing. Separation of the core into layers was done so that the specific gravities of individual layers could be compared and differences in densities detected.

Bulk Specific Gravity

The extent of water absorption of the core samples during specific gravity determinations was evaluated by comparing the results of two series of tests. In one series, the bulk specific gravities of five samples, comprising the subdivisions from one core specimen cut from a pavement constructed on Black Base (BB) material, were determined by weighing the sample in air then weighing it in water and computing its bulk specific gravity.

The five samples were then allowed to dry at room temperature, 77°F (25°C), and their specific gravities were remeasured with the samples coated with paraffin. Comparison of the results from the two series of tests on the same samples showed large differences. The observed specific gravities of the uncoated samples were much larger than the specific gravities of the same samples coated with paraffin. It was concluded that the extent of water absorption of the field core samples were high enough to appreciably affect their observed bulk specific gravity values. Based on this finding, it was decided that all the core samples be tested for bulk specific gravity using ASTM method of test D-1188 (5).

Rice's Specific Gravity

The ASTM method of test D-2041 (36), for the determination of the maximum theoretical specific gravity (Rice's vacuum saturation method) was slightly modified so existing equipment in the O.S.U. Civil Engineering Asphalt Laboratory could be used. The following modifications were made:

1) Container: a 0.5 gallon (1.8925 liter) Mason fruit jar with rubber gasket, conical cap with #40 U.S. standard mesh strainer, and a hose connection was used instead of the suggested 1000 ml. volumetric flask. Each jar was calibrated prior to use.

2) Vacuum Pump: a Nelson vacuum pump capable of holding 30 psi (2.11 kg/sq. cm.) vacuum pressure was used to evacuate the entrapped air. The specimen was subjected to full vacuum for 15 minutes.

3) Preparation of Test Samples: the core sample used in the bulk specific gravity test was heated in a temperature controlled oven until the asphalt in the sample attained a fluid consistency. A spatula was used to separate the coarse aggregate particles from the matrix material. Lumps of the finer material were also broken down into as small a size as possible with the spatula. The separated mixture was allowed to cool to room temperature and thoroughly stirred during cooling to prevent the particles from caking together. Where the volume of a core sample was significantly larger than was specified, the standard "quartering" method of sampling was employed to reduce the volume of the separated sample to the proper size.

4) Wetting Agent: to facilitate release of entrapped air, Calgon was added to the deaired-distilled water used in the test.

Percent Density

The percent density values for the individual test samples were calculated using the relationship:

$$\text{Percent Density} = \frac{\text{Bulk Specific Gravity}}{\text{Rice's Specific Gravity}} \times 100$$

The percent density values, expressed as a percentage of the maximum theoretical specific gravity (voidless mix), were used to determine the volume of voids in the sample as follows:

$$\text{Percent Air Voids} = (100 - \text{Percent Density Value})$$

Comparison of the percent density values for the core samples at the individual test points on a test site were made and significant differences in these percent density values were assumed to be a result of densification under traffic loads.

Stereo-Photo Interpretation

In surface mixtures incorporating non-polishing aggregates, only the fine materials and the asphaltic binder tend to wear or abrade under traffic. This leaves the larger aggregate particles projecting above the partially worn background fines in the form of angular to sub-angular shapes, depending on the polish-resistant characteristics of the material. In the case of mixtures made with polishing aggregates, both the surface aggregates and the background fines tend to wear under traffic at different rates, depending on the relative wear-resistance of the surface materials. In either case, the amount of wear due to traffic action

is greater on heavily traveled surfaces (wheelpaths) than on less frequented surfaces (surfaces other than wheelpaths).

Based on this discussion, the projection of the coarser aggregate particles at the pavement surface should be relatively higher in the wheelpaths than outside the wheelpaths. This assumes that the background fines do not wear to an extent that would permit the dislodging of the surface aggregates, that raveling due to stripping of the asphalt binder from the aggregates does not occur, and that bleeding of excess asphalt onto the surface does not take place. If these assumptions are reasonable, comparison of the projections of surface aggregates in the wheelpaths to those outside the wheelpaths should give a reasonably good estimate of the differential wear that has occurred.

To obtain estimates of these projections, the stereo-slide pairs were viewed under a telescopic lens with six power magnification on a flourescent light desk. By comparing the heights of projections with that of a calibrated wedge scale placed on the pavement at the time the photographs were taken, estimates of maximum projections were recorded in terms of the calibrated scale. These scale values were later converted to inches by means of a calibration curve.

Other surface characteristics were observed during the microscopic study. These included the degree of polishing of the surface aggregate, geometry of projections, raveling, bleeding, fracture of surface aggregates, cracking, and erosion of the surface. This supplementary information aided the evaluation of the general condition of the pavement surface at the individual test points at a site.

CHAPTER VI

TEST RESULTS AND DISCUSSION

Density Measurements

If the initial percent density values of the individual core subdivisions, i.e., the pavement layers, were known, then comparison with the test values would indicate any changes in density caused by traffic compaction. The contribution to rutting of these changes could then be estimated, using the procedure discussed earlier. Since the initial values were unknown, classical statistical methods were employed to test for differences in the observed percent density values. Significant point differences were considered as changes resulting from traffic action.

Tests for evidence of differences were conducted for each test site using the Statistical Analysis System (SAS) standard computer program (2). A flow diagram for this program is presented in Appendix C. The results of these tests indicated the Observed Significance Level (10) and acceptance or rejection of the null-hypothesis (no differences) depended on choice of a significance level. Choice of this significance level depends on several factors including: 1) expected variability in the initial values, 2) degree of certainty or accuracy required, 3) accuracy of test results and, 4) consistency with which the tests were conducted. For this study, a value of 0.1 was considered as the significance criterion for the rejection or acceptance of the hypothesis of

no differences. The results of the computer analysis for the individual test sites are discussed in the following paragraphs under the four types of base course materials. Information on the individual test sites is presented in Appendix A.

HMSA Base

All four test sites on this base material showed strong evidence of layer differences in the percent density values. The observed significance level was 0.0001 in each case. The percent density values of the surface materials (surface and leveling courses) were essentially within the specified limits for these materials and ranged from a high value of 99 percent to a low value of 82 percent. The percent density values of the HMSA base course materials contributed a greater portion of the observed variability and ranged from a high value of 93 percent to a low value of 77 percent.

The computer analysis did not show much evidence of point differences in the percent density values for test site 10. The observed significance level was 0.2465. However, a plot of percent density values versus transverse location of test points indicated peak values occuring at the wheelpath locations (Fig. 14) for both the surface and the base course materials and is an indication of some differential densification (wheelpath versus outside wheelpaths) at these locations. (Note that the base course plots on this and the following figures are the average of the values for the top, middle and bottom thirds of the base layer.) For the surface materials the maximum values occurred at test points #2 and #7, which are the respective transverse locations of the outer wheelpaths in the outer and the inner traffic lanes. For the base course materials, the maximum values occurred at test points #2 and #9, the outer and

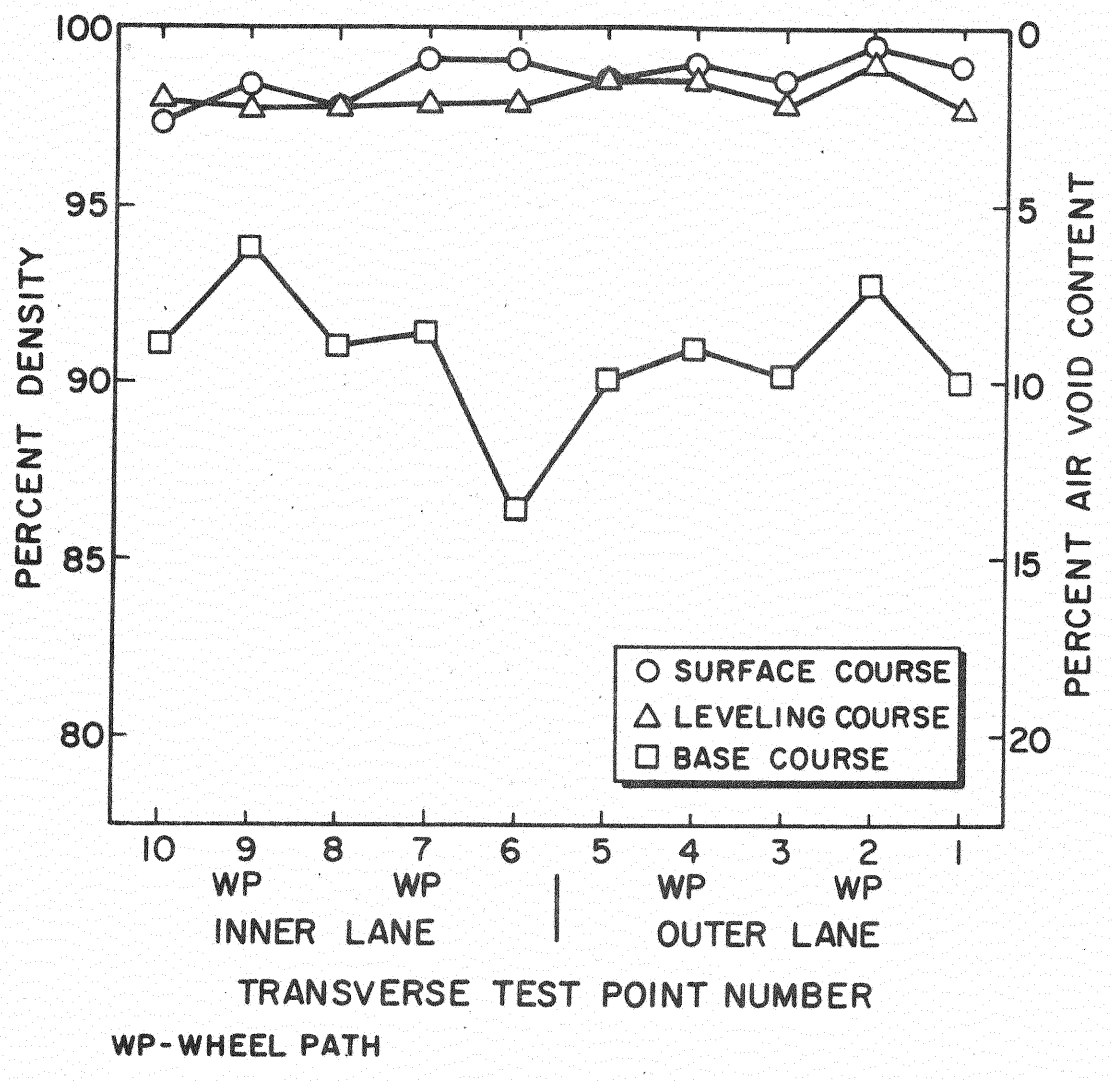

Figure 14. Percent Density Versus Transverse Test Point Site #10, Base Type--HMSA

the inner wheelpath locations in the outer and the inner traffic lanes, respectively.

The Analysis of Variance (AOV) for test site 60 indicated strong evidence of point differences in the percent density values. The observed Significance Level was 0.0001. A plot of percent density versus transverse test point (Fig. 15) associated the peak values with wheelpath locations. For the surface course, differential densification is indicated at test points #2 and #4, with a maximum value of 3.6 density units occurring at point #2. Extremely low density values in the leveling course at test points #7 and #8 correspond to low values in the base material at these locations. The density of the base course material was uniformly low, averaging approximately 78% across the full pavement width.

At test site 70, the AOV indicated strong evidence of both layer and point differences. The curves show consistent differential densification in the surface course material at the wheelpath locations (Fig. 16). In the inner traffic lane, a differential value of 2.3 percent density units was recorded at test points #7 and #9. For the outer traffic lane, the maximum differential densification was 4.0 percent density units and occurred at the outer wheelpath location. The percent density values for the leveling course materials were consistently high and uniform across the pavement and were greater than the surface course at all but three points. A differential densification of 1.6 units can be observed at test point #2. At the inner wheelpath location (outer lane), however, both the surface course and the base course materials showed similar differential densification and these were 2.8 and 3.4 percent density units respectively.

The percent density curves for test site 120 (Fig.17) were similar to those of test site #70. Major differential densification occurred in

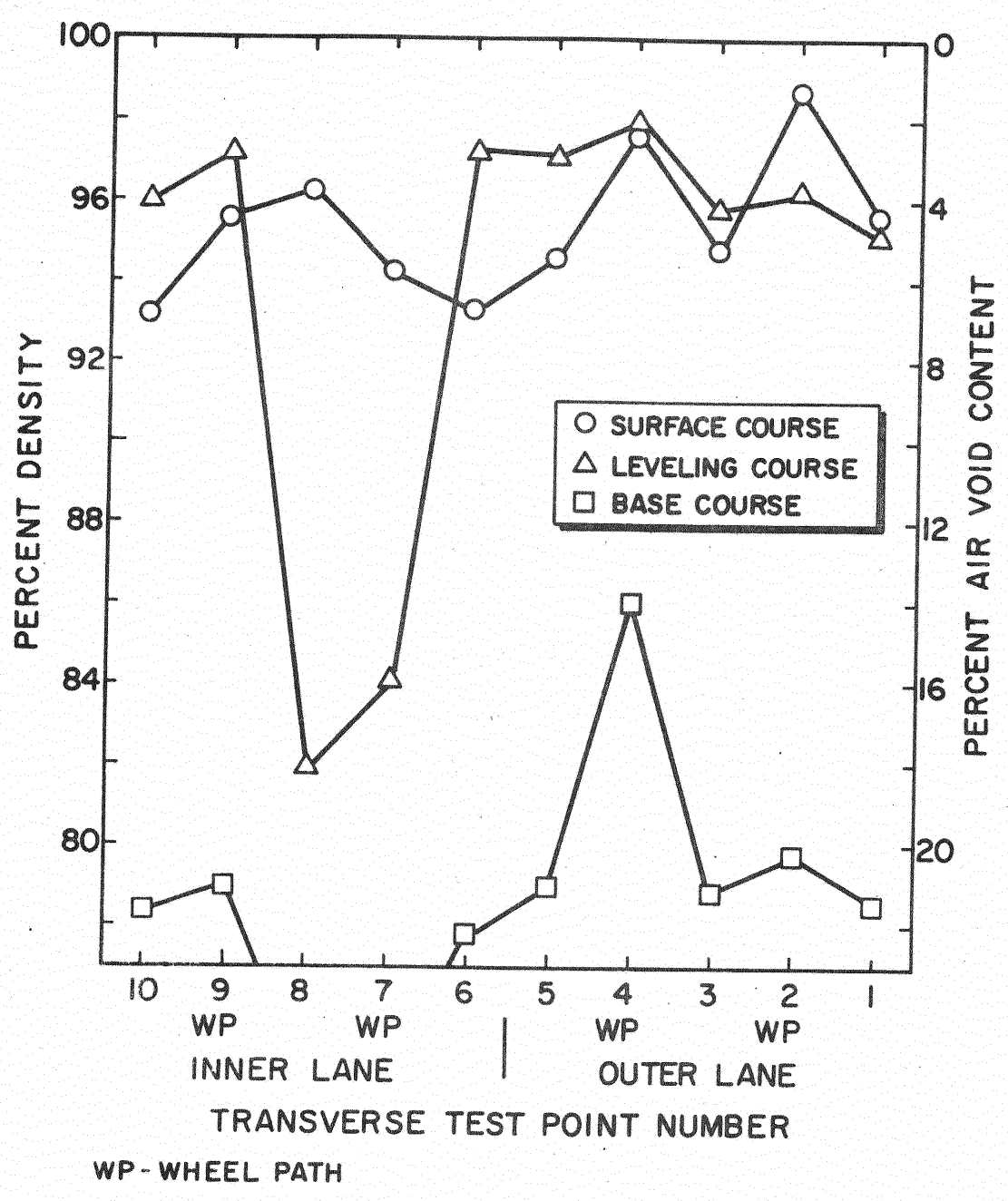

Figure 15. Percent Density Versus Transverse Test Point Site #60, Base Type--HMSA

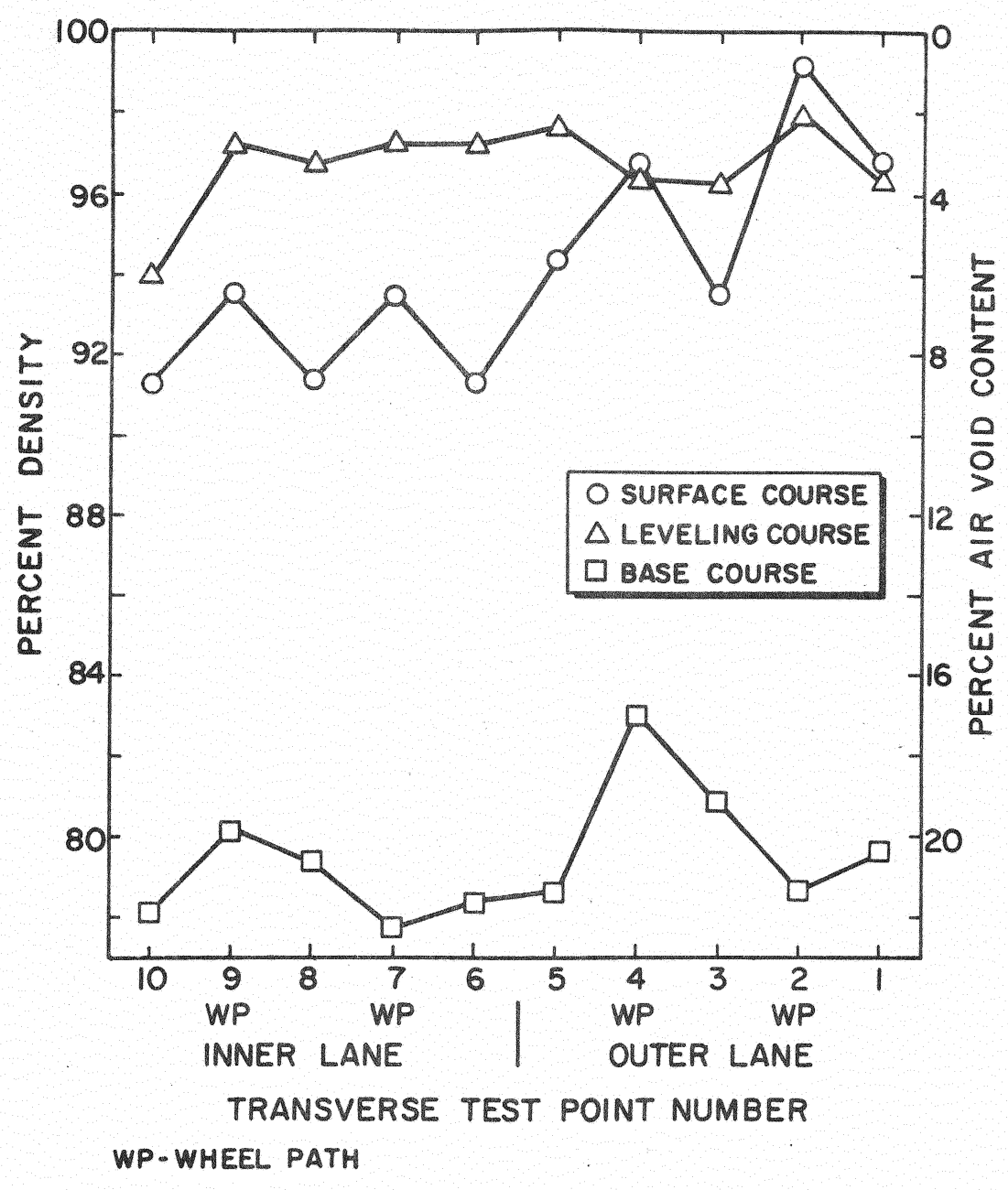

Figure 16. Percent Density Versus Transverse Test Point Site #70, Base Type--HMSA

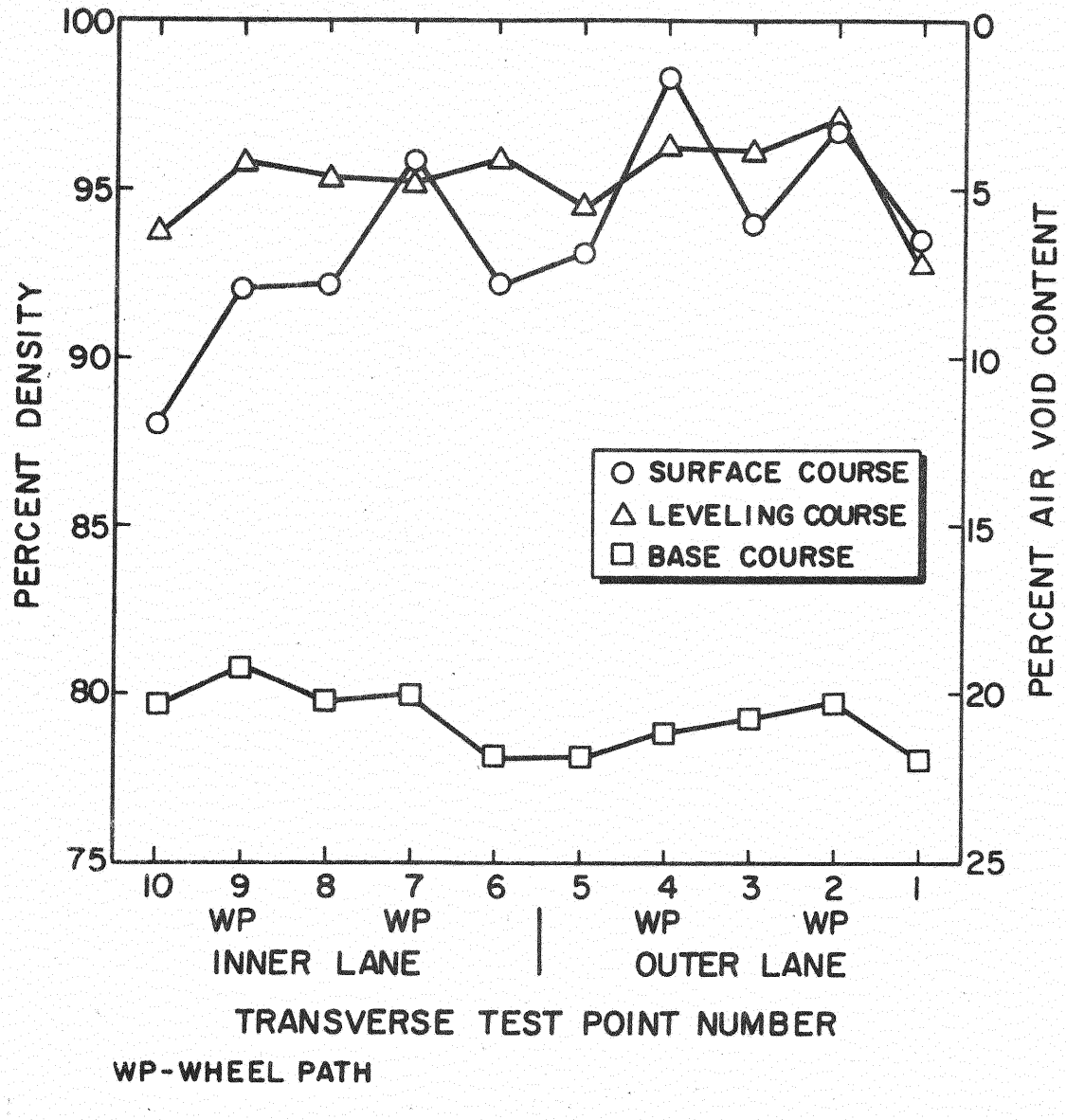

Figure 17. Percent Density Versus Transverse Test Point Site #120, Base Type--HMSA

the surface course materials and relatively uniform percent density values in the leveling course material are indicated. While the density of the base course was uniformly low (approximately 80%), there was some evidence of differential densification in the wheelpaths. It is interting that the density of the leveling course layer was frequently greater than the surface layer at test site No's 60, 70, and 120. Conditions such as this were found at nine of the sixteen test sites. This may be the result of inadequate compaction of the surface course material during construction, however, it can also be an indication that a certain amount of decompaction is occurring in the surface layers from the kneading action of vehicle tires. Low density and/or stability in surface course materials results in poor load - distributing characteristics. This causes a higher concentration of traffic stresses on the underlying materials and encourages densification and lateral creep.

Black Base

Like the pavement sections on HMSA base materials, the percent density values of the surface layers on the sections with black base materials were found to be relatively high and ranged from about 90 to 98 percent. However, the densities of the BB materials were consistently higher than those of HMSA. The analysis of variance on the percent density values indicated strong evidence of point differences for all four of the test sites and strong evidence of layer differences for three test sites.

For test site 30, the analysis did not indicate any strong evidence of layer differences. Accordingly, the percent density values of the layers were averaged for each test point on the percent density versus test point curve for this test site (Fig. 18). Two peak values at the outer and the

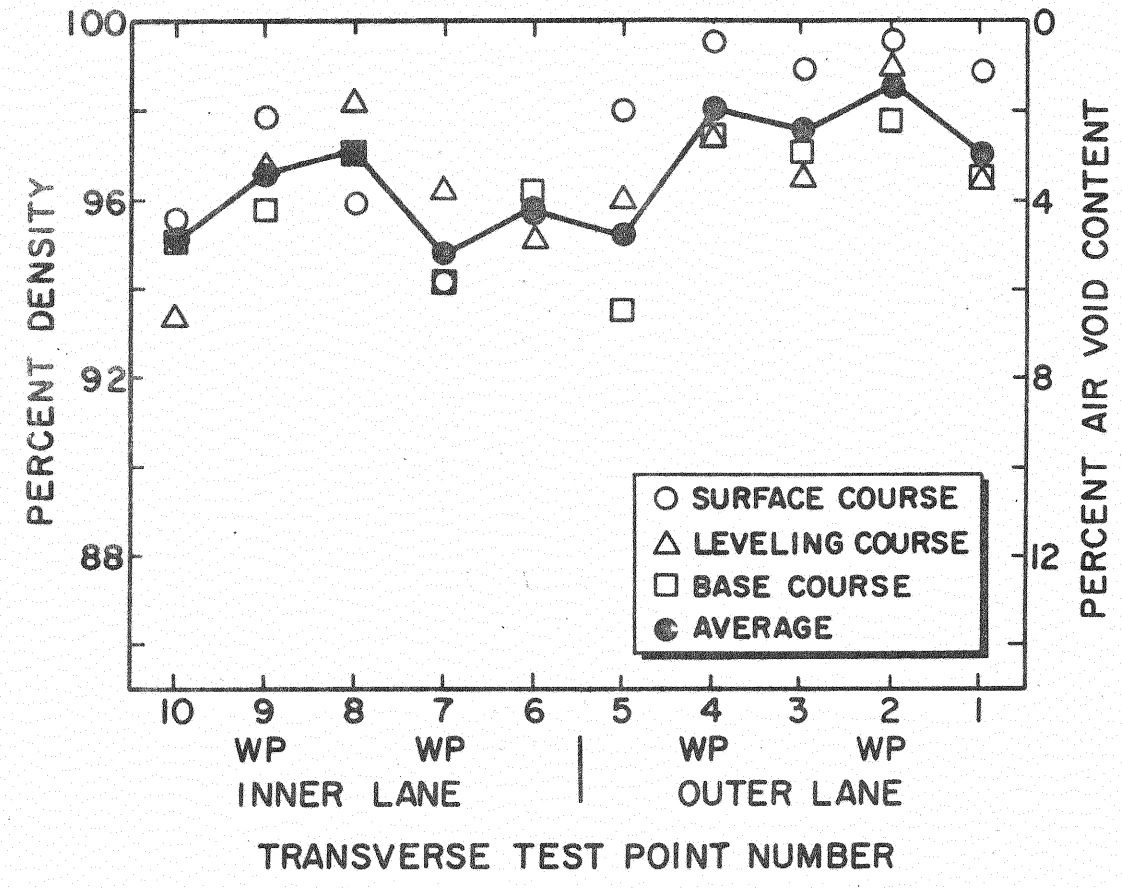

Figure 18. Percent Density Versus Transverse Test Point Site #30, Base Type--BB

inner wheelpath locations in the outer traffic lane can be seen on this plot. The differential densification at these wheelpath locations (test points #2 and #4) was estimated as 1.6 percent density units for each layer. In this case, the AOV showed strong evidence of point differences in the respective layers and this is an indication of differential densification.

In the inner traffic lane, the plotted density values were quite scattered. In fact, the only peak value shown on the curve occurred at a non-wheelpath location. The recorded density values for the materials in this lane were considered inconsistent and this was attributed to experimental error in the density determinations. However, the average density values were lower than in the outer lane, indicating the compactive influence of traffic in the more frequently traveled right hand lane.

The AOV for test site 50 indicated significant layer and point differences in the percent density values. Therefore, separate curves were plotted for each layer (Fig. 19). Although the difference in percent density values was not great from one layer to another, the peak values were generally associated with wheelpath locations. The average density curve for the base course material showed very little change across the roadway. The densities of the respective test samples in this layer ranged from approximately 87 to 91 percent. Maximum differential densification in the surface course was 1.4 percent density units and this occurred at test point #4 in the outer lane. Peak density values in the leveling course are quite distinct in the inner traffic lane. The maximum differential densification in the leveling course occurred at test point #9 and was 2.5 units.

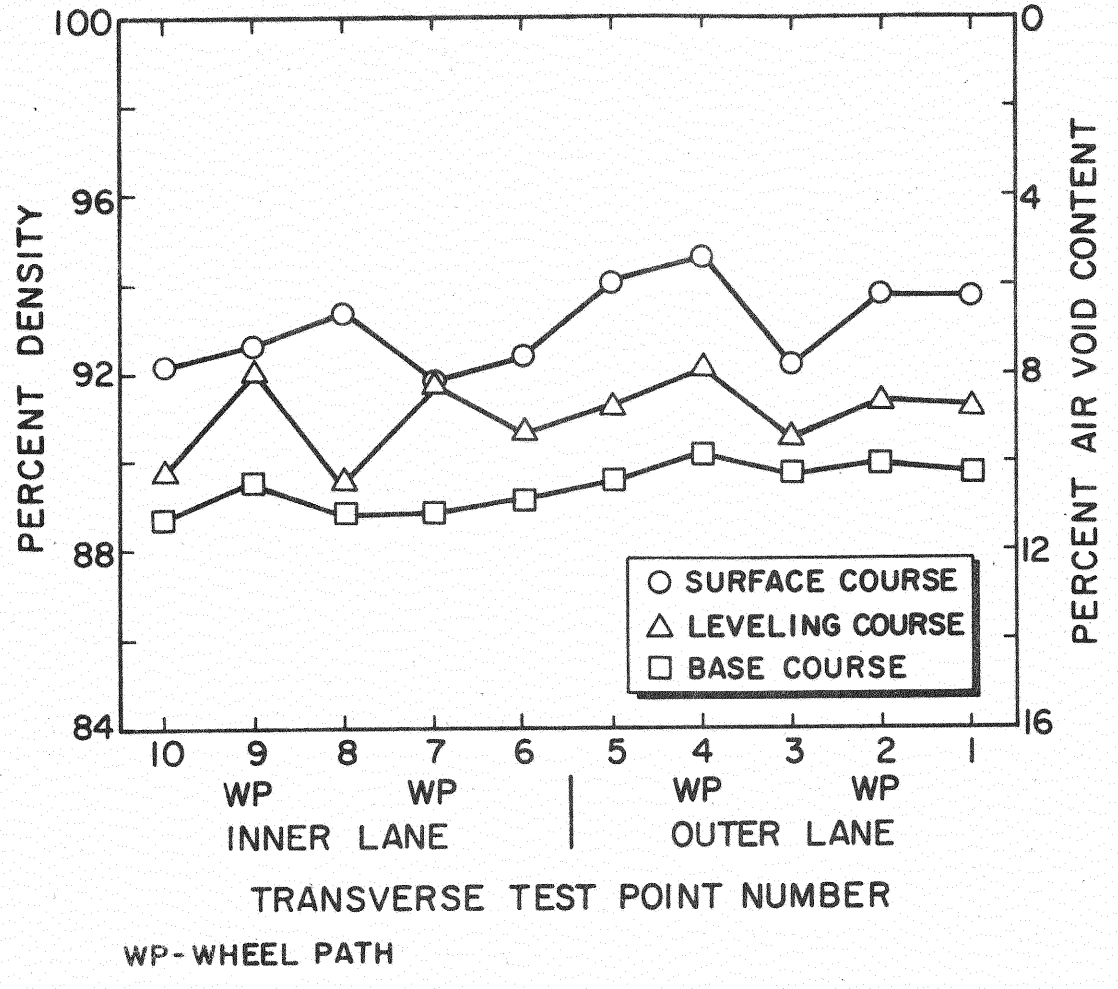

Figure 19. Percent Density Versus Transverse Test Point
Site #50, Base Type--BB

The density curves for test site 20 (Fig. 20) showed higher percent density values in the base course materials than in the leveling course materials at all but two test points. This type of situation should be avoided in pavement construction. That is, a low density layer between two layers of higher density materials will almost certainly result in pavement rutting due to either differential densification and/or lateral creep of material in the sandwiched layer. The curves for the base and leveling courses did not show major peak values, however, the surface course materials, which had relatively high percent density values (98 percent average), exhibited a differential densification of 2.5 percent density units at test point #9. Densification was observed at all four wheelpath locations in the surface layer.

On test site 40, the density curves showed the lowest percent density values in the surface course materials (Fig. 21). A differential densification value of 3.9 percent density units occurred in this layer at test point #4. Some peak density values for the leveling and base course layers were evidenced at wheelpath locations but this tendency was not consistent at this test site. Interestingly, there was a rather substantial difference in density of the leveling course materials in the two traffic lanes. In the outer lane the leveling course materials had percent density values averaging about 98 percent as compared to 94 percent in the inner lane. While this may be an indication of increased compaction in the more heavily traveled outer lane, it is also possible that such a difference existed at the time of construction. The latter possibility is strengthened by the differential densification of 2.2 percent density units in this layer at test point #7.

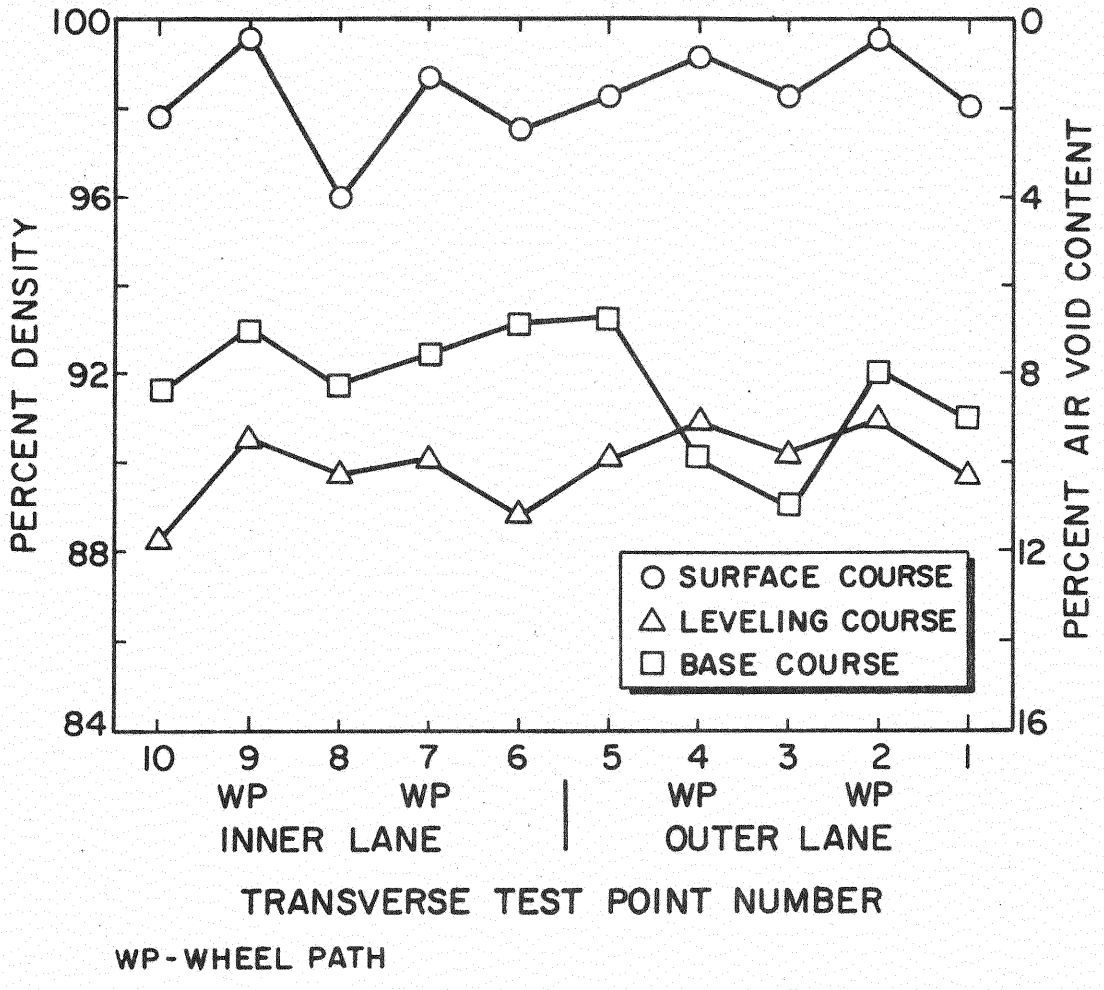

Figure 20. Percent Density Versus Transverse Test Point Site #20, Base Type--BB

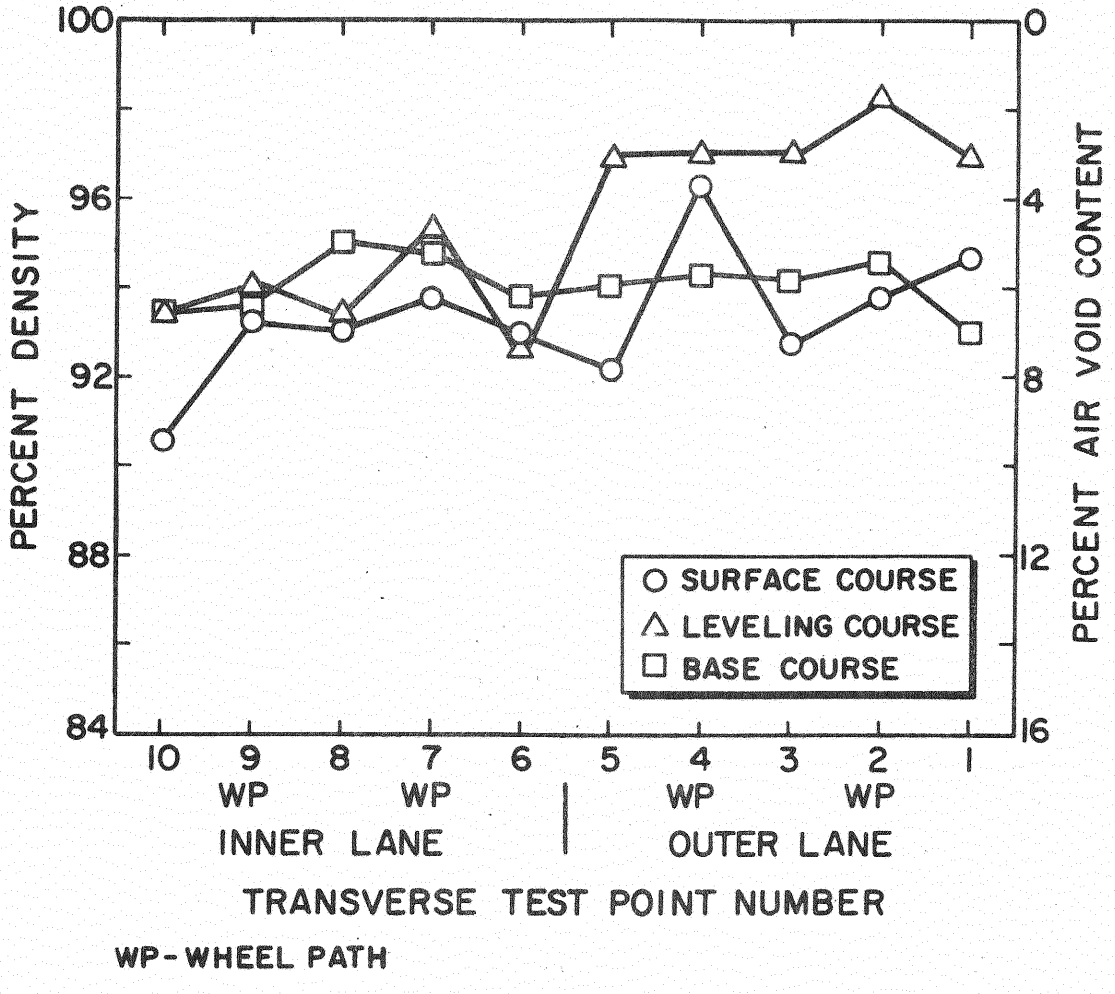

Figure 21. Percent Density Versus Transverse Test Point Site #40, Base Type--BB

SABC Materials

The percent density curves for all the pavement sections utilizing this type of base course material showed peak values in both the surface and the leveling course materials at the wheelpath locations. At three of the pavement test sites, the measured percent density values for the leveling course materials were found to be higher than those of the surface course materials. The AOV on the percent density values indicated strong evidence of point differences for all four test sites and strong evidence of layer differences for three of the test sites.

The AOV did not indicate strong evidence of layer differences for test site 100 and, thus, only an average curve is plotted in Fig. 22. The surface course materials which showed larger values in the outer traffic lane had percent density values lower than those of the leveling course materials in the inner traffic lane. If the initial percent density values were approximately equal in both lanes, then it can be inferred that the change in trend is due to densification of the surface course materials. The initial density in both layers may have been relatively low. According to the density curve, peak values occurred at the four wheelpath locations and a maximum differential densification of 2.1 percent density units occurred at test point #4 compared with 3.7 units at test point #7.

Except at test point #7, the percent density values recorded for the leveling course materials were higher than those of the surface course materials at test site 80 (Fig. 23). Accordingly, large amounts of differential densification were observed at the wheelpath locations in the surface layer. Maximum differential densification values of 4.6 units and 2.5 units occurred at test points #7 and #2 in the surface course material.

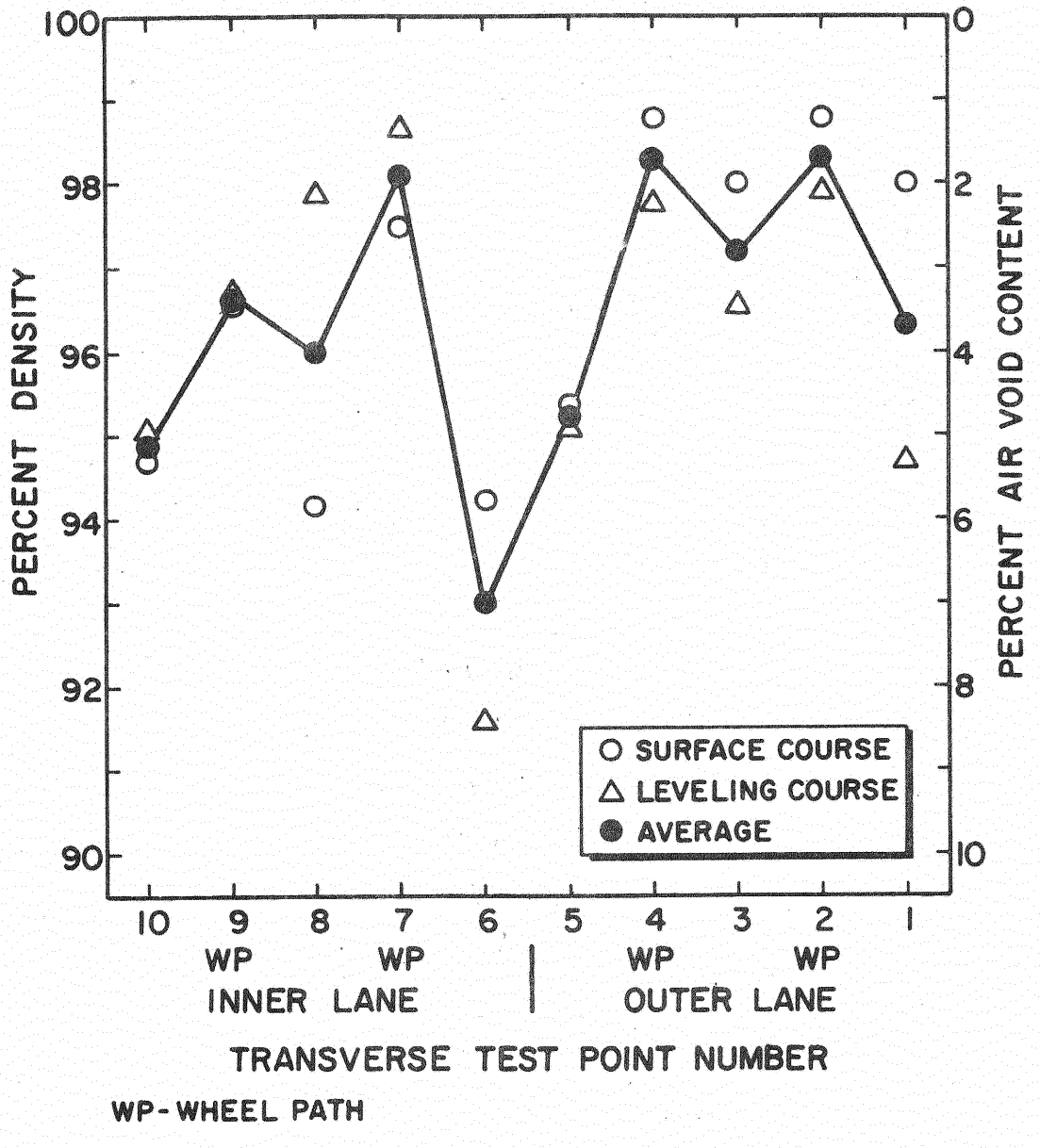

Figure 22. Percent Density Versus Transverse Test Point Site #100, Base Type--SABC

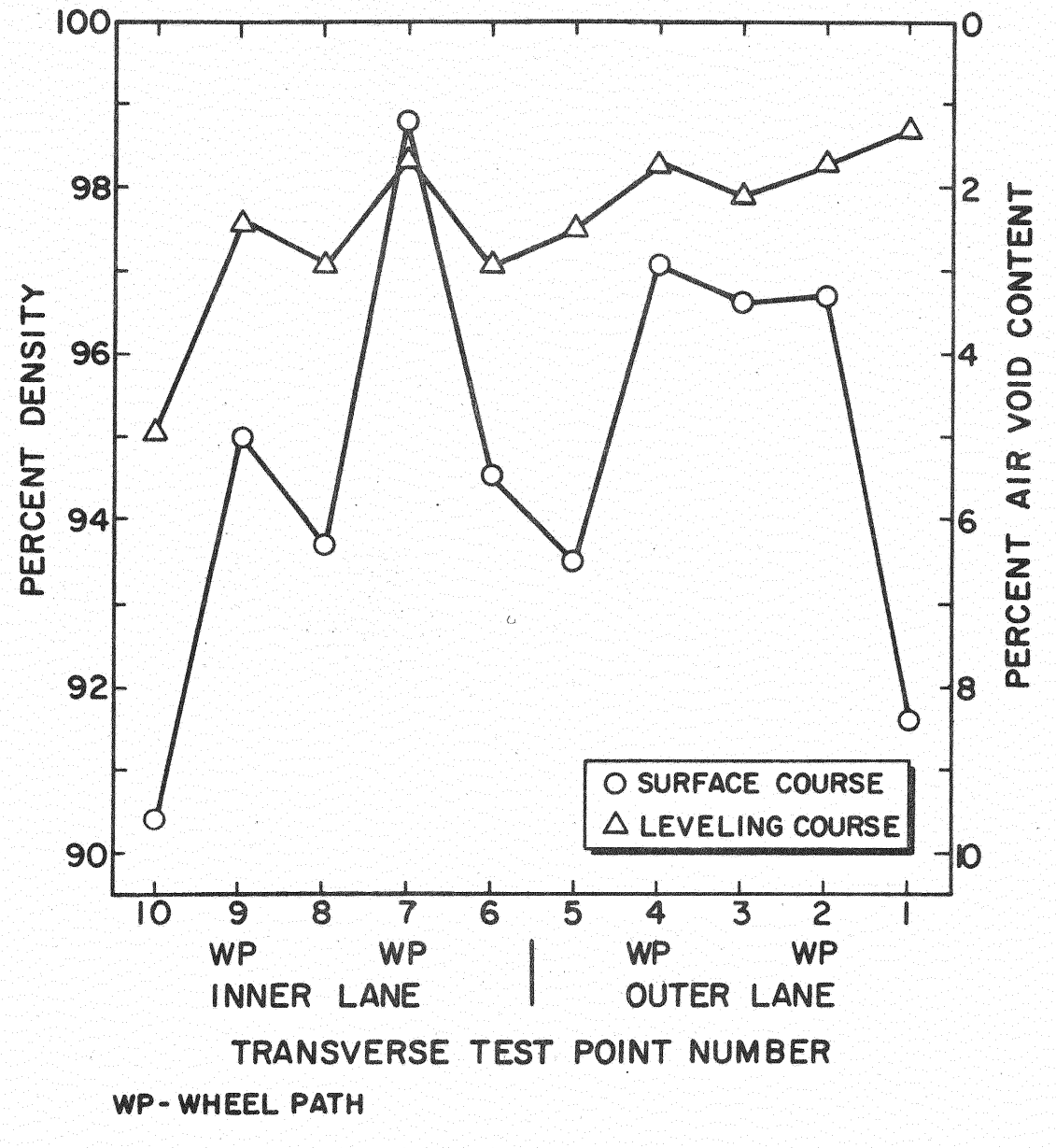

Figure 23. Percent Density Versus Transverse Test Point Site #80, Base Type--SABC

The density values for the leveling course material were relatively uniform in the outer traffic lane but significant densification was evidenced in the inner lane. The maximum differential densification of 1.5 percent density units in this layer was observed at test point #9.

The density curves for test site 90 (Fig. 24) had similar trends, i.e., the surface course materials exhibited lower percent density values than the leveling course, and the curves showed peak values at the wheelpath locations in both layers. Maximum differential densification of 2.1 percent density units was observed at test point #4 in the outer traffic lane. The densities of the materials in both layers in the outer traffic lane were generally higher than those in the inner lane and this is again an indication of the compactive influence of the more frequently applied traffic loads.

For site 110 (Fig.25), the density curves appeared somewhat erratic. The surface layer had higher density values at all the transverse test points except at points #5 and #6. Nevertheless, peak values were observed in both the surface and leveling course materials at the wheelpath locations. The maximum densification in the surface course occurred at test point #7 and was 2.9 percent density units. Densification values at the other wheelpath locations were only slightly lower.

Soil-Cement Base

The percent density curves for the four test sites on soil-cement base course materials (SCB) showed the densities of the surface course to be about the same as those of the leveling course in the outer traffic lane, however, in the inner traffic lane, at three of the sites the densities of the leveling course were considerably higher. Generally, the densities of the respective layers decreased from the outer to the inner

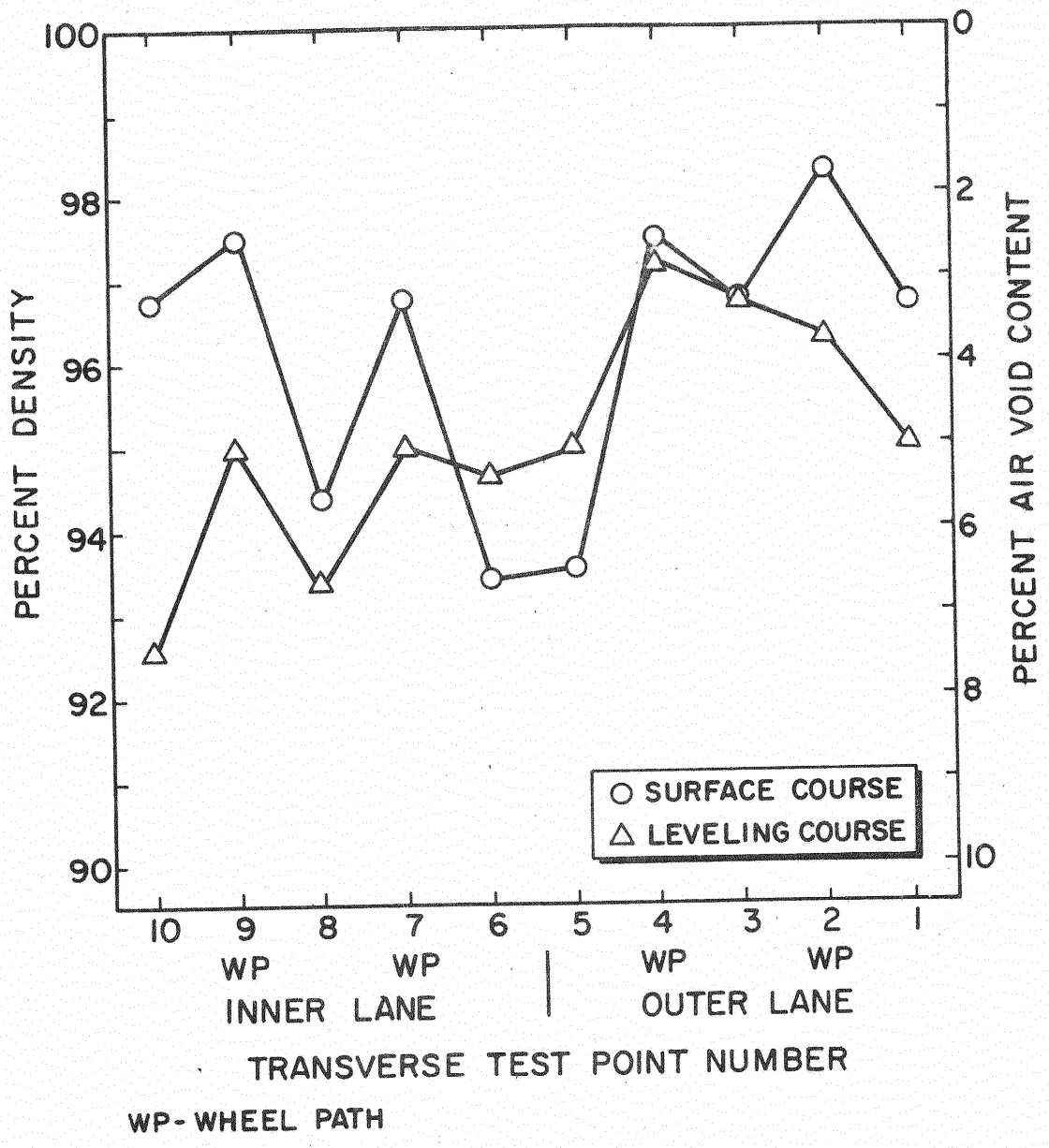

Figure 25. Percent Density Versus Transverse Test Point Site #110, Base Type--SABC

traffic lanes. Since the initial density values of the layers were unknown a good explanation of these conditions was difficult. Considering the rigidity of the soil-cement base and heavier traffic volumes in the outer traffic lanes, however, it might be inferred that this behavior is due to a greater rate of densification in the outer traffic lanes. The rigidity of the base course material may also have facilitated compaction of the leveling course materials to a high density during construction. Assuming that the surface course material had relatively lower initial densities, traffic compaction of this layer could be easily achieved, especially during the early stages of pavement life.

For test site 130, the densities of the surface course material were essentially the same as those of the leveling course in the outer lane and ranged from 96.8 to 97.6 percent (Fig. 26). The maximum differential densification was 1.6 percent density units for the surface layer and this occurred at test point #2. For the leveling course, a densification of 1.4 percent density units was evidenced at test point #4. In the inner lane, the percent density values of the surface course material ranged from 95.5 percent at the outer wheelpath location to 92.7 percent at the shoulder compared with an average value of 97.8 percent for the leveling course material. Generally, the curves showed peak values in both layers at all the wheelpath locations.

The percent density curves for test site 140 (Fig. 27) were similar to those at test site 130. Again, density values of the respective layers were higher in the outer traffic lane and the density curves peaked at the wheelpath locations. The amounts of differential densification were also similar to those observed at test site 130.

For site 170, the AOV did not indicate any strong evidence of layer differences. The average curve indicated peak values at three of the wheel-

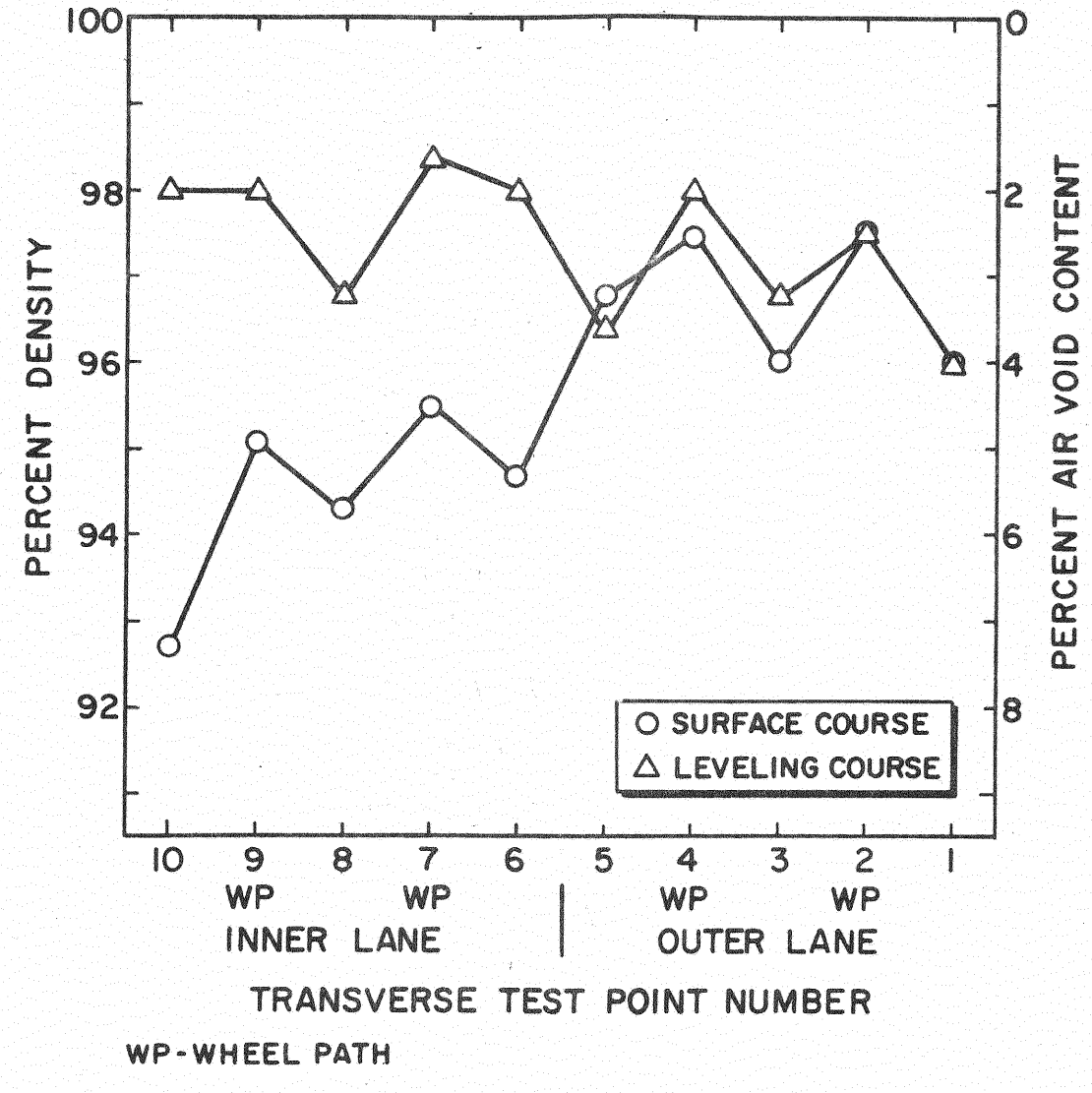

Figure 26. Percent Density Versus Transverse Test Point Site #130, Base Type--SCB

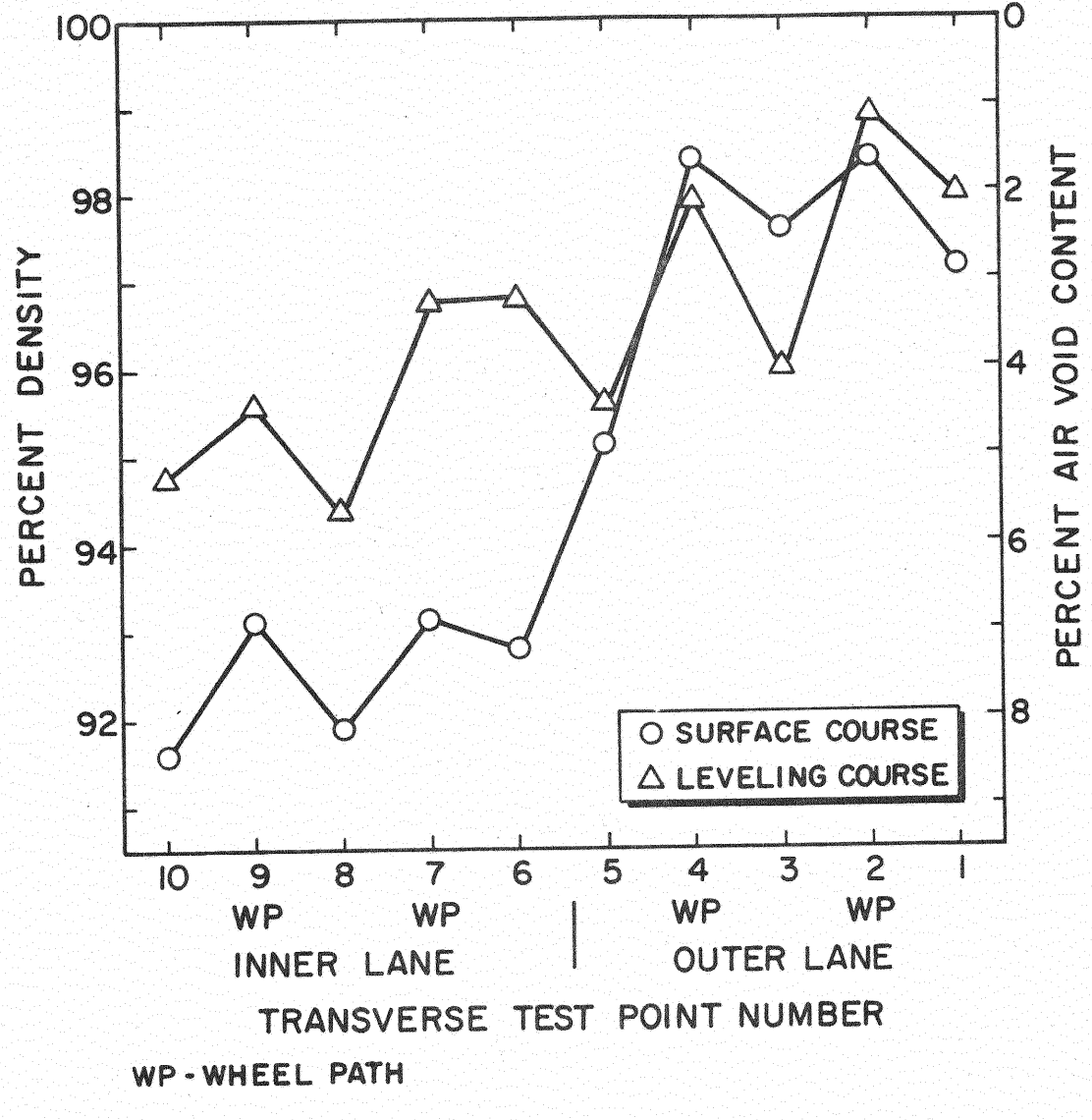

Figure 27. Percent Density Versus Transverse Test Point Site #140, Base Type--SCB

path locations (Fig. 28). The differential densification occurring at the two wheelpath locations in the outer traffic lane was the same and amounted to 1.1 percent density units. A maximum densification of 1.4 percent density units was observed at test point #9 in the inner traffic lane.

The percent density curves for the materials at test site 180 (Fig. 29) showed the density of the surface course to be less than that of the leveling course at all test points. While the two curves were approximately parallel the surface course showed more pronounced peaks in the wheelpaths. The maximum differential densification was found in the surface course at test point #2 in the outer lane. This amounted to 4.2 percent density units.

Surface Wear Measurements

Initially, several assumptions were made relative to estimating amounts of surface wear from the stereo-photos of the pavement surface (see Stereo-Photo Interpretation). Two of these assumptions did not hold true at the time the photographs were taken, the surfaces at many of the sites showed substantial dislodgement of the coarse aggregate particles from the matrix, and often this condition had progressed to the "raveling" stage.

These conditions weakened the estimating procedure used, in that the estimate of wear depth obtained by comparing the height of projection of the surface aggregates did not account for the depth of material lost by dislodgement. Even on the more extensively raveled sites evidence of differential wear could be detected. However, the amounts of wear were considered to be minimal at these locations.

Table I shows a summary of the results of the stereo-photo interpretation for each of the test sites. The tabulated values are averages of the amounts of differential wear determined at the wheelpath locations for

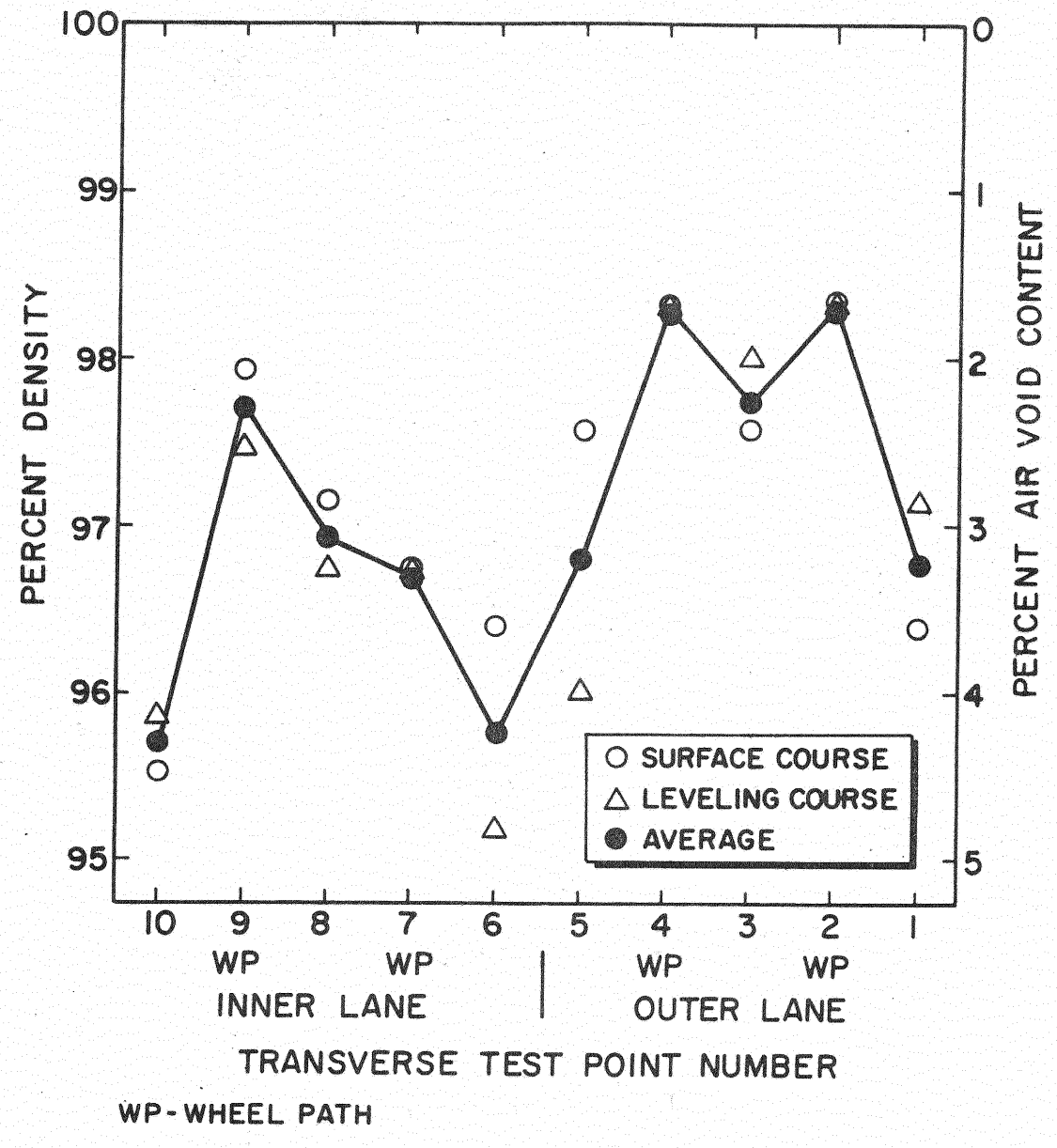

Figure 28. Percent Density Versus Transverse Test Point
Site #170, Base Type--SCB

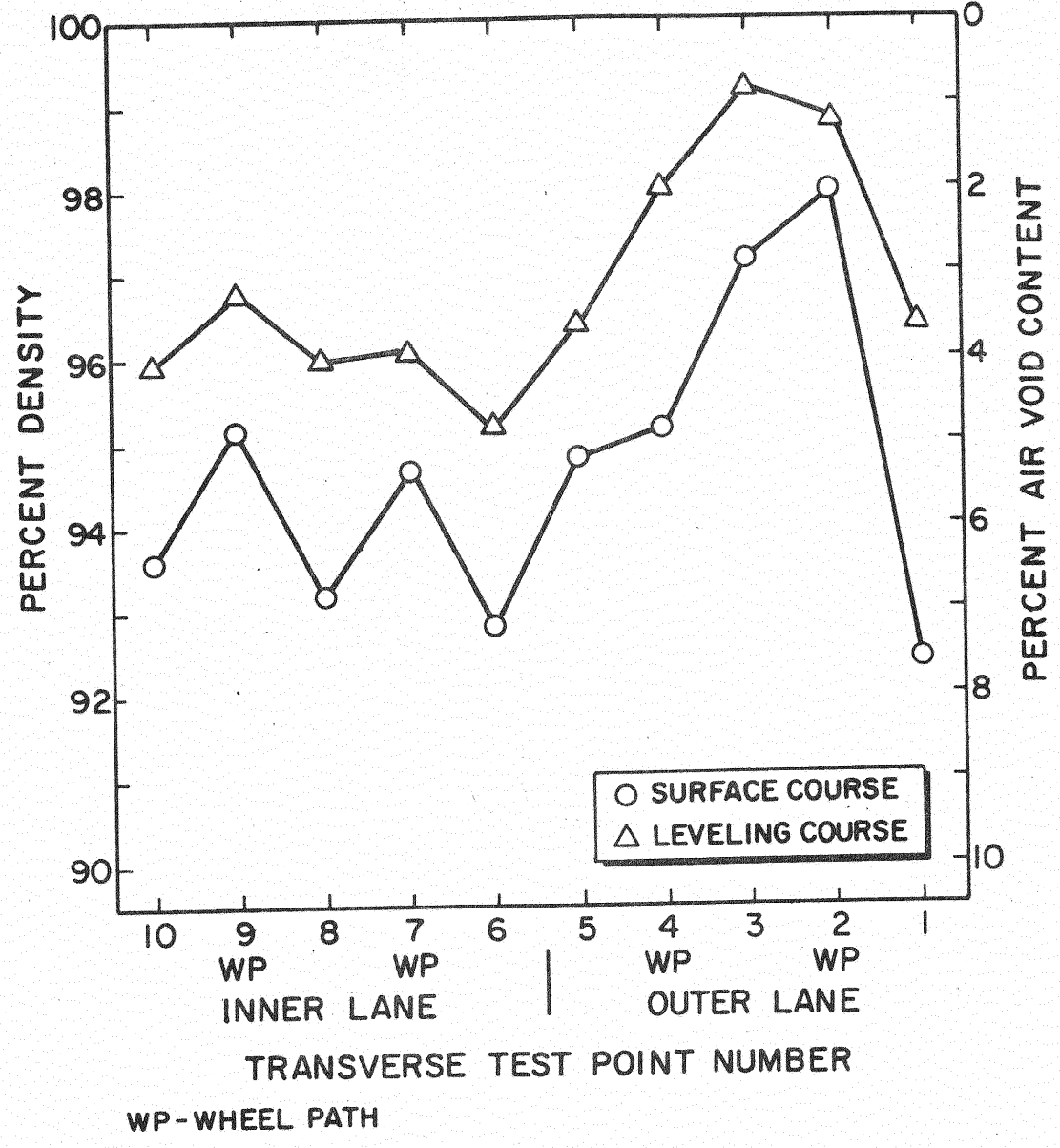

Figure 29. Percent Density Versus Transverse Test Point Site #180, Base Type--SCB

TABLE I

DIFFERENTIAL WEAR

BASE COURSE MATL.	SITE #	AGE MO.	AVERAGE DIFFERENTIAL WEAR (INS.)[1] AT WHEELPATH LOCATIONS	
			INNER LANE	OUTER LANE
HMSA	10	36	0.012	0.020
	60	169	0.016	0.023
	70	169	0.018	0.027
	120	105	0.016	0.029
BB	20	82	0.008	0.071
	30	56	**	**
	40	56	**	0.016
	50	86	0.015	0.016
SABC	80	165	0.016	0.031
	90	165	0.023	0.078
	100	158	**	**
	110	158	**	**
SCB	130	148	0.010	0.017
	140	148	0.005	0.014
	170	169	0.028	0.039
	180	169	0.031	0.031

** MISSING VALUES

1. CONVERSION: 1.0 in. = 2.54 cm

a given lane. As would be expected, the larger values occurred in the outer pavement lane. Missing data reflects poor quality photographs resulting from a malfunction of the camera shutter system. While the magnitudes of wear were smaller than anticipated, the results indicate that wear is definitely a contributing factor to rutting.

Profile Measurements

As discussed earlier, a transverse profile graph was made for each pavement lane at a given test site. The two graphs for each site were put together and a continuous tracing made of the transverse profile of the pavement surface. These tracings were reduced photographically to a convenient size for presentation (see following graphs). Vertical and horizontal scales are indicated on these graphs and the graphs are oriented as they would appear when viewed in the direction of traffic on the pavement. The graphs are not inclined to correspond to the measured pavement cross-slope. The transverse locations of the test points are marked and numbered sequentially from right to left. This numbering system corresponds to that shown in Fig. 1.

Subsidence and/or rut depth measurements were designated as "positive" values and the measurements of heave were considered "negative" values. These profile measurements were scaled directly from the original profile graphs and are shown immediately below their respective locations on the tracing. Rut depth was measured as the maximum vertical displacement of the surface in the wheelpath (a minimum point) from a straight line tangent to the profile curve at the adjacent maximum points.

The traffic lanes at each test site were designed to have a uniform cross-slope and it was assumed that they were constructed in this manner.

(6.35 cm.) Type B leveling course and 9.0 in. (22.86 cm.) of HMSA base on a slight fill section. Based on the method of measurement, heave is indicated at test points #1, #3, and #8, and the maximum rut depth of 0.99 in 2.52 cm.) occurred at test points #2 and #4. The density curves for the layers showed relatively high and uniform densities of about 98% in the surface and leveling courses and an average of about 90% in the base course.

At test point #2, the observed increase in density, i.e., the differential densification, in all of the layers will account for approximately 0.28 in. (0.71 cm.) of the toal rut depth. The average amount of surface wear in the outer lane was 0.02 in. (0.05 cm.). Thus, the remaining 0.69 in.)1.75 cm.) of the total rut depth can be attributed to lateral creep of the material in one or more of the pavement layers. In this case, lateral creep, densification, and surface wear accounted for 70, 28 and 2 percent of the observed rutting, respectively.

Because of the relatively low density of the sand asphalt base course, it is likely that a preponderance of the lateral creep took place in this layer. Difficulty was encountered in removing full depth pavement cores at several test points at this site. The base material washed out during coring and indicated stripping and/or a lack of coherence in the sand asphalt base. Also, visual examination of the pavement surface noted narrow longitudinal cracking between the wheelpaths in the outer lane and wide longitudinal cracks at the outer shoulder and at the pavement center line. There is a definite possibility that subgrade softening and displacement may also have occurred at this site.

The profile tracing for test site 60 is shown in Fig. 31. The pavement section at the location was a 2.0 in. (5.08 cm.) surface course, a 2.5 in. (6.35 cm.) leveling course and 8.5 in (21.59 cm.) of HMSA base.

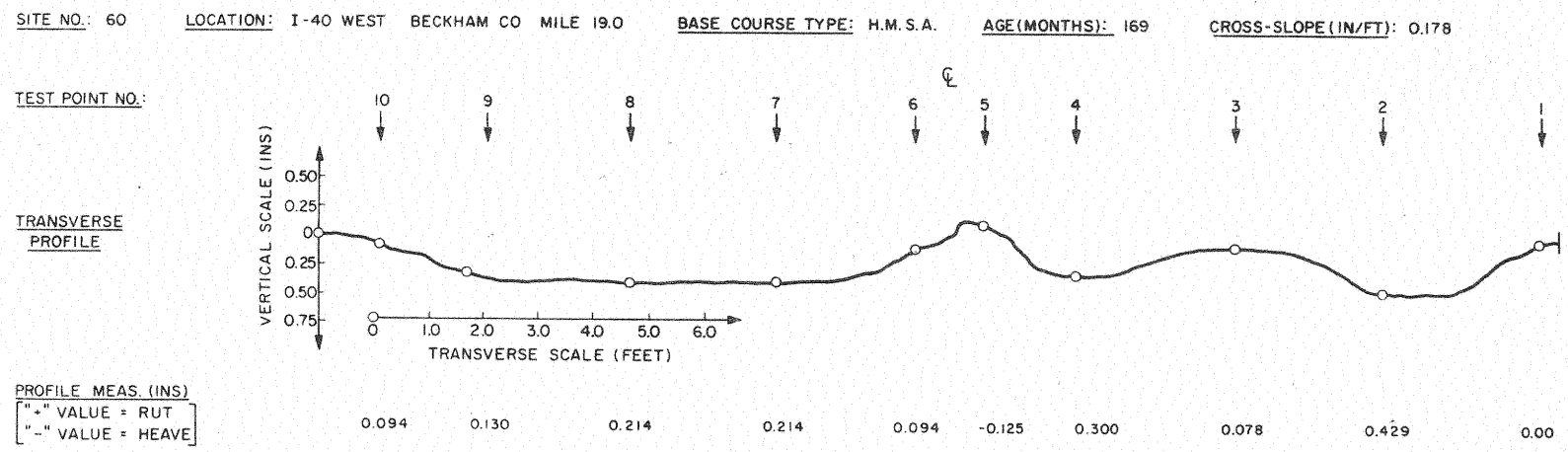

Figure 31. Transverse Profile Tracing, Test Site 60

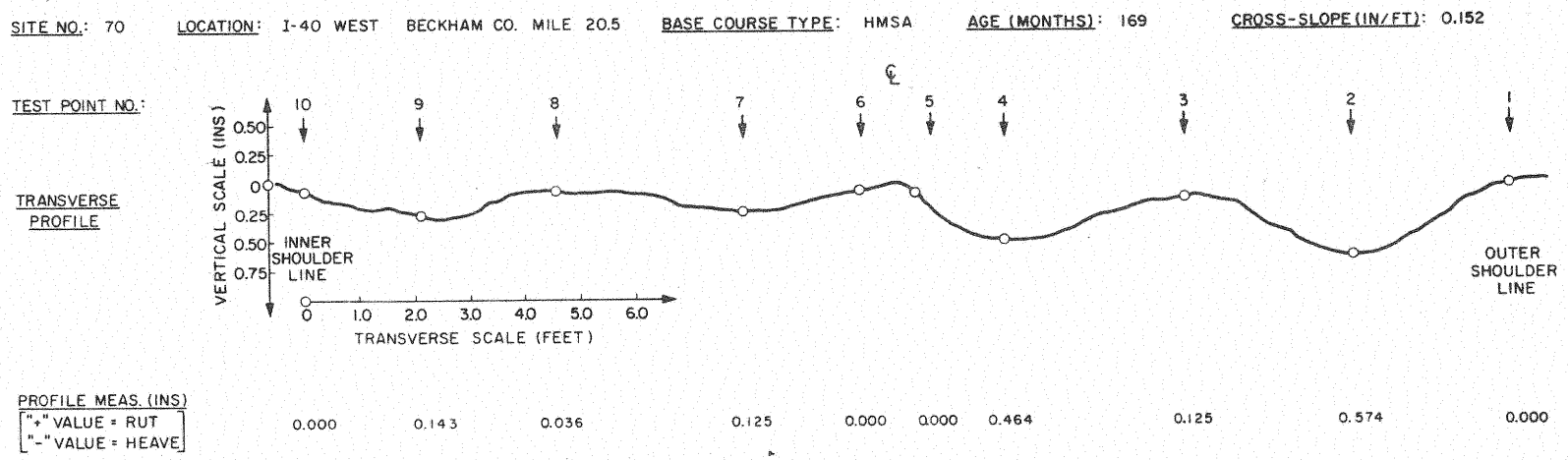

Figure 32. Transverse Profile tracing, Test Site 70

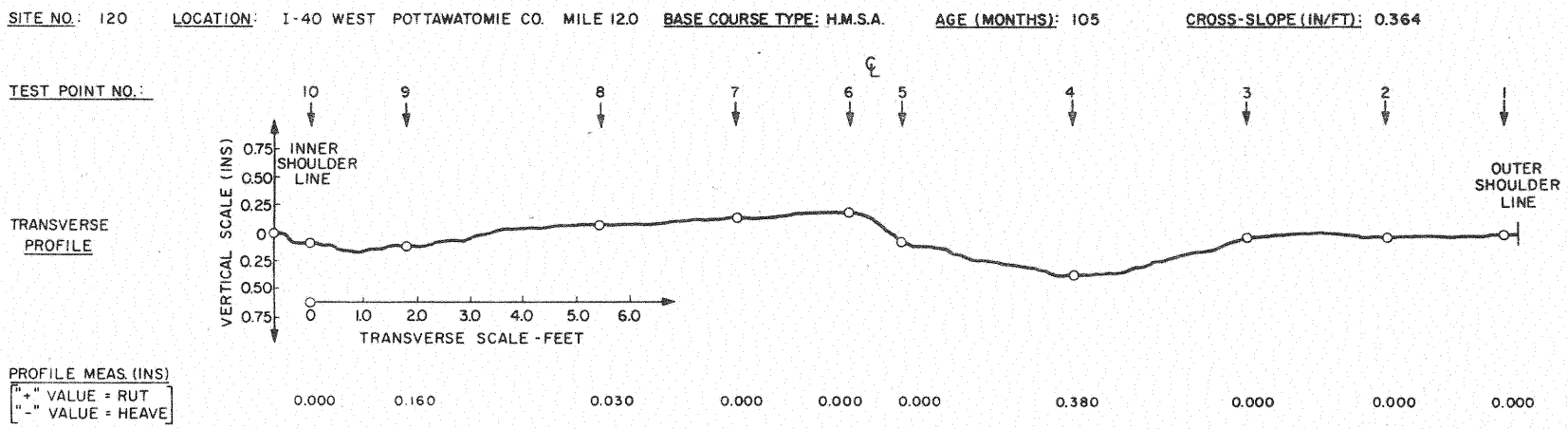

Figure 33. Transverse Profile Tracing, Test Site 120

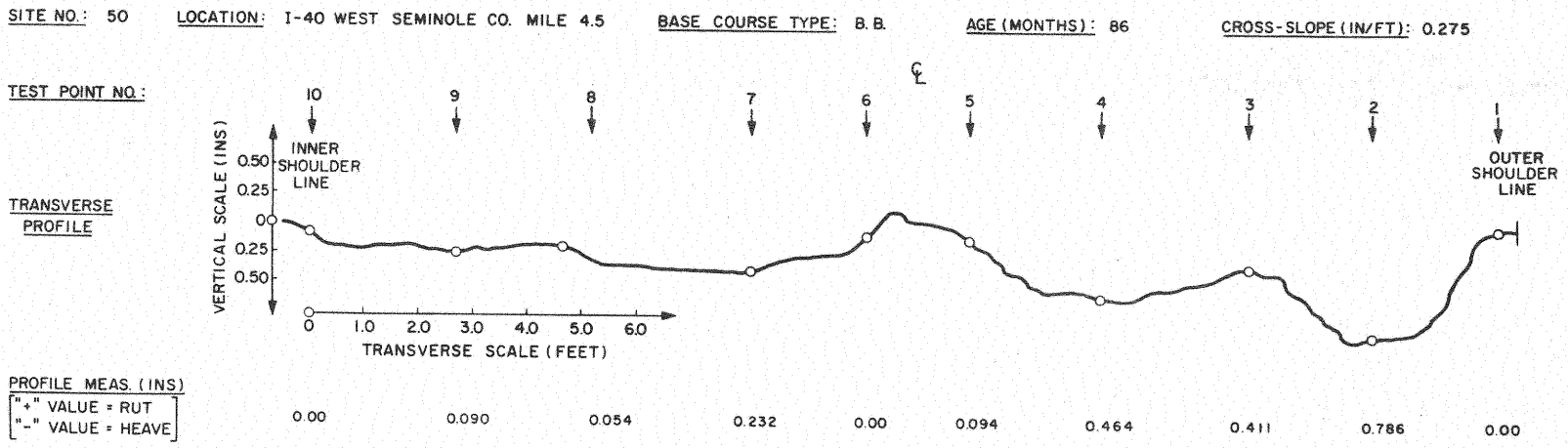

Figure 34. Transverse Profile Tracing, Test Site 50

However, this pattern did not hold true for all sections.

At test site 20 (Fig. 35) the maximum rut depth occurred at test point #4, the inner wheelpath in the outer lane. The differential densification in the respective layers and the surface wear at this point indicate that approximately 70% of the total rut depth of 0.571 in. (1.45 cm.) can be attributed to these factors. At test point #2, these same factors account for about 78% of the total rut depth. Again, the balance of the rutting must be assigned to subgrade consolidation because of the relatively high density of the black base and lack of evidence of surface heave in the vicinity. Some heave was determined at test point #8 but this was in the other lane and the magnitude was very low.

Surface heave was observed in the outer lane at test site 30 (Fig. 36) and the maximum rut depth of 0.607 in. (1.54 cm.) occurred at test point #2 in this lane. The average percent density values of the three bituminous bound layers [2.0 in. (5.08 cm.) of surface course, 2.0 in. (5.08 cm.) of leveling course, and 9.0 in. (22.86 cm.) of black base] were quite high and relatively small amounts of differential densification in the respective layers was indicated. Therefore, between 70 and 75% of the total rut depth must be attributed to something other than densification and surface wear. The density, coherence and general appearance of the core samples at this site seemed to rule out the possibility of lateral creep in these materials. Wide longitudinal cracking in the outer lane at test point #2 and general subsidence in the inner lane, again, indicate problems in the subgrade.

The profile tracing at test site 40 (Fig. 37) presented some problems in trying to deduce what had happened at this location. At the time the tracing was made, the profile of the inner lane was questioned and several

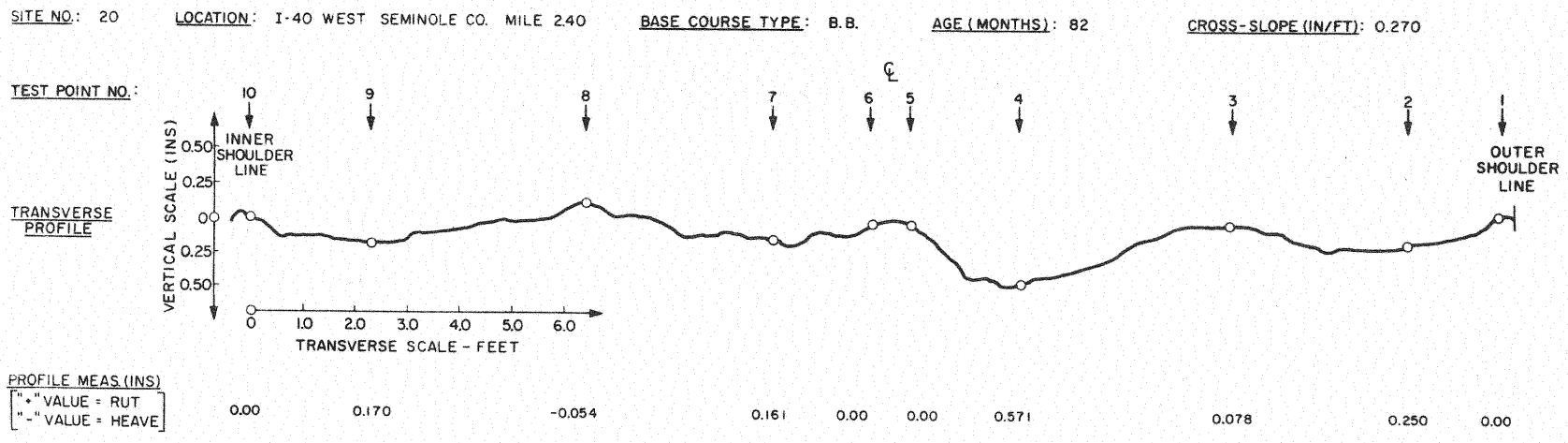

Figure 35. Transverse Profile Tracing, Test Site 20.

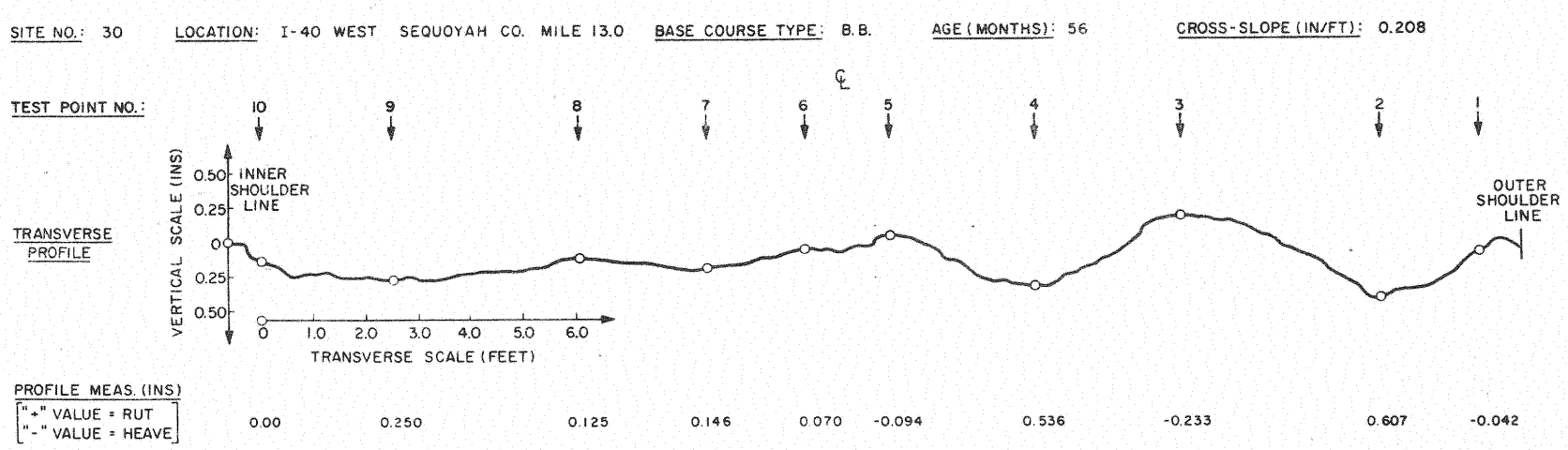

Figure 36. Transverse Profile Tracing, Test Site 30

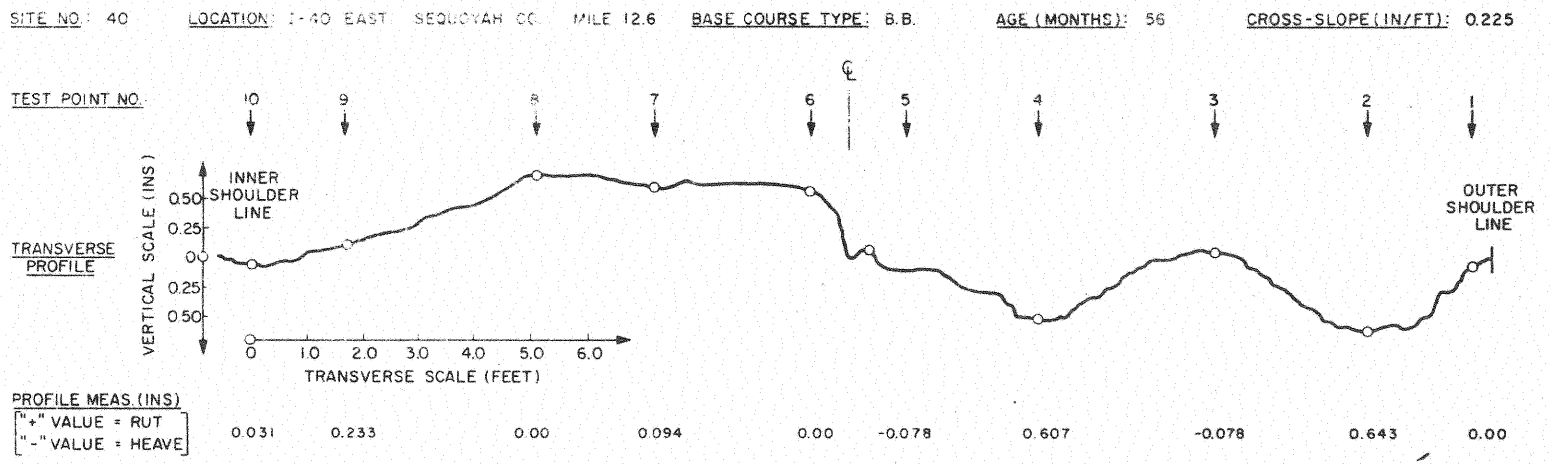

Figure 37. Transverse Profile Tracing, Test Site 40

different traces were made using various recorder scales with similar results. An elevation difference of approximately 0.5 in. (1.27 cm.) between the lanes at the center line was observed in the field. Subsidence across the entire width of the outer lane and upheaval in the inner lane between the center line and test point #9 is a possible explanation, however, it is more likely that this is due to failure to achieve proper grade and cross-slope in the pavement surface at the time of construction. A maximum rut depth of 0.643 in. (1.63 cm.) was measured at test point #2 in the outer lane. Only about 25% of this total rutting can be attributed to densification in the bituminous bound layers (cross section same as that at test site 30) and surface wear.

Stabilized Aggregate Base Sections

The pavement at test site 80 consisted of 2.0 in. (5.08 cm.) of type C surface course mix and 3.0 in. (7.62 cm.) of Type B leveling course mix on a stabilized aggregate base. The transverse profile tracing (Fig. 38) indicated a maximum rut depth of 0.571 in. (1.45 cm.) at test point #4 and a 0.200 in. (0.51 cm.) heave at test point #3. A total of 0.083 in. (0.21 cm.) could be assigned to densification and surface wear at test point #4. This is only about 15% of the total rut depth at this point. Longitudinal cracking in the wheelpaths of the outer lane and a general map cracking pattern across the pavement surface was noted. Also, stabilizing operations (lime injection) on the base materials were being carried out in the vicinity of this site at the time of testing. Based on these observations, it is reasonable to attribute the substantial rutting and heave at this test site to instability of the base course material. It should be noted that all of the test sites on SABC were relatively old (the ages ranged from about 13 to 14 years). The fatigue

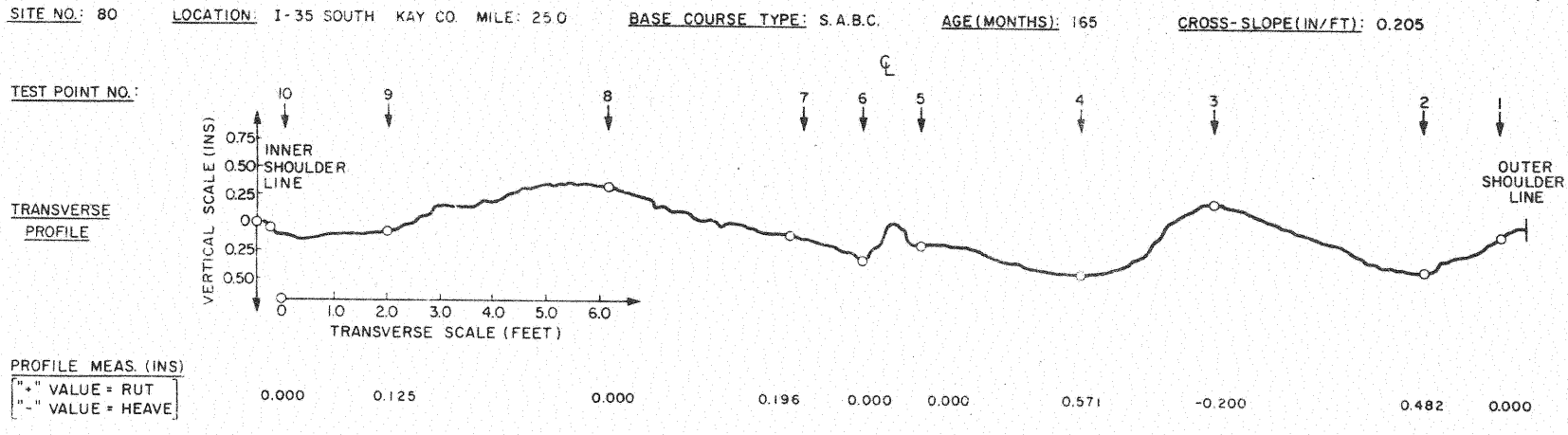

Figure 38. Transverse Profile Tracing, Test Site 80

life of this type of unbound base material is probably a definite factor relating to deformations in the surfacing layers.

The profile tracing at test site 90 is shown in Fig. 39. Rather deep rutting occurred in the outer traffic lane and heave is indicated at test points #3, #5 and #8. The pavement had a cross-section similar to that at test site 80. While densification was evident in the surface and leveling courses and there was a substantial amount of surface wear in the outer lane, only a small percentage (22%) of the maximum rut depth could be attributed to these factors. A lane elevation differential of approximately 0.5 in. (1.27 cm.) was observed at the centerline. Whether this was due to settlement in the inner lane or was a construction aberration is open to speculation. Base problems were suspected.

Test site 100 and test site 110 had similar cross sections, i.e., 3.0 in. (5.08 cm.) of surface course and 3.5 in. (8.89 cm.) of leveling course, and similar profile tracings (Fig. 40 and Fig. 41). Severe cracking of the pavement surface had occurred in the outer and inner lanes at these sites. In both instances, the maximum rut was found at test point #4 and surface heave was indicated in the outer lanes. According to the visual rating, only slight to moderate surface wear had occurred. Approximately 20% of the maximum rut depths could be assigned to densification in the surface and leveling courses at these locations. The surface heave and the balance of the rutting were attributed to base deformation. The generally convex shape of the inner lane profiles may also be due to base problems, but in these two cases a parabolic curve was used as the assumed initial shape of the surface for profile measurements.

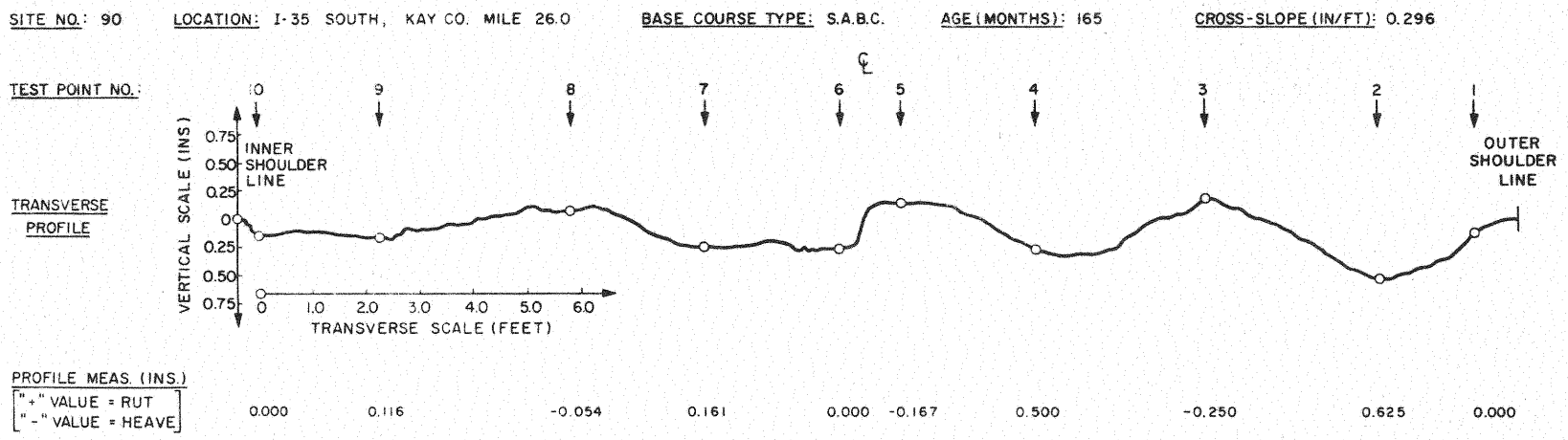

Figure 39. Transverse Profile Tracing, Test Site 90

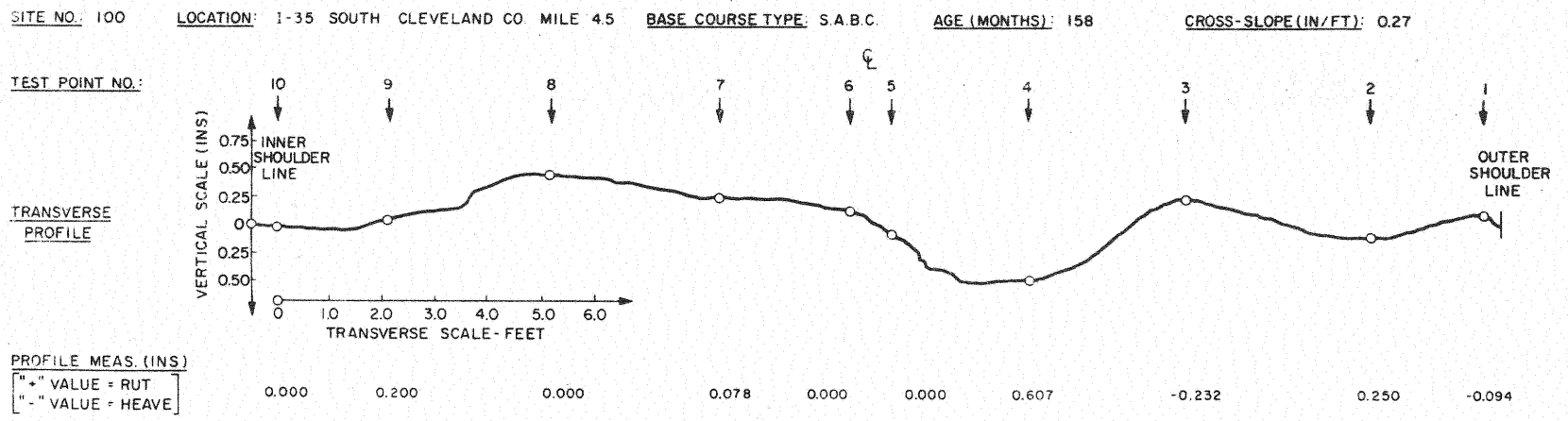

Figure 40. Transverse Profile Tracing, Test Site 100

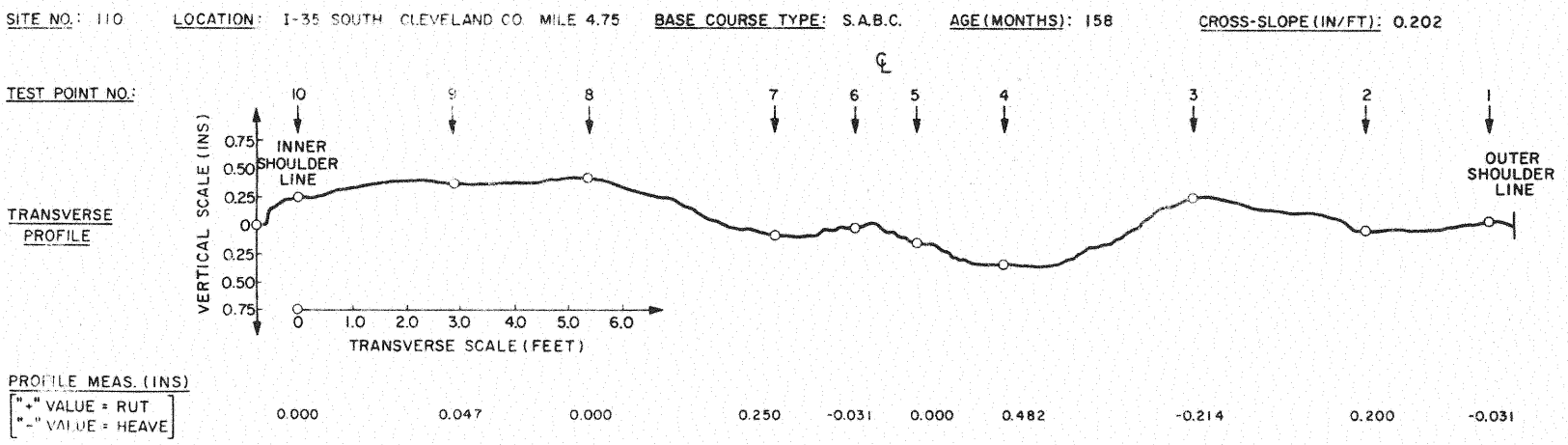

Figure 41. Transverse Profile Tracing, Test Site 110

Soil-Cement Base Sections

Generally, rutting and other surface distortions were minimal at the test sites on pavements constructed over soil-cement bases, although these pavements were among the oldest studied. This is undoubtedly due to the rigid nature of this base material and, in comparison with the rutting and surface distortions encountered on the other types of bases, demonstrates the desirability of a high density - high stability base course for bituminous pavements. The old cliche, "a pavement is only as good as its base", still -holds true.

Despite the apparent good performance of the soil-cement base materials some problems were noted. The pavement surfaces at the respective sites showed transverse longitudinal and dendritic type cracking. These surface cracks are reflections of shrinkage cracks in the base. While only minor amounts of break-outs or material erosion adjacent to the crack joints were observed, subsequent traffic will progressively deteriorate the surface at these locations. Also, surface water will drain into and through these cracks to soften the underlying subgrade soil. A weakened subgrade condition was suspected at two of the test sites. Because of this, the cracks are detrimental to the structural integrity of the pavement system and require appropriate remedial action, i.e., sealing.

At test site 130 (Fig. 42), the greatest amount of rutting occurred in the outer traffic lane at test point #2. Differential densification in the respective asphalt bound layers and surface wear will account for about 51% of the rut depth of 0.219 in. (0.556 cm.) at this wheelpath location. Due to the rigid nature of the base, the remaining 49% of the total rut depth can be attributed to lateral creep of the bituminous materials. This is indicated by the slight surface heave at test points #1 and #3.

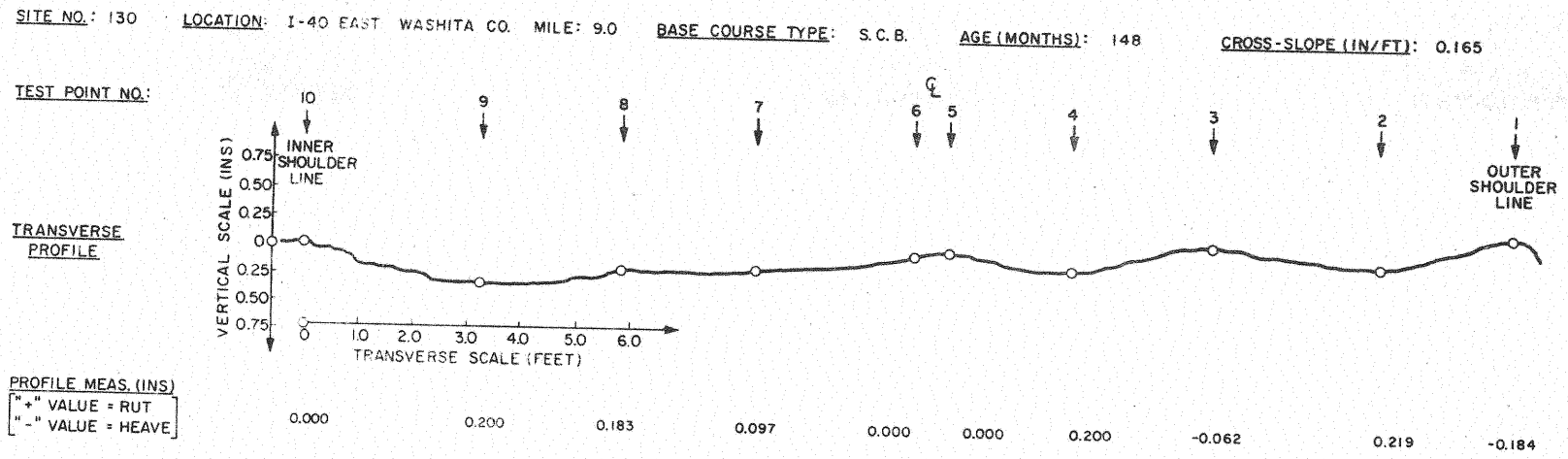

Figure 42. Transverse Profile Tracing, Test Site 130

Rut depths in the outer lane at test site 140 were slightly greater than those at test site 130 (Fig. 43). At the point of maximum rut depth, test point #2, approximately 0.086 in. (0.218 cm.) of the rut can be ascribed to densification and 0.014 in. (0.036 cm.) to surface wear. The total of these measurements amounted to about 35% of the total rut depth. These factors, densification and wear, accounted for 48% of the rut depth at test point #4 and all of the rutting that occurred in the inner traffic lane. While no surface heave was evident in the outer lane, lateral creep must be responsible for the balance of rutting that occurred in this lane. This points out some of the fallacies inherent to the measurment technique that was used.

The rather wide depression basins at the wheelpaths in the outer lane indicate a lateral shift of the traffic to avoid driving in the ruts that develop. This transverse shifting of the vehicles using the pavement spreads out the effects of densification and wear and, over a long period of time, may have subdued any heave that occurred in this lane. Similar indications of a lateral shift of traffic in the lanes were noted at many of the test site locations.

Substantial amounts of heave were indicated in the outer lane at test site 170 (Fig. 44) and the deepest ruts on all of the pavement sections with a soil-cement base occurred at this site. Severe raveling had taken place in all of the wheelpaths. This, of course, influenced the magnitude of differential wear determined at these points, but there was no way of ascertaining the depth of this erosion and its contribution to rutting. Based on previous analysis, approximately half of the 0.50 in. (1.27 cm.) rut depth can be blaimed on lateral creep of the bituminous paving materials.

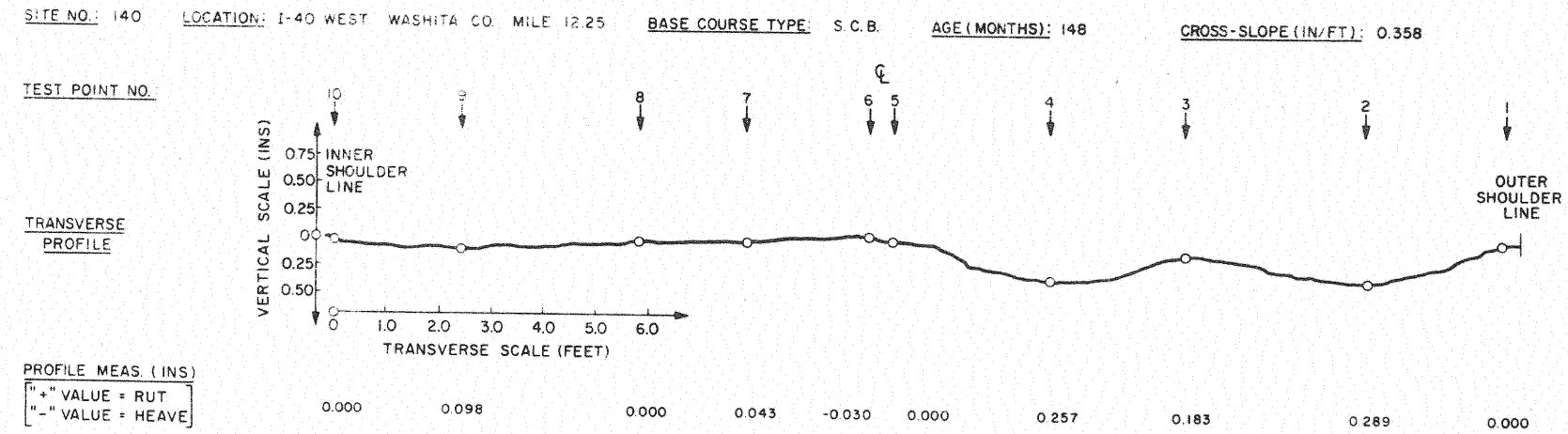

Figure 43. Transverse Profile Tracing, Test Site 140

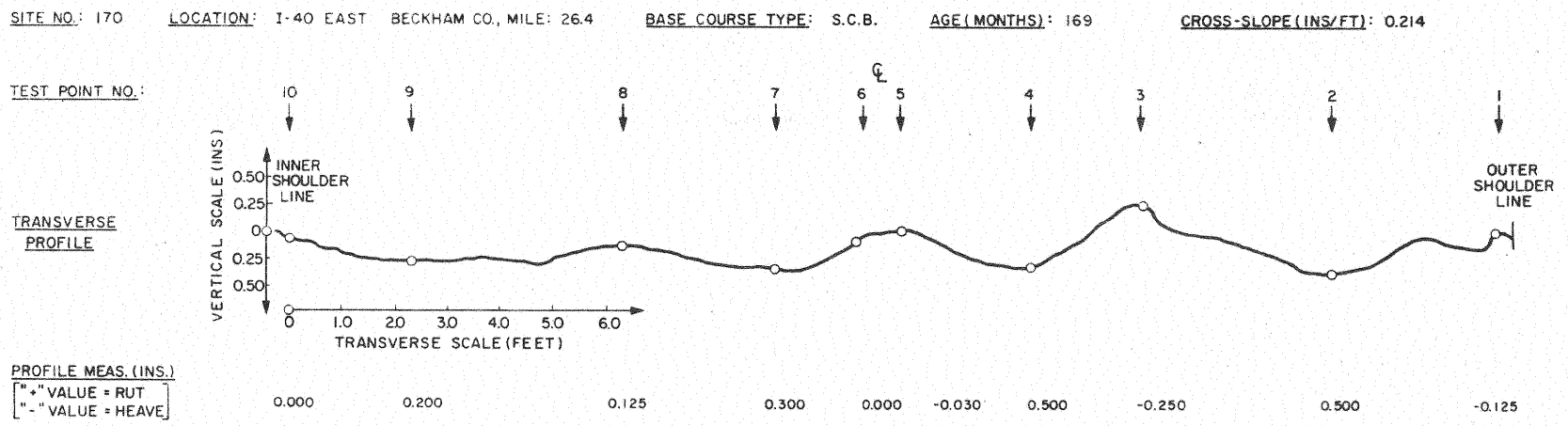

Figure 44. Transverse Profile Tracing, Test Site 170

Severe raveling was also in evidence in the wheelpaths of the outer lane at test site 180 but no indication of heave could be found (Fig. 45). By the method of analysis used, 31% of the maximum rut depth at test point #2 could be assigned to densification and wear. Lateral creep is probably responsible for a portion of the remaining depth. In this case, however, the profile tracing showed a general subsidence of the outer lane. Surface cracking was extensive in this lane and it is believed that subgrade softening also contributed to the rutting that took place. The convex shape of the inner lane profile could be interpreted as a general heave extending across the lane but it probably represents closely the "as constructed" profile.

Nuclear Density Measurements

The Troxler density gage utilizes Compton scattering and photoelectric absorption of gamma photons to measure the density of materials being tested. In this study, the gage was used to determine the density of the pavement surface (approximately the upper 3 inches) at each of the selected test points at a site. The backscatter method or technique of measurement was employed. While completely non-destructive, i.e., no disturbance of the surface was required, this technique is the least accurate method of measuring density and resulted in many extremely low and unrealistic density values.

For comparison, the specific gravity values of the top 2.0 in. (5.04 cm.) of the bituminous surfacing materials from the core samples were converted to density units. (It should be recalled that these cores were obtained from the selected test points following the nuclear density determinations). The SAS computer program was employed to determine the corresponding values obtained using the nuclear density gage. A plot of this

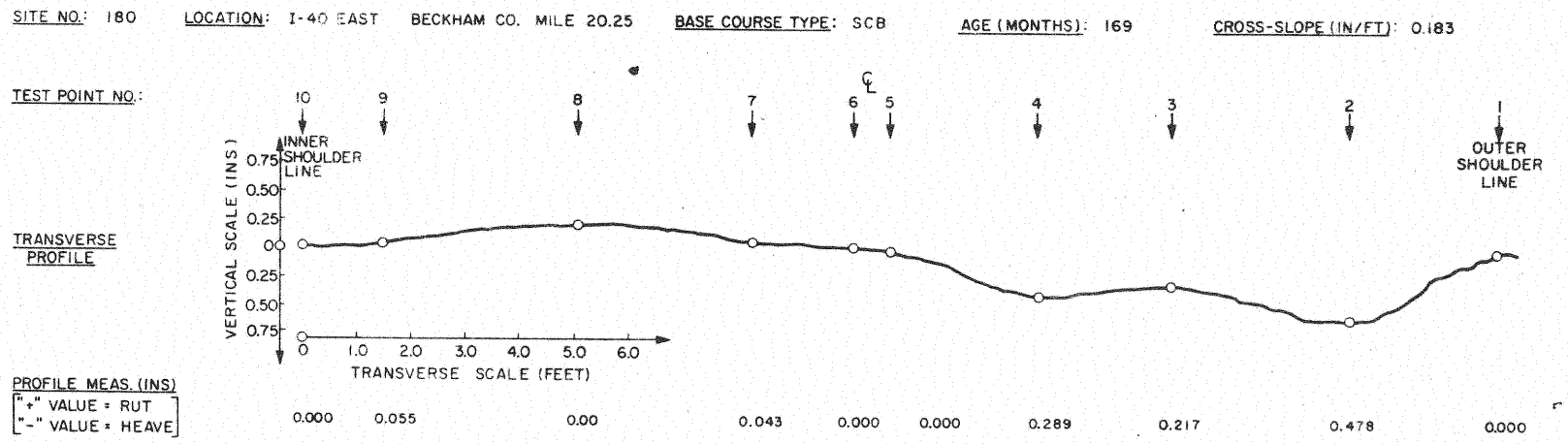

Figure 45. Transverse Profile Tracing, Test Site 180

data is shown in Fig. 46. For the two data sets of 160 observations each, the correlation coefficient was 0.31 and the OSL was 0.0001. The least squares curve fit method was used to obtain the correlation curve shown in Fig. 47.

Although some error in the laboratory density values was likely, the poor correlation obtained was largely attributed to the nuclear density measurement technique. The accuracy of the backscatter method is affected by surface roughness since the nuclear source and the detectors are both on the surface of the pavement. Photon streaming through surface voids induces errors in the measurements. Even when the surface voids (at raveled or badly worn locations) were filled with sand, the density values were frequently so low that they were considered unreliable. Backscatter density measurements are also heavily weighted by the density of the top 0.5 in. (1.27 cm.) of surfacing material.

Summary of Results

Table II shows the contributions of the various modes of rutting at the respective test sites. The measurements of heave, surface wear, and differential densification determined in this study were subject to some maccuracies, due primarily to the lack of initial data on the pavement sections. Thus, the tabulated values should be regarded as indications of the component contributions. Despite this, however, the data in this summary consistently show that the bituminous mixes were responsible for a significant amount of the rutting that occurred.

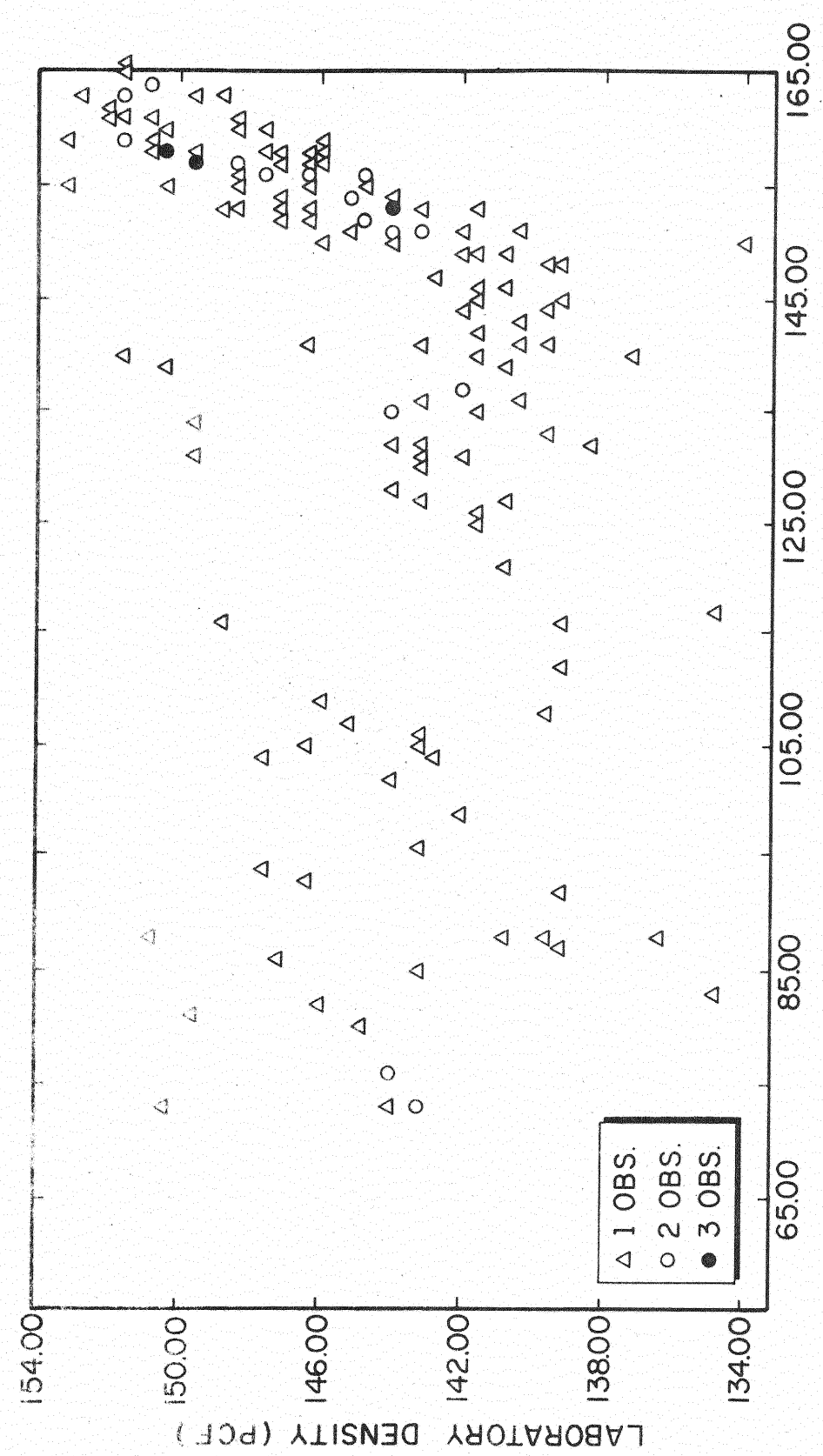

Figure 46. Plot of Nuclear Density Versus Laboratory Density

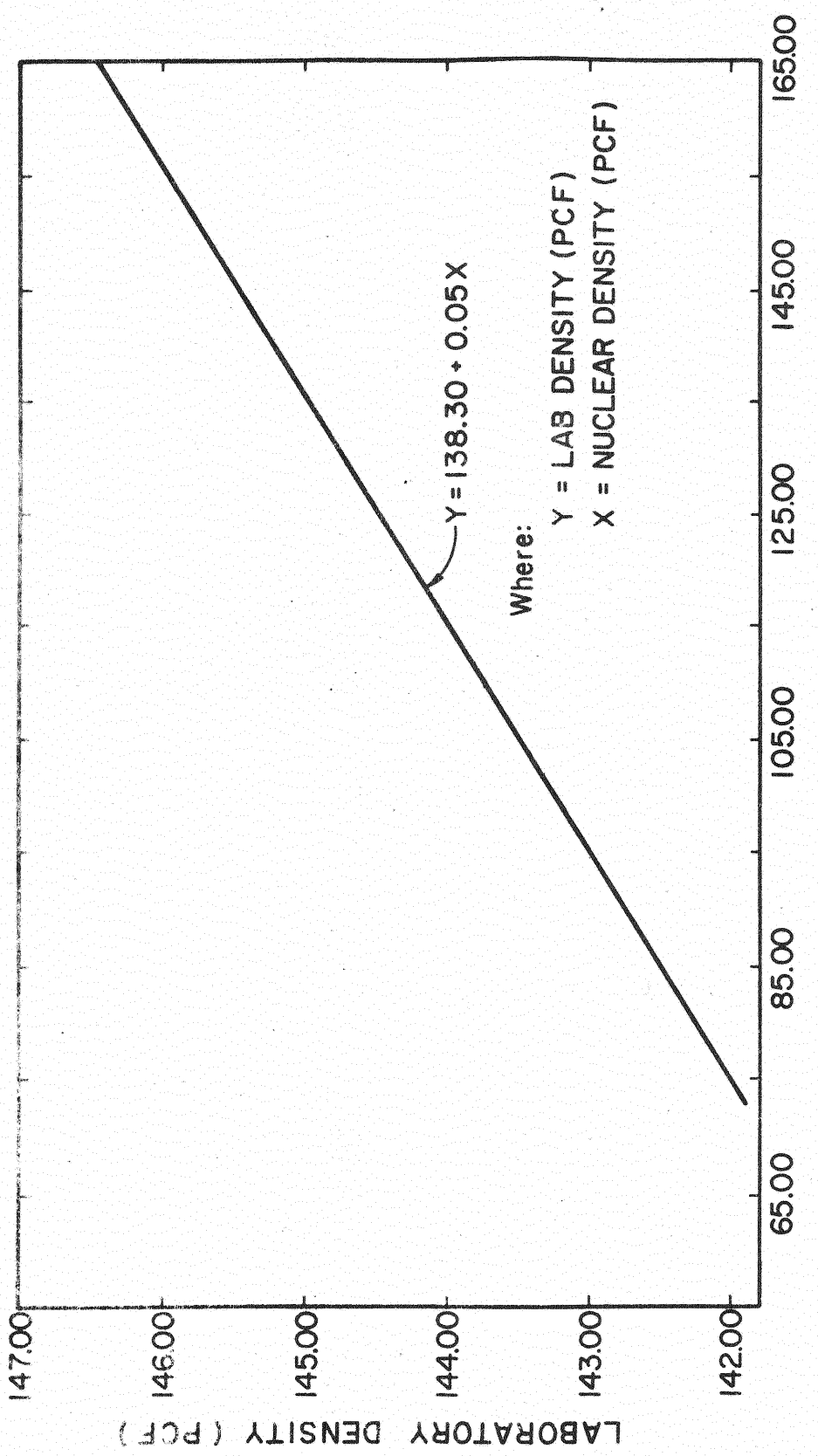

Figure 47. Correlation Curve

TABLE II

MODAL CONTRIBUTIONS TO RUTTING

Site No.	Base Course	Age (Mo.)	Max. Rut (in)	Approximate Percentage Contribution to Rutting			
				Densification	Surface Wear	Lateral Creep	Base or Subgrade Deformation
10	HMSA	36	0.990	28%	2%	70%	*
60	HMSA	169	0.429	40%	5%	55%	*
70	HMSA	169	0.574	40%	5%	55%	*
120	HMSA	105	0.380	42%	8%	50%	*
20	BB	82	0.571	58%	12%	30%	*
30	BB	56	0.607	25%	--	*	73%
40	BB	56	0.643	22%	2%	*	76%
50	BB	86	0.786	8%	2%	*	90%
80	SABC	165	0.571	9%	5%	*	86%
90	SABC	165	0.625	9%	13%	*	78%
100	SABC	156	0.607	18%	--	*	77%
110	SABC	156	0.482	20%	--	*	74%
130	SCB	148	0.219	43%	8%	49%	
140	SCB	148	0.289	30%	5%	65%	
170	SCB	169	0.500	14%	8%	78%	*
180	SCB	169	0.478	25%	6%	69%	*

* Not a major factor - some contribution indicated

CHAPTER VII

CONCLUSIONS AND RECOMMENDATIONS

Conclusions

Based on the test procedures employed and the pavement sections studied, the following conclusions are made:

1. The transverse profile gage provides a portable and accurate means of obtaining continuous profile tracings of a pavement surface.

2. In addition to measurement of surface deformations, the plotted profile graphs can provide permanent records of these conditions at a specific time in the service life of a pavement and can be used for future studies.

3. Densification under traffic loading occurred in all asphalt bound material layers. Increases of up to 7 percent density units at wheelpath locations in the outer traffic lanes were found.

4. Densification contributed a significant amount to the total surface rut depth. On the thicker pavements, i.e., sections employing black base or sand-asphalt base, the amount of rut depth ascribed to densification ranged from 8 to 58 percent for the outer pavement lanes.

5. Surface wear or attrition in the wheelpaths on heavily travelled lanes was an important contributing factor to rutting. Stereo-photography provided a means of determining the amount of surface wear that had occurred.

6. Evidence of creep or instability in the bituminous material layers

was found at eleven of the sixteen test sites. This occurred in high as well as low density materials and contributed from 30 to 78 percent of the rutting at these locations. More prominent surface heaves were noticed at sites where the bituminous material layers had low densities.

7. Base and/or subgrade deformations influenced the magnitude of rutting at many of the test sites. Extensive surface cracking and indications of surface subsidence were found at these sites. Consolidation and shear failure in these layers concealed the effects of lateral creep in the bituminous-bound materials.

8. No satisfactory correlation between laboratory density values and the values obtained using the surface nuclear density gage was found. The accuracy of measurements obtained using the backscatter method appeared to depend greatly on the pavement surface characteristics, i.e., surface roughness and density of the top 0.5 in. (1.27 cm.) of the surface material.

Recommendations

In view of the results of this research investigation, the following recommendations are made:

1. In order to follow surface deformations due to traffic action, profile tracings at a site should be made prior to opening the highway to traffic. This would provide an initial tracing at time "zero" for subsequent comparisons.

2. Following the above recommendation, additional studies could ascertain exact amounts of surface heave, and determine the bituminous pavement layer(s) responsible for this type of displacement. With careful monitoring and trenching of selected test sections, it should be possible to distinguish between surface heave resulting from lateral creep (shear failure)

in these layers and that due to deformations in the non-bituminous base or subgrade.

3. Increased surveillance of operations at hot-mix plant sites and more stability checks on the mixture being produced could be instituted to insure conformance with the stability requirements for a given type of mix. Special studies of this nature on selected projects would indicate the adequacy of present inspection and check test procedures.

4. To minimize the contributions of densification and lateral creep to rutting, construction methods and specifications should be reviewed to determine if changes are necessary to insure adequate compaction and density of all asphalt bound pavement materials.

5. The accuracy of current laboratory procedures for determining percent density values of both laboratory and field compacted specimens should be investigated. Error in the determination of the maximum specific gravity of a mixture can easily result in very low in-place density values. Due to this error, the measured pecent density values of field specimens can be above the specified minimum value but the actual density of these specimens may be a great deal below the desired value.

6. A more accurate technique of determining the amount of surface wear from stereo-photographs should be devised. A tentative approach would be to utilize a non-wearing surface such as the head of a nail (driven into a new pavement surface in the expected wheelpath) as a datum. Subsequent wear of the adjacent pavement surface could then be measured more exactly through stereoscopic comparison with this reference surface.

7. A comprehensive study of the effectiveness of the various types of base course material used in flexible pavement construction in Oklahoma should be made. A feasible approach to such a study would be to use stage construction test sections at various geographical locations in Oklahoma.

That is, for a given type of base, design and construct test sections with varying thicknesses of the surface course material and follow subsequent behavior in terms of appropriate performance variables including 1) rutting, 2) surface heave, 3) subsidence and 4) longitudinal and transverse cracking. Other variables, e.g., initial density of material layers, layer thickness, type of section, etc., could be included in such a study.

Addendum to Recommendations

More specific comments and suggestions relative to Recommendations 3, 4, and 5 are warranted since these are the recommendations primarily addressed to improving or minimizing the rutting propensities of asphalt pavements.

Recommendation 3. Instability or lack of resistance to lateral displacement of the asphalt bound materials was considered a major contributing factor to rutting at many of the test sites. Thus, adequate stability of the field compacted plant mixtures is necessary and should be corroborated through special studies by the Oklahoma Department of Highways. The following suggestions are made for this purpose:

1. There is a direct relationship between density of a mix and its stability, such that, a low density can correspond with a very low stability value. One approach to checking the field stability of a mixture would be to (a) mold additional specimens during the mix-design procedure with varying amounts of compactive effort; (b) determine the lab densities and Hveem stabilities of these additional specimens and plot a curve relating these values; (c) density values of field cores entered on such a curve would indicate the approximate stability value of the field compacted mix. This approach should be tried on selected paving projects to determine whether

the in-situ mixtures have the requisite stability and to ascertain the value or need for such a procedure.

2. Along with the preceding suggestion, the number of stability test specimens made from mix produced at the plant site should be substantially increased on the selected paving projects. This will insure conformance with the applicable stability requirements for a greater portion of the total production of a given mix. Such a measure would also serve to verify the adequacy of present inspection procedures and the number of test specimens being made.

Recommendation 4. Based on the results of this study and a review of the pertinent Standard Specifications, it seems evident that flexible pavement layers are presently being constructed with a built-in rutting capability. This statement applies to the surface and binder courses and to the fine aggregate bituminous base course and relates to the allowable density and stability of the mixtures used in these layers. For example, the allowable density range for field compacted surface mixes is 89.3 to 93.1 percent with corresponding air void contents of 10.7 to 6.9 percent. This range of air void content is too high if a minimum amount of post construction densification, i.e., rutting, from imposed traffic loads is desired. Specific suggestions regarding more stringent specifications and increased inspection of construction are as follows:

1. The minimum roadway or field density for surface and binder mixtures should be specified as 94 percent of the maximum theoretical density fo the mix.

2. The specifications for fine aggregate bituminous base (HMSA) should be changed to:

(a) Eliminate the use of AC-3A and AC-4.

(b) Require 5-8 percent asphalt content.

(c) Narrow the percent passing range for the No. 10 and No. 40 sieves in the gradational requirements.

(d) Increase the allowable laboratory compacted density to not less than 92 percent of maximum theoretical density.

(e) Increase the allowable Hveem stability value to not less than 30.

Note: It may be difficult to adhere to the above specification changes using materials indigenous to some areas of Oklahoma. Consideration should be given to the use of these as "alternate" specifications in areas where plentiful supplies of coarse aggregates are available and the use of present specifications in other areas.

3. Inspection or surveillance during the rolling operations and the number of density test samples should be increased to insure that the pavement layers are being compacted to an adequate density during construction. Surface nuclear density gages or electronic density recorders could be used for in-place measurements to check compliance with density specifications during the rolling operations.

Recommendation 5. Experience with the Oklahoma Department of Highway's method of test for bulk impregnated specific gravity of the combined aggregate in a mix (OHD-L-7) indicates that the determined values may be on the low side of what might be termed the "actual" specific gravity values of the combined aggregate. This influences the calculated theoretical maximum specific gravity values of the mixtures and results in measured percent density (percent of solids by volume) values of compacted laboratory specimens and field samples that are greater than the percent densities that actually exist. Thus, the current laboratory mix design procedures may be partly

responsibile for the relatively low field densities found in this study. It is suggested that an in-house investigation of these laboratory procedures be instituted to compare percent density values determined by the OHD method with those determined by ASTM Method D 2041.

BIBLIOGRAPHY

1. Barksdale, R.D., and G.A. Leonards, "Predicting Performance of Bituminous Surface Pavements". Proceedings 2nd International Conference on Structural Design of Asphalt Pavements, Ann Arbor, Michigan 1967.

2. Barr, A.J., et al, "A User's Guide to the Statistical Analysis System". North Carolina State University Press, Raleigh, August 1972.

3. Bonitzer, J., and P.H. Leger, "Studies on Pavement Design". Proceedings International Conference on Structural Design of Asphalt Pavements, August 1967.

4. Britton, W.S.G., "Effects of Aggregate Size, Shape and Surface Texture on the Durability of Bituminous Mixtures". Highway Research Board Special Report 109, 1970, pp 23-24.

5. "Bulk Specific Gravity of Compacted Bituminous Mixtures Using Paraffin Coated Specimens". ASTM Designation: D1188, 1971.

6. Burmister, D.M., "The General Theory of Stresses and Displacements in Layered Systems". Journal of Applied Physics, Vol. 16, 1945, pp 89-302.

7. Defoe, J.H., and A.P. Chritz, "Evaluation of Nuclear Method for Asphalt Testing". Highway Research Record Report No. R-745, July 1970.

8. Ellis, D.S., et al, "Thermally Induced Densification of Asphalt Concrete". Proceedings Association of Asphalt Paving Technologists, Vol. 38, February 1969, p 660.

9. "Evaluation of Studded Tires - Performance Data and Pavement Wear Measurement". Highway Research Board Special Report 61, p 66.

10. Finney, D.J., "An Introduction to the Theory of Experimental Design". University of Chicago Press, Chicago, 1960.

11. Ford, M.C., Jr., "Stripping in Bituminous Mixtures". (Unpub. Ph.D. dissertation, Oklahoma State University, Stillwater, 1973).

12. Foster, C., "Dominant Effect of Fine Aggregate on Strength of Dense-Graded Asphalt Mixes". Highway Research Board, Special Report 109, 1968, pp 1-3.

13. "General Discussion of Effects of Aggregate Size, Shape, and Surface Texture on Properties of Bituminous Mixtures." Highway Research Board Special Report 109, January 1968, pp 33-41.

14. Hadley, W.O., et al, "Correlation of Direct Tensile Test Results with Stability and Cohesiometer Values for Asphalt Treated Materials". Proceedings Association of Asphalt Technologists Volume 39, 1970, pp 745-765.

15. Hveem, F.N., "Pavement Deflections and Fatigue Failures". Highway Research Board Bulletin 114, 1955, pp 43-87.

16. "Density of Bituminous Concrete in Place by Nuclear Method". ASTM Designation: D 2950, 1974.

17. "Instruction Manual for Series 2400 Compac Surface Moisture/Density Gages". Troxler Electronic Laboratories, Inc., Raleigh, North Carolina.

18. Kamel, Nabil, "Developing Structural Design Models for Ontario Pavements". Transportation Research Record 521, 1974, p 60.

19. Keyser, J.H., "The Effect of Studded Tires on the Durability of Road Surfacings". Highway Research Record 331, 1970.

20. Lee, A.R., and D. Croney, "British Full-Scale Pavement Design Experiments". Proceedings, International Conference on Asphalt Pavements, University of Michigan, August 1962, pp 114-136.

21. Manke, P.G., "Asphalt Mix Design Procedures". Laboratory Manual for CIVEN 5653, Department of Civil Engineering, Oklahoma State University, 1970.

22. Marks, D., and H.O. Ford, "Density of Bituminous Surface Courses" Proceedings, 55th Annual Tennessee Highway Conference, Bulletin No. 40, January 1974, pp 1-13.

23. McLeod, N.W., "Influence of Viscosity of Asphalt Cements on Compaction of Paving Mixtures in the Field". Highway Research Record 158, 1967, pp 76-115.

24. Nair, K., and C.Y. Chang, "Flexible Pavement Design and Management: Materials Characterization". NCHRP Report 140, 1973.

25. "Pavement Evaluation." Proceedings American Association of Asphalt Technologists, Volume 38, 1969, p 660.

26. "Pavement Evaluation Using Road Meters". Highway Research Special Report 133, Washington D.C., 1973.

27. Preus, C.K., "Studded Tire Effects on Pavements and Traffic Safety". Highway Research Record 418, 1972, pp 44-54.

28. Ramsey, W.J., and O.L. Lund, "Experimental Lime Stabilization in Nebraska". Highway Research Record 263, December 1969, p 9.

29. Regal, F.V., "Factors Governing Selection of Aggregates: Practice in Missouri". Proceeding 13th National Asphalt Conference, 1940, pp 181-186.

30. Schonfeld, R., "Photo Interpretation of Skid Resistance". Highway Research Record 311, 1970.

31. Schonfeld, R., "Skid Numbers from Stereo-Photographs". Ontario Department of Highways, Report No. RR 155, January 1970.

32. Shook, J.F., and J.R. Lambrechts, "Performance of Full-Depth Asphalt Bases on San Diego County Experimental Base Project". Transportation Research Record 521, 1974, pp 47-59.

33. Snedecor, W.J., and W.G. Cochran, "Statistical Methods". (6th ed.) Iowa State University Press, 1972.

34. "Standard Specifications for Highway Construction". Oklahoma State Highway Commission, 1967.

35. "The AASHO Road Test Report No. 5: Flexible Pavement Research". Highway Research Special Report No. 61 E, 1962, p 60.

36. "Theoretical Maximum Specific Gravity of Bituminous Paving Mixtures". ASTM Designation: D 2041, 1971.

37. Volterra, E., and J.H. Gaines, "Beams on Elastic Foundations". Advanced Strength of Materials, Englewood, N.J.: Prentice-Hall, 1971.

38. Winnitoy, W.E., "Rating Flexible Pavement Surface Condition". Highway Research Record 300, 1969.

39. Yoder, E.J. Principles of Pavement Design, New York: Wiley & Sons Book Co., 1959.

APPENDIX A

TEST SITE INFORMATION

TABLE III

TEST SITE INFORMATION

TEST SITE #	LOCATION	SECTION TYPE	BASE TYPE	AGE (MONTHS)	LOCATION OF MARKER (ORANGE PLATE)
10	Interstate 40, Westbound Lanes, Muskogee,County, Oklahoma, approx. 12.50 miles East of McIntosh County line	Fill	Hot Mix Sand Asphalt	36	North right-of-way fence
20	Interstate 40, Westbound Lanes, Seminole County, Oklahoma, approx. 2.4 miles East of Pottawatomie County line	Fill	Black Base	82	North right-of-way fence
30	Interstate 40, Westbound Lanes, Sequoyah County, Oklahoma, approx. 13.0 miles East of Muskogee County line	Cut	Black Base	56	North right-of way fence
40	Interstate 40, Eastbound Lanes, Sequoyah County, Oklahoma, approx. 12.6 miles East of Muskogee County line	Fill	Black Base	56	South right-of-way fence
50	Interstate 40, Westbound Lanes, Seminole County, Oklahoma, approx. 4.5 miles East of Pottawatomie County line	Slight Cut	Black Base	86	North right-of-way fence
60	Interstate 40, Westbound Lanes, Beckham County, Oklahoma, approx. 19.0 miles East of Texas-Oklahoma State line	Slight Fill	Hot Mix Sand Asphalt	169	North right-of-way fence
70	Interstate 40, Westbound Lanes, Beckham County, Oklahoma, approx. 20.50 miles East of Texas-Oklahoma State line	Slight Fill	Hot Mix Sand Asphalt	169	North right-of-way fence
80	Interstate 35, Southbound Lanes, Kay County, Oklahoma, approx. 25.0 miles North of Noble County line	Slight Fill	Stabilized Aggregate Base Course	165	West right-of-way fence
90	Interstate 35, Southbound Lanes, Kay County, Oklahoma, approx. 26.0 miles North of Noble County line	Slight Fill	Stabilized Aggregate Base Course	165	West right-of-way fence
100	Interstate 35, Southbound Lanes, Cleveland County, Oklahoma, approx. 4.5 miles North of McClain County line	Slight Fill	Stabilized Aggregate Base Course	158	West right-of-way fence
110	Interstate 40, Westbound Lanes, Cleveland County, Oklahoma, approx. 12.0 miles East of Oklahoma County line	Slight Fill	Stabilized Aggregate Base Course	158	West right-of-way fence
120	Interstate 40, Eastbound Lanes, Pottawatomie County, Oklahoma, approx. 12.0 miles East of Oklahoma County line	Slight Fill	HMSA	105	North right-of-way fence
130	Interstate 40, Eastbound Lanes, Washita County, Oklahoma, approx. 9.0 miles East of Beckham County line	Slight Fill	Soil-Cement Base	148	South right-of-way fence
140	Interstate 40, Westbound Lanes, Washita County, Oklahoma, approx. 12.25 miles East of Beckham County line	Fill	Soil-Cement Base	148	North right-of-way fence
170	Interstate 40, Eastbound Lanes, Beckham County, Oklahoma, approx. 26.4 miles East of Texas-Oklahoma State line	Fill	Soil-Cement Base	169	South right-of way fence
180	Interstate 40, Eastbound Lanes, Beckham County, Oklahoma, approx. 20.25 miles East of Texas-Oklahoma State line	Fill	Soil-Cement Base	196	South right-of-way fence

APPENDIX B

FLOW DIAGRAM

COMPUTER ANALYSIS OF TEST DATA

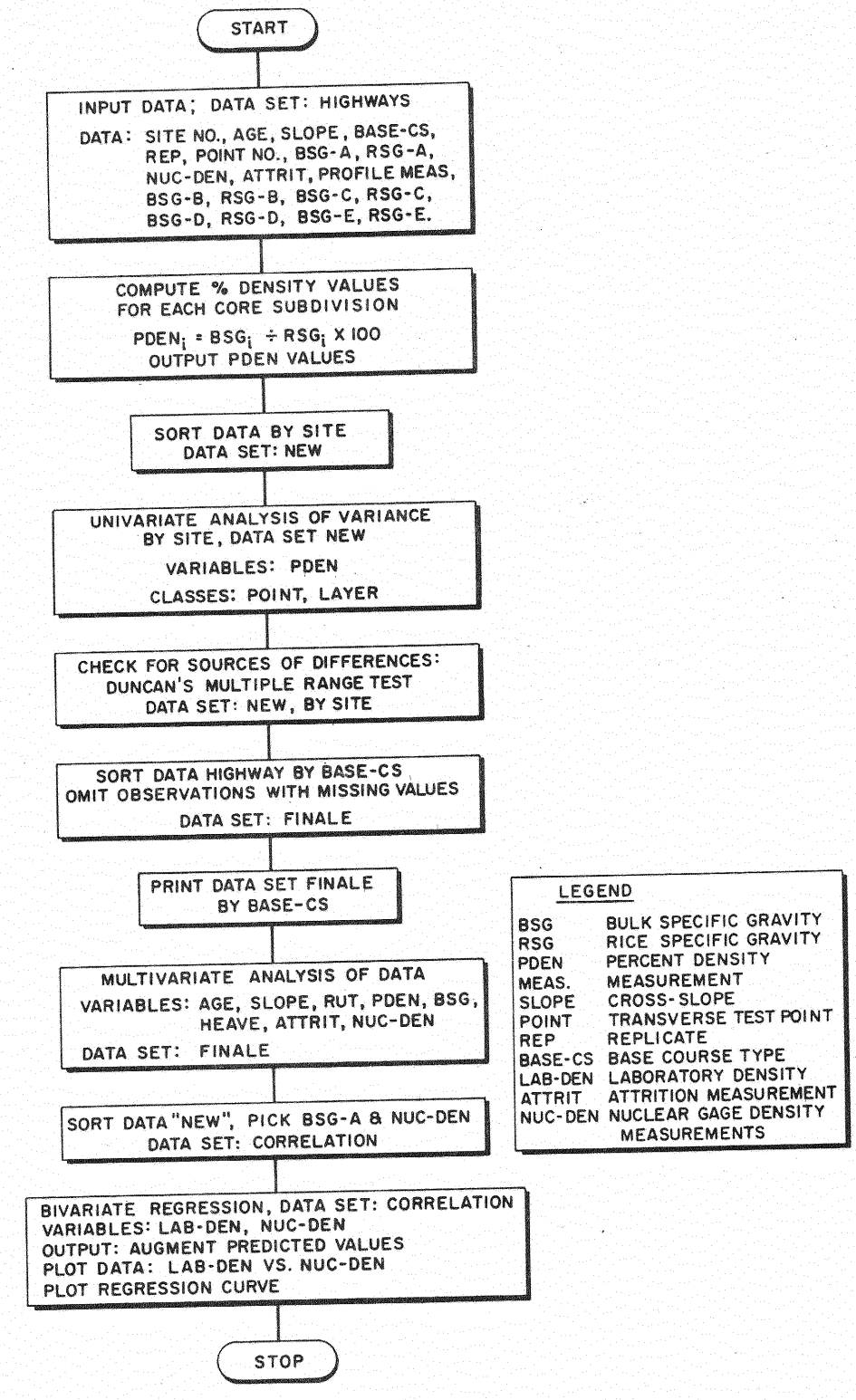

Figure 48 Flow Diagram: Computer Analysis of Test Data Using the SAS Computer Program